

File B) Proposed Area of Review (AoR) and Corrective Action Plan

Note: This document contains Area of Review and Corrective Action information for the Kansas Small Scale Test Wellington Field. The contents were extracted from the original KGS permit document that was prepared prior to the new EPA submission format introduced to KGS on June 3rd 2014. This explains why the information in this Area of Review and Corrective Action document may contain references to figures, tables, and sub-sections in other permit sections that may not be included in this Area of Review and Corrective Action document. Therefore, to facilitate the review process, the entire original permit application has been submitted as a separate document titled “L - Other Information Required by the UIC Program Director”, which also contains an Executive Summary, cover letter, application forms, complete table of contents, list of tables and figures, appendices, and a cross reference table which lists sub-sections that address all Class VI 40 CFR sections 146.82 – 146.93 requirements.

The Proposed Area of Review (AoR) and Corrective Action Plan is documented in the following sections:

Table of Contents

File B: Proposed Area of Review and Corrective Action Plan

Section 5	5-1
Reservoir Modeling	5-1
5.1 Introduction	5-1
5.2 Conceptual Model and Arbuckle Hydrogeologic State Information	5-2
5.2.1 Modeled Formation	5-2
5.2.2 Modeled Processes	5-4
5.2.3 Geologic Structure	5-4
5.2.4 Arbuckle Hydrogeologic State Information	5-5
5.2.5 Arbuckle Groundwater Velocity	5-5
5.2.6 Model Operational Constraints	5-6
5.3 Geostatistical Reservoir Characterization of Arbuckle Group	5-6
5.3.1 Conceptual Model	5-8
5.3.2 Facies Modeling	5-8
5.3.3 Petrophysical Properties Modeling	5-9
5.4 Arbuckle Reservoir Flow and Transport Model	5-13
5.4.1 Simulation Software Description	5-16
5.4.2 Model Mesh and Boundary Conditions	5-16
5.4.3 Hydrogeologic Properties	5-17
5.4.4 Initial Conditions and Injection Rates	5-18
5.4.5 Alternative Models	5-23
5.4.6 Reservoir Simulation Results	5-23
5.4.6.1 CO ₂ Plume Migration	5-24
5.4.6.2 Simulated Pressure Distribution	5-41

Section 9	9-1
Area of Review Delineation Re-Evaluation and Corrective Action Plan.	9-1
9.1 Introduction	9-1
9.2 EPA Area of Review (AoR)	9-3
9.2.1 Pressure-Based AoR	9-3
9.2.2 Plume-Based AoR	9-5
9.3 Corrective Action Plan	9-5
9.3.1 Area of Review Plan and Schedule	9-7
9.3.2 Corrective Action Plan and Schedule Following AoR Re-evaluation (§146.8 [b][2][iv])	9-9
9.3.3 Site Access (§146.8 [b][2][iv]):	9-9
9.4 Compatibility of CO ₂ with Arbuckle Brine and Minerals	9-10
9.5 Period of Data Retention	9-10

Section 5

Reservoir Modeling

5.1 Introduction

This section presents details of the Arbuckle reservoir simulation model that was constructed to project the results of the Wellington Field short-term Arbuckle CO₂ pilot injection project and delineate the EPA Area of Review (AoR) documented in Section 9. As required under §146.84(c), the AoR must be delineated using a computational model that can accurately predict the projected lateral and vertical migration of the CO₂ plume and formation fluids in the subsurface from the commencement of injection activities until the plume movement ceases and until pressure differentials sufficient to cause the movement of injected fluids or formation fluids into a USDW are no longer present. The model must:

- (i) Be based on detailed geologic data collected to characterize the injection zone(s), confining zone(s), and any additional zones; and anticipated operating data, including injection pressures, rates, and total volumes over the proposed life of the geologic sequestration project;
- (ii) Take into account any geologic heterogeneities, other discontinuities, data quality, and their possible impact on model predictions; and
- (iii) Consider potential migration through faults, fractures, and artificial penetrations.

This section presents the reservoir simulations conducted to fulfill §146.84 requirements stated above. The simulations were conducted assuming a maximum injection of 40,000 metric tons of CO₂ over a period of nine months. As indicated in Section 1, the exact quantity of CO₂ to be injected is subject to budgetary considerations and availability of CO₂ and could be as low as 10,000 tons. The simulation results, therefore, represent impacts of the maximum quantity of CO₂ that may be injected during the Wellington Arbuckle injection pilot project.

The modeling results indicate that the induced pore pressures in the Arbuckle aquifer away from the injection well are of insufficient magnitude to cause the Arbuckle brines to migrate up

into the USDW even if there were any artificial or natural penetration in the Arbuckle Group or the overlying confining units.

The simulation results also indicate that the free-phase CO₂ plume is contained within the total CO₂ plume (i.e., in the free plus dissolved phases) and that it extends to a maximum lateral distance of 1,700 ft from the injection well. The EPA Area of Review (AoR) is defined by the 1% saturation isoline of the stabilized free-phase plume.

5.2 Conceptual Model and Arbuckle Hydrogeologic State Information

5.2.1 Modeled Formation

The simulation model spans the entire thickness of the Arbuckle aquifer (Figure 5.1). The CO₂ is to be injected in the lower portion of the Arbuckle in the interval 4,910–5,050 feet which has relatively high permeability based on the core data collected at the site. Preliminary simulations indicated that the bulk of the CO₂ will remain confined in the lower portions of the Arbuckle because of the low permeability intervals in the baffle zones as discussed in Section 4.6.6 and also shown in analysis of geologic logs at wells KGS 1-28 and KGS 1-32 (Figure 4.32 a-b). Therefore, no-flow boundary conditions were specified along the top of the Arbuckle. The specification of a no-flow boundary at the top is also in agreement with hydrogeologic analyses presented in Section 4.7, which indicates that the upper confining zone—comprising the Simpson Group, the Chattanooga Shale, and the Pierson formation—has very low permeability, which should impede any vertical movement of groundwater from the Arbuckle Group. Additionally, entry pressure analyses (documented in Section 4.7.4) indicate that an increase in pore pressure of more than 956 psi within the confining zone at the injection well site is required for the CO₂-brine to penetrate through the confining zone. As discussed in the model simulation results section below (Section 5.4.6), the maximum increase in pore pressure at the top of the Arbuckle is approximately 13.1 psi under the worst-case scenario, which corresponds to a low permeability–low porosity alternative model case as discussed in Section 5.4.5. This small pressure rise at the top of the Arbuckle is due to CO₂ injection below the lower vertical-permeability baffle zones present in the middle of the Arbuck-

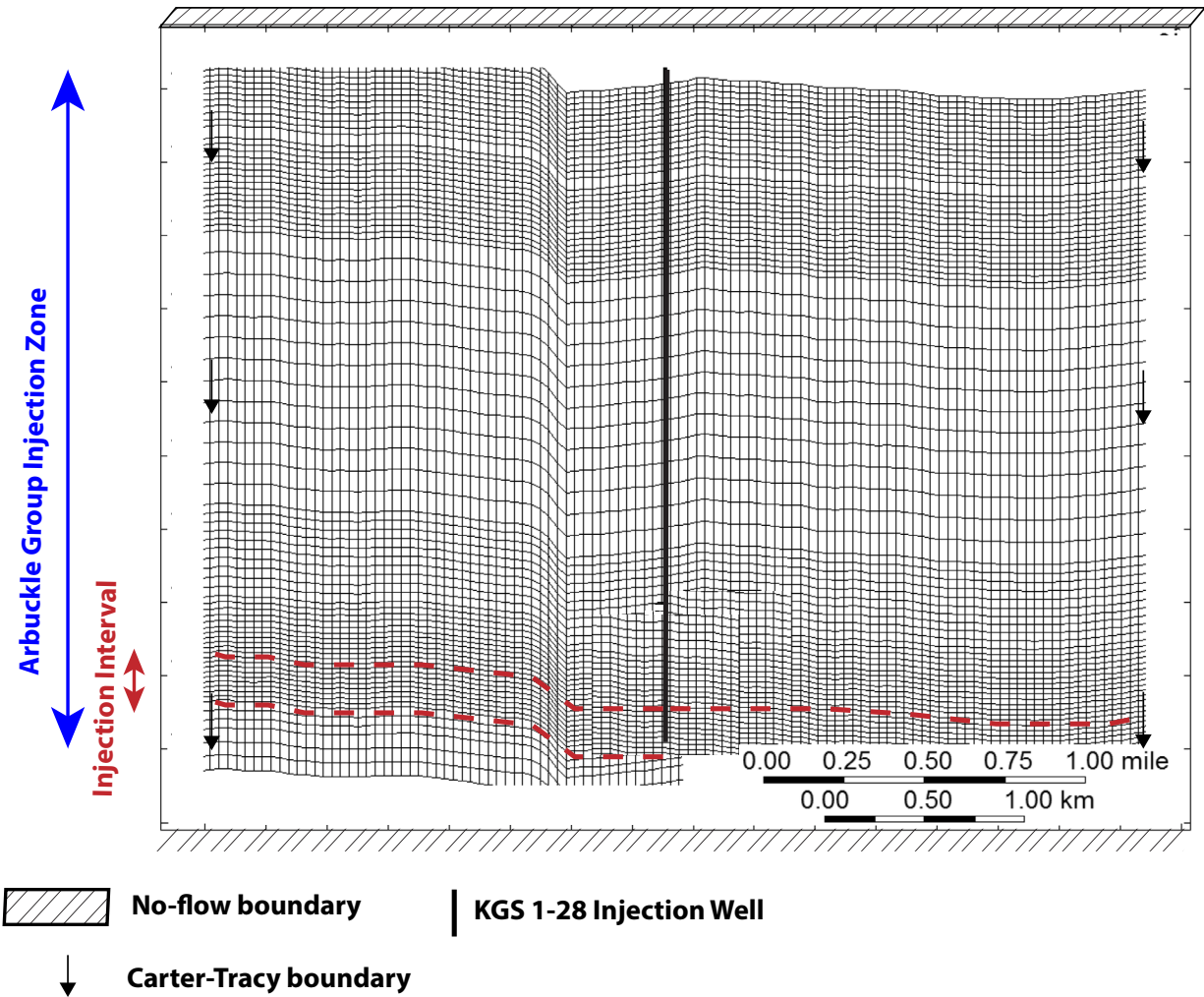


Figure 5.1—Typical east-west cross section of model grid showing boundary conditions.

le Group, which confines the CO₂ in the injection interval in the lower portions of the Arbuckle Group. The confining zone is also documented to be locally free of transmissive fractures based on fracture analysis conducted at KGS 1-28 (injection well) and documented in Section 4.7.5. There are no known faults in the area, as documented in Section 6. Based on the above evidence, it is technically appropriate to restrict the simulation region within the Arbuckle Group for purposes of numerical efficiency, without compromising predictions of the effects of injection on the plume or pressure fronts. Because of the presence of the Precambrian granitic basement under the Arbuckle Group, which is expected to provide hydraulic confinement, the bottom of the model domain was also specified as a no-flow boundary.

5.2.2 Modeled Processes

Physical processes modeled in the reservoir simulations included isothermal multi-phase flow and transport of brine and CO₂. Isothermal conditions were modeled because the total variation in subsurface temperature in the Arbuckle Group from the top to the base is only slightly more than 10°F, which should not significantly affect the various storage modes away from the injection well, and because it is assumed that the temperature of the injected CO₂ will equilibrate to formation temperature close to the well. Uniform salinity concentration was assumed because geochemical evidence shows a lack of communication between upper and lower layers and because of the relatively small area of impact due to CO₂ injection. Subsurface storage of CO₂ occurs via the following four main mechanisms:

- structural trapping,
- aqueous dissolution,
- hydraulic trapping, and
- mineralization.

The first three mechanisms were simulated in the Wellington model. Mineralization was not simulated as preliminary geochemical modeling indicated that due to the short-term and small-scale nature of the pilot project, mineral precipitation is not expected to cause any problems with clogging of pore space that may reduce permeability and negatively impact injectivity. Therefore, any mineral storage that may occur will only result in faster stabilization of the CO₂ plume and make projections presented in this model somewhat more conservative.

5.2.3 Geologic Structure

There are no faults in the Arbuckle Group or the overlying confining zone or in proximity to the AoR derived from the model results. The closest fault is approximately 12.5 mi southeast of Wellington, as shown in Figure 6.4. Known faults mapped on top of Arbuckle and Mississippian system structures are presented in Figure 6.8. The seismic data at the Wellington site, presented in Section 4.8, also points to the absence of faults in the vicinity of Wellington.

5.2.4 Arbuckle Hydrogeologic State Information

As shown in Figures 4.29, 4.31, and 4.35, the ambient pore pressure, temperature, and salinity vary nearly linearly with depth in the Arbuckle Group. By linear extrapolation, the relationship between depth and these three parameters can be expressed by the following equations using the data in Figures 4.29, 4.31, and 4.35:

$$\text{Temperature (}^\circ\text{F)} = (0.011 * \text{Depth} + 73.25)$$

$$\text{Pressure (psi)} = (0.487 * \text{Depth} - 324.8)$$

$$\text{Chloride (mg/l)} = (100.9 * \text{Depth} - 394.786)$$

where depth is in feet below kelly bushing (KB)

Using the above relationships, the temperature, pressure, and salinity at the top and bottom of the Arbuckle Group at the injection well site (KGS 1-28) are presented in Table 5.1.

Table 5.1—Temperature, pressure, and salinity at the top and bottom of the Arbuckle Group at the injection well site (KGS 1-28).

	Top of Arbuckle (4,168 ft)	Bottom of Arbuckle (5,160 ft)
Temperature (°F)	115	130
Pressure (psi)	1,705	2,188
Chloride (mg/l)	25,765	125,858

5.2.5 Arbuckle Groundwater Velocity

On a regional basis in the Arbuckle, groundwater flows from east to west, as shown in the potentiometric surface map presented in Figure 4.37. Groundwater velocity, however, is estimated to be very slow. The head in Sumner County drops approximately 100 ft over 20 mi (Figure 4.37), resulting in a head gradient of approximately 1.0e-03 ft/ft. Assuming an average large-scale Arbuckle porosity of approximately 6% and an average permeability of 10 mD, the pore velocity in the Arbuckle is approximately 0.2 ft/year, which is fairly small and can be neglected in specification of ambient boundary conditions for the purpose of this modeling study.

5.2.6 Model Operational Constraints

The bottomhole injection pressure in the Arbuckle should not exceed 90% of the estimated fracture gradient of 0.75 psi/ft (measured from land surface) as derived in Section 4.6.9. Therefore, the maximum induced pressure at the top and bottom of the Arbuckle Group should be less than 2,813 and 3,483 psi, respectively, as specified in Table 5.2. At the top of the perforations (4,910 ft), pressure will not exceed 2,563 psi.

Table 5.2—Maximum allowable pressure at the top and bottom of the Arbuckle Group based on 90% fracture gradient of 0.675 psi/ft.

Depth (feet, bls)	Maximum Pore Pressure (psi)
4,168 (Top of Arbuckle)	2,813
4,910 (Top of Perforation)	3,314
5,050 (Bottom of Perforation)	3,408
5,160 (Bottom of Arbuckle)	3,483

5.3 Geostatistical Reservoir Characterization of Arbuckle Group

Statistical reservoir geomodeling software packages have been used in the oil and gas industry for decades. The motivation for developing reservoir models was to provide a tool for better reconciliation and use of available hard and soft data (Figure 5.2). Benefits of such numerical models include 1) transfer of data between disciplines, 2) a tool to focus attention on critical unknowns, and 3) a 3-D visualization tool to present spatial variations to optimize reservoir development. Other reasons for creating high-resolution geologic models include the following:

- volumetric estimates
- multiple realizations that allow unbiased evaluation of uncertainties before finalizing a drilling program
- lateral and top seal analyses
- integration (i.e., by gridding) of 3-D seismic surveys and their derived attributes
- assessments of 3-D connectivity

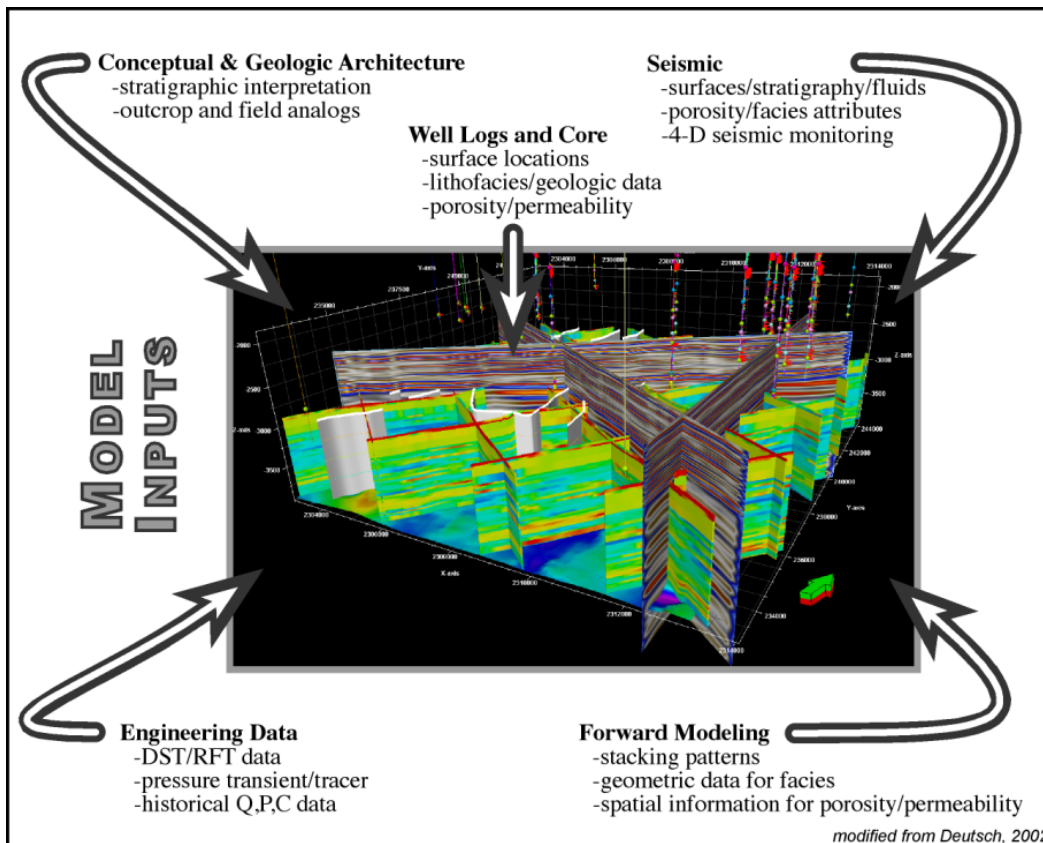


Figure 5.2—A static, geocellular reservoir model showing the categories of data that can be incorporated (source: modified from Deutsch, 2002)

- flow-simulation-based production forecasting using different well designs
- optimizing long-term development strategies to maximize return on investment.

Although geocellular modeling software has largely flourished in the energy industry, its utility can be important for reservoir characterization in CO₂ research and geologic storage projects, such as the Wellington Field. The objective in the Wellington project is to integrate various data sets of different scales into a cohesive model of key petrophysical properties, especially porosity and permeability. The general steps for applying this technology are to model the large-scale features followed by modeling progressively smaller, more uncertain, features. The first step applied at the Wellington field was to establish a conceptual depositional model and its characteristic stratigraphic layering. The stratigraphic architecture provided a first-order constraint on the spatial continuity of facies, porosity, permeability, saturations, and other attributes within each layer. Next, facies (i.e., rock fabrics) were modeled for each stratigraphic layer using cell-based

or object-based techniques. Porosity was modeled by facies and conditioned to “soft” trend data, such as seismic inversion attribute volumes. Likewise, permeability was modeled by facies and collocated, co-Kriged to the porosity model.

5.3.1 Conceptual Model

Lower Arbuckle core from Wellington reflects sub-meter-scale, shallowing-upward peritidal cycles. The two common motifs are cycles passing from basal dolo-mudstones/wackestones into algal dolo-laminites or matrix-poor monomict breccias. Bioclasts are conspicuously absent. Breccias are clast-supported, monomictic, and angular, and their matrix dominantly consists of cement (Figure 5.3). They are best classified as crackle to mosaic breccias (Loucks, 1999) because there is little evidence of transportation. Lithofacies and stacking patterns (i.e., sub-meter scale, peritidal cycles) are consistent with an intertidal to supratidal setting. Breccia morphologies, scale (<0.1 m), mineralogy (e.g., dolomite, anhydrite, length-slow chalcedony), depositional setting, greenhouse climate, and paleo-latitude (~15° S) support mechanical breakdown processes associated with evaporite dissolution. The Arbuckle-Simpson contact (~800 ft above the proposed injection interval) records the super-sequence scale, Sauk-Tipppecanoe unconformity, which records subaerial-related karst landforms across the Early Phanerozoic supercontinent Laurentia.

5.3.2 Facies Modeling

The primary depositional lithofacies were documented during core description at KGS 1-32. A key issue was reconciling inconsistencies (order of magnitude) between permeability measurements derived from wireline logs (i.e., nuclear resonance tool), whole core, and step-rate tests. Poor core recovery from the injection zone resulted from persistent jamming, which is commonly experienced in fractured or vuggy rocks. Image logs acquired over this interval record some intervals with large pores (cm scale) that are likely solution-enlarged vugs (touching-vugs of Lucia, 1999; Figure 5.4). Touching-vug fabrics commonly form a reservoir-scale, interconnected pore system characterized by Darcy-scale permeability. It is hypothesized that a touching-vug pore

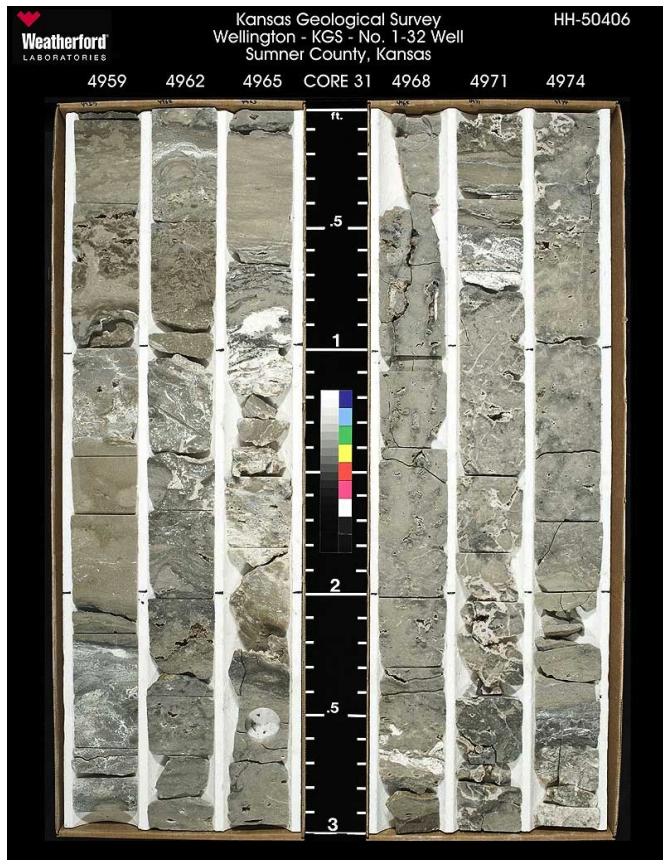


Figure 5.3—Example of the carbonate facies and porosity in the injection zone in the lower Arbuckle (part of the Gasconade Dolomite Formation). Upper half is light olive-gray, medium-grained dolomitic packstone with crackle breccia. Scattered subvertical fractures and limited cross stratification. Lower half of interval shown has occasional large vugs that crosscut the core consisting of a light olive-gray dolopackstone that is medium grained. Variable-sized vugs range from cm-size irregular to subhorizontal.

system preferentially developed within fracture-dominated crackle and mosaic breccias—*formed in response to evaporite removal*—which functioned as a strataform conduit for undersaturated meteoric fluids (Figure 5.5). As such, this high-permeability, interwell-scale, touching-vug pore system is largely strataform and, therefore, predictable.

5.3.3 Petrophysical Properties Modeling

The approach taken for modeling a particular reservoir can vary greatly based on available information and often involves a complicated orchestration of well logs, core analysis, seismic surveys, literature, depositional analogs, and statistics. Because well log data were available in only two wells (KGS 1-28 and KGS 1-32) that penetrate the Arbuckle reservoir at the Wellington site, the geologic model also relied on seismic data, step-rate test, and drill-stem test information. Schlumberger’s Petrel™ geologic modeling software package was used to produce the current geologic model of the Arbuckle saline aquifer for the pilot project area. This geomodel extends

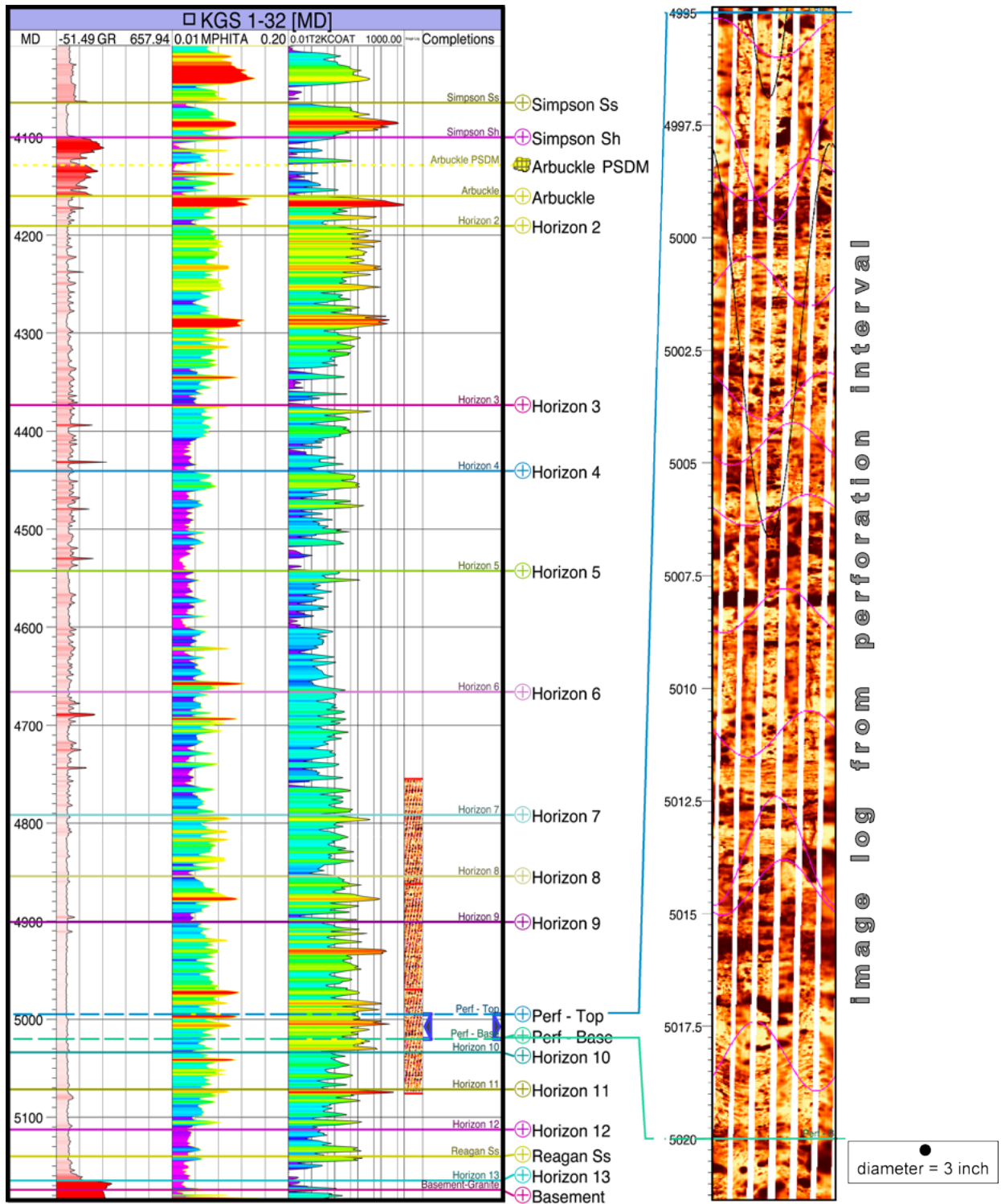


Figure 5.4—Geophysical logs within the Arbuckle Group at KGS 1-32. (Notes: MPHITA represents Haliburton porosity. Horizon markers represent porosity package. Image log on right presented to provide example of vugs; 3-in diameter symbol represents size of vug).

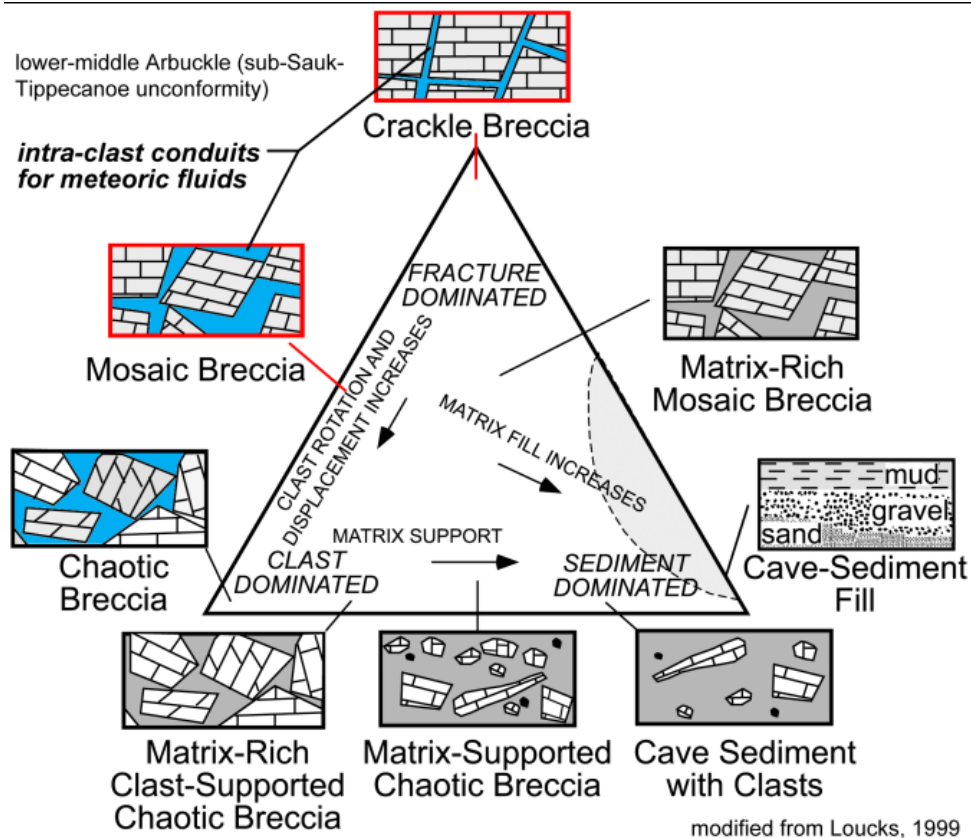


Figure 5.5—Classification of breccias and clastic deposits in cave systems exhibiting relationship between chaotic breccias, crackle breccias, and cave-sediment fill (source: Loucks, 1999).

4.25 mi by 4 mi laterally and is 1,075 ft deep, spanning the entire Arbuckle Group as well as a portion of the sealing units (Simpson/Chattanooga shale).

Porosity Modeling

In contrast to well data, seismic data are extensive over the reservoir and are, therefore, of great value for constraining facies and porosity trends within the geomodel. Petrel’s volume attribute processing (i.e., genetic inversion) was used to derive a porosity attribute from the prestack depth migration (PSDM) volume to generate the porosity model (Figure 5.6). The seismic volume was created by re-sampling (using the original exact amplitude values) the PSDM 50 ft above the Arbuckle and 500 ft below the Arbuckle (i.e., approximate basement). The cropped PSDM volume and conditioned porosity logs were used as learning inputs during neural network processing. A

correlation threshold of 0.85 was selected and 10,000 iterations were run to provide the best correlation. The resulting porosity attribute was then re-sampled, or upscaled (by averaging), into the corresponding 3-D property grid cell.

The porosity model was constructed using sequential Gaussian simulation (SGS). The porosity logs were upscaled using arithmetic averaging. The raw upscaled porosity histogram was used during SGS. The final porosity model was then smoothed. The following parameters were used as inputs:

I. Variogram

- a. Type: spherical
- b. Nugget: 0.001
- c. Anisotropy range and orientation
 - i. Lateral range (isotropic): 5,000 ft
 - ii. Vertical range: 10 ft

II. Distribution: actual histogram range (0.06–0.11) from upscaled logs

III. Co-Kriging

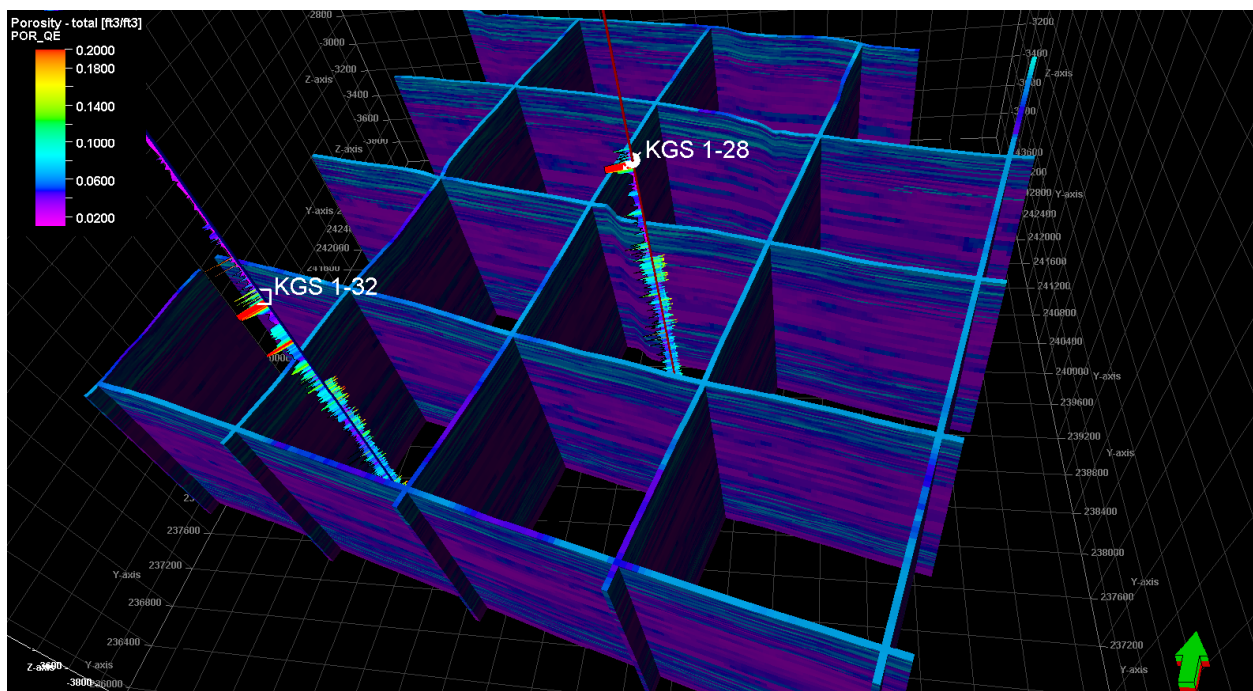


Figure 5.6—Upscaled porosity distribution in the Arbuckle Group based on the Petrel geomodel.

- a. Secondary 3-D variable: inverted porosity attribute grid
- b. Correlation coefficient: 0.75

Table 5.3 presents the minimum, maximum, and average porosity within the Arbuckle Group in the geomodel.

Table 5.3—Hydrogeologic property statistics in hydrogeologic characterization and simulation models.

Property	Reservoir Characterization Geomodel			Reservoir Simulation Numerical Model		
	min	max	avg	min	max	avg
Porosity (%)	3.2	12.9	6.8	3.2	12.9	6.7
Horizontal Permeability (mD)	0.05	2,955	134.2	0.05	2,955	130.7
Vertical Permeability (mD)	.005	1,567	387	0.005	1,567	385

Permeability Modeling

The upscaled permeability logs shown in Figure 5.4 were created using the following controls: geometric averaging method; logs were treated as points; and method was set to simple. The permeability model was constructed using SGS. Isotropic semi-variogram ranges were set to 3,000 ft horizontally and 10 ft vertically. The permeability was collocated and co-Kriged to the porosity model using the calculated correlation coefficient (~0.70). The resulting SGS-based horizontal and vertical permeability distributions are presented in Figure 5.7a-b.

Table 5.3 presents the minimum, maximum, and average permeabilities within the Arbuckle Group in the geomodel. An east-west cross-section of horizontal permeability through injection well (KGS 1-28) is presented in Figure 5.7c, which shows the relatively high permeability zone selected for completion within the injection interval.

5.4 Arbuckle Reservoir Flow and Transport Model

An extensive set of computer simulations were conducted to estimate the potential impacts of CO₂ injection in the Arbuckle injection zone. The key objectives were to determine the resulting rise in pore fluid pressure and the extent of CO₂ plume migration. The underlying motivation was to determine whether the injected CO₂ could affect the USDW or potentially escape into the atmosphere

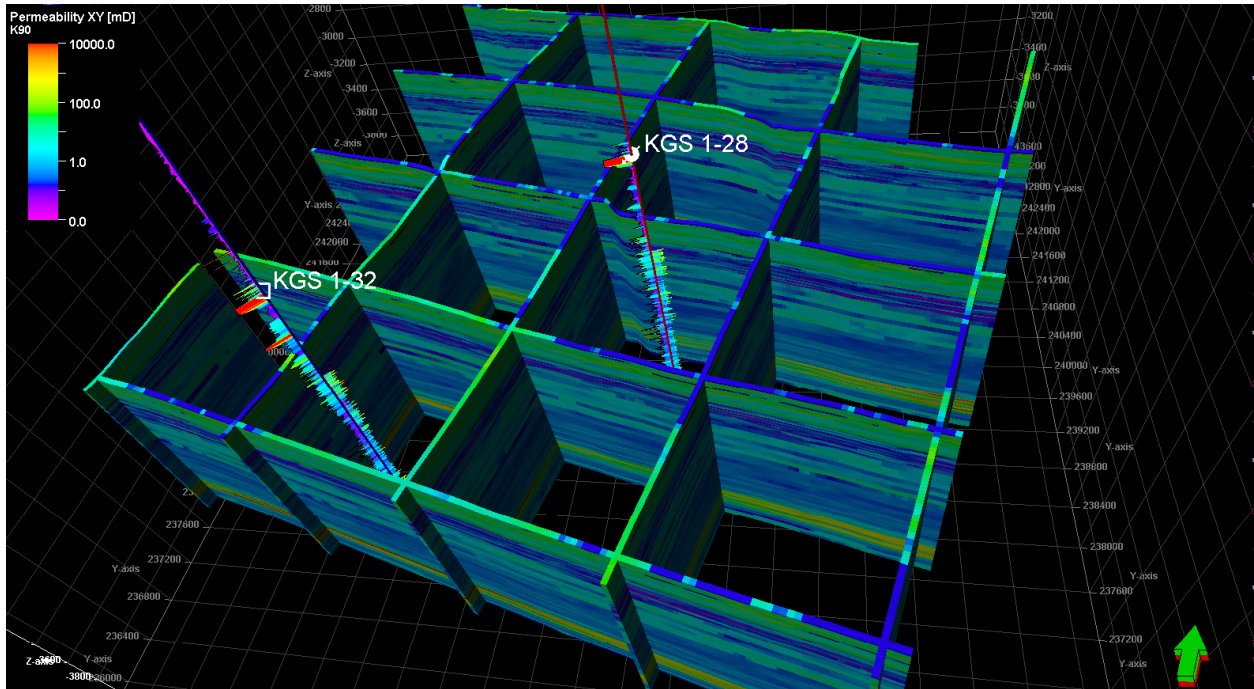


Figure 5.7a—Upscaled horizontal permeability (mD) distributions in the Arbuckle Group derived from Petrel geomodel.

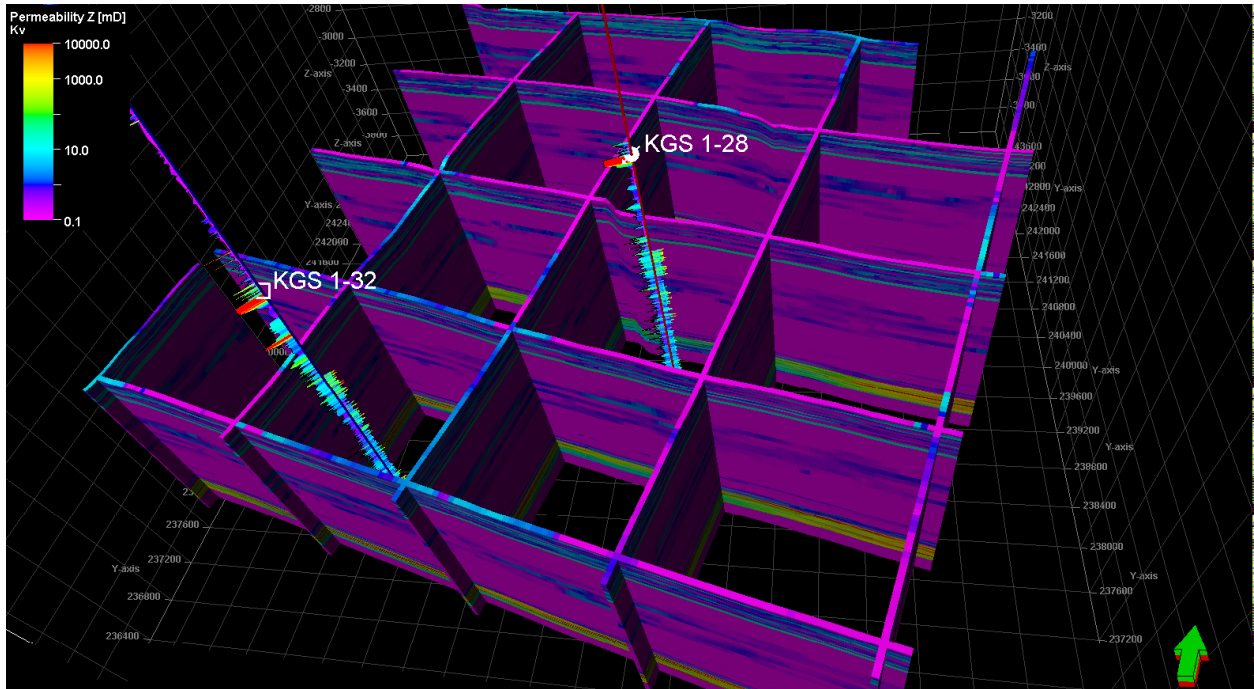


Figure 5.7b—Upscaled vertical permeability (mD) distributions in the Arbuckle Group derived from Petrel geomodel.

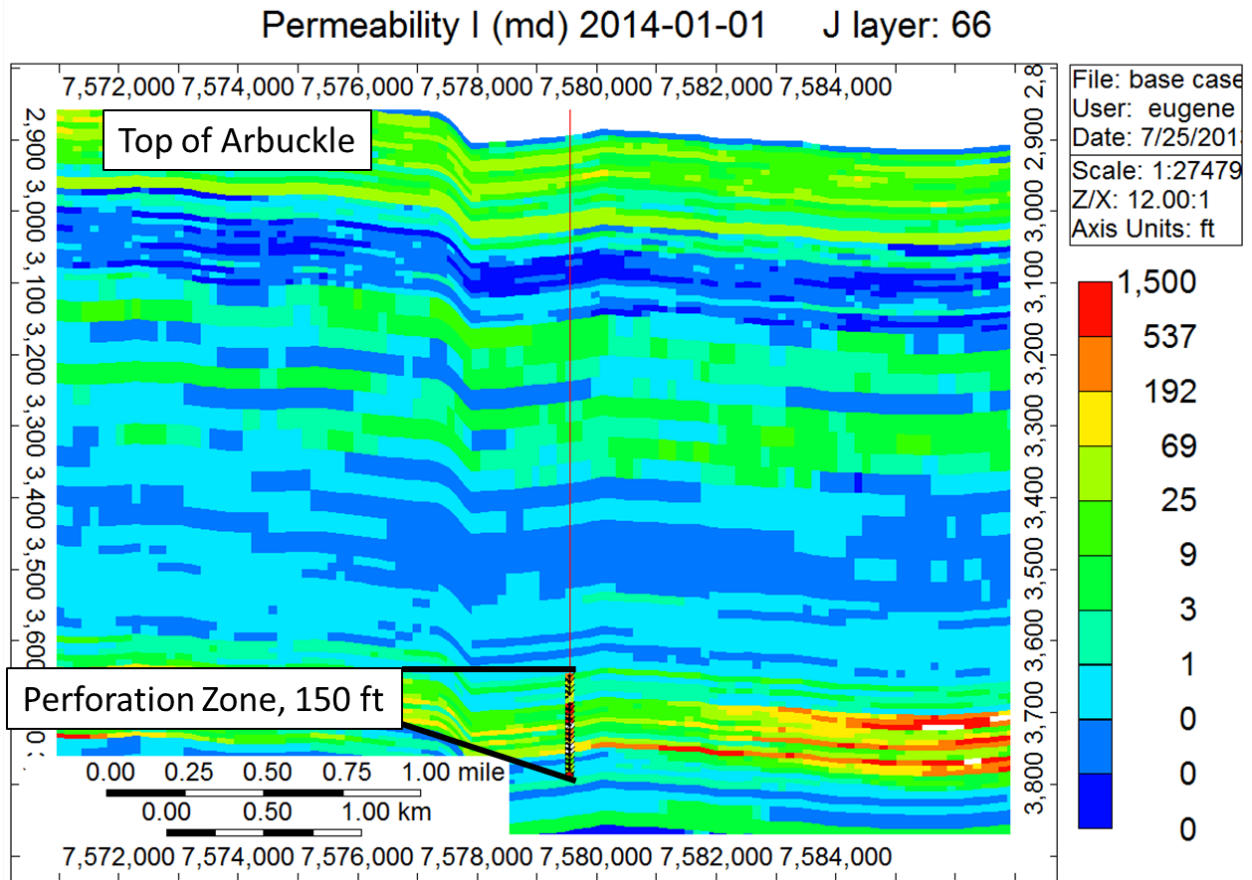


Figure 5.7c—Horizontal permeability (mD) distribution within an east-west cross section through the injection well (KGS 1-28).

through existing wells or hypothetical faults/fractures that might be affected by the injected fluid.

As in all reservoirs, there are data gaps that prevent an absolute or unique characterization of the geology and petrophysical properties. This results in conceptual, parametric, and boundary condition uncertainties. To address these uncertainties, a comprehensive set of simulations were conducted to perform a sensitivity analysis using alternative parameter sets. A key objective was to ensure specification of parameter sets that would result in the most negative impacts (the worst-case scenario; i.e., maximum formation pressures and largest extent of plume migration). However, simulations involving alternative parameter and boundary conditions that resulted in more favorable outcomes were also conducted to bracket the range of possible induced system states and outcomes.

5.4.1 Simulation Software Description

The reservoir simulations were conducted using the Computer Modeling Group (CMG) GEM simulator. GEM is a full equation of state compositional reservoir simulator with advanced features for modeling the flow of three-phase, multi-component fluids and has been used to conduct numerous CO₂ studies (Chang et al., 2009; Bui et al., 2010). It is considered by DOE to be an industry standard for oil/gas and CO₂ geologic storage applications. GEM is an essential engineering tool for modeling complex reservoirs with complicated phase behavior interactions that have the potential to impact CO₂ injection and transport. The code can account for the thermodynamic interactions between three phases: liquid, gas, and solid (for salt precipitates). Mutual solubilities and physical properties can be dynamic variables depending on the phase composition/system state and are subject to well-established constitutive relationships that are a function of the system state (pressures, saturation, concentrations, temperatures, etc.). In particular, the following assumptions govern the phase interactions:

- Gas solubility obeys Henry's Law (Li and Nghiem, June 1986)
- The fluid phase is calculated using Schmit-Wenzel or Peng-Robinson (SW-PR) equations of state (Soreide-Whitson, 1992)
- Changes in aqueous phase density with CO₂ solubility, mineral precipitations, etc., are accounted for with the standard or Rowe and Chou correlations.
- Aqueous phase viscosity is calculated based on Kestin, Khalifa, and Correia (1981).

5.4.2 Model Mesh and Boundary Conditions

The Petrel-based geomodel mesh discussed above consists of a 706 x 654 horizontal grid and 79 vertical layers for a total of 36,476,196 cells. The model domain encompasses a 17 mi² area and the formations from the base of the Arbuckle Group to Chattanooga and Simpson Group formations from depths of 4,100 to 5,175 ft BGL at KGS 1-28. To reduce reservoir simulation time, this model was upscaled to a 157 x 145 horizontal mesh with 79 layers for a total of 1,798,435 cells to represent the same rock volume for use in the CMG simulator. The fluid flow model was

divided into 79 layers. The thickness of the layers varies from 5 to 20 ft based on the geomodel, with an average of 13 feet.

Based on preliminary simulations, it was determined that due to the small scale of injection and the presence of a competent confining zone, the plume would be contained within the Arbuckle system for all alternative realizations of reservoir parameters. Therefore, the reservoir model domain was restricted to the Arbuckle aquifer with no-flow boundaries specified along the top (Simpson Group) and bottom (Precambrian basement) of the Arbuckle group. As discussed in Section 5.2.1, the specification of no-flow boundaries along the top and bottom of the Arbuckle Group is justified because of the low permeabilities in the overlying and underlying confining zones as discussed in Section 4.7.3. The permeability in the Pierson formation was estimated to be as low as 1.6 nanoDarcy (nD; 1.0^{-9} Darcy).

The simulation model, centered approximately on the injection well (KGS 1-28), extends approximately 4 mi in the east-west and 4.25 mi in the north-south orientations. Vertically, the model extends approximately 1,050 ft from the top of the Precambrian basement to the bottom of the Simpson Group. As discussed above, the model domain was discretized laterally by 157 x 145 cells in the east-west and north-south directions and vertically in 79 layers. The lateral boundary conditions were set as an infinite-acting Carter-Tracy aquifer (Dake, 1978; Carter and Tracy, 1960) without leakage. Sensitivity analyses indicated that there was negligible difference in the simulation results pressures due to specification of non-leaky Carter-Tracy boundary as compared to a leaky Carter-Tracy boundary or a closed no-flow lateral boundary.

5.4.3 Hydrogeologic Properties

Geologic and hydrologic data pertaining to the Arbuckle Group are detailed in Sections 3 and 4 of the permit application. As discussed in Section 5.3, site-specific hydrogeologic properties were used to construct a geomodel at the Wellington site. The porosity and permeability of the geomodel were upscaled to the coarser grid using a weighted averaging approach so that the total pore space volume (2.99×10^{10} ft³) in the Petrel geomodel was maintained in the upscaled reser-

voir simulation model. As shown in Figures 5.8a-b and 5.9, the qualitative representation (i.e., the shape) of the permeability and porosity distribution remained similar in both the geo and reservoir models. The upscaled reservoir grid was imported from Petrel into CMG Builder, where the model was prepared for dynamic simulations assuming an equivalent porous medium model with flow limited to only the rock matrix. The minimum, maximum, and average porosity and permeabilities in the reservoir model are documented in Table 5.3 alongside the statistics for the geomodel.

Because of the absence of published capillary pressure and relative permeability relationships for the Arbuckle in Kansas, the simulations used the relative permeability function governing multi-phase flow in fractured carbonate-CO₂-brine system as proposed by Bennion and Bachu (2007) (Figure 5.10).

5.4.4 Initial Conditions and Injection Rates

The initial conditions specified in the reservoir model are specified in Table 5.4. The simulations were conducted assuming isothermal conditions. Although isothermal conditions were assumed, a thermal gradient of 0.008 °C/ft was considered for specifying petrophysical properties that vary with layer depth and temperature such as CO₂ relative permeability, CO₂ dissolution in formation water, etc. The original static pressure in the injection zone (at a reference depth of 4,960 ft) was set to 2,093 psi and the Arbuckle pressure gradient of 0.48 psi/ft (discussed in Section 4) was assumed for specifying petrophysical properties. A 140-ft thick perforation zone in well KGS 1-28 was specified between 4,910 and 5,050 ft. A constant brine density of 68.64 lbs/ft³ (specific gravity of 1.1) was assumed. A total of 40,000 metric tons of CO₂ was injected in the Arbuckle formation over a period of nine months at an average injection rate of 150 tons/day.

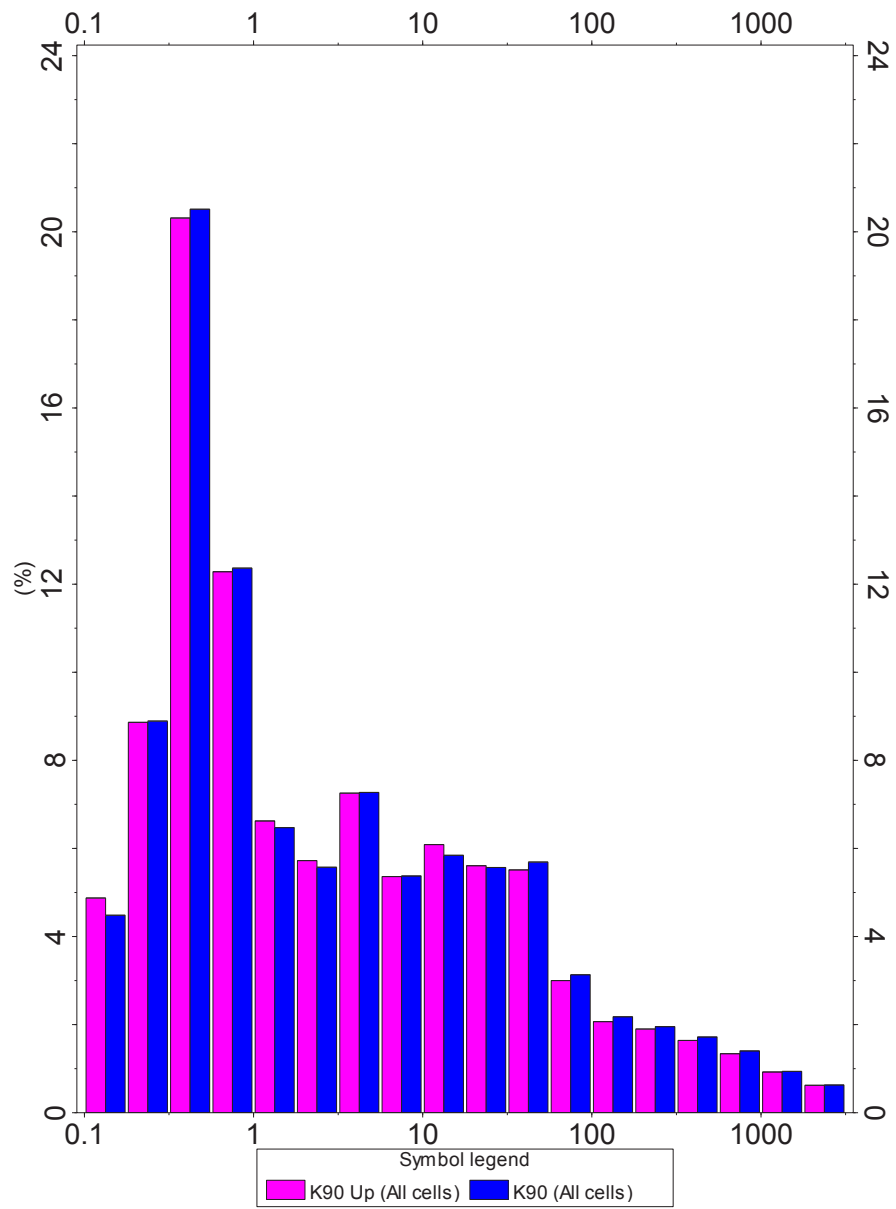


Figure 5.8a—Horizontal permeability distribution histogram comparison for original and upscaled model properties. (Note: x-axis represents permeability in milliDarcy, mD.)

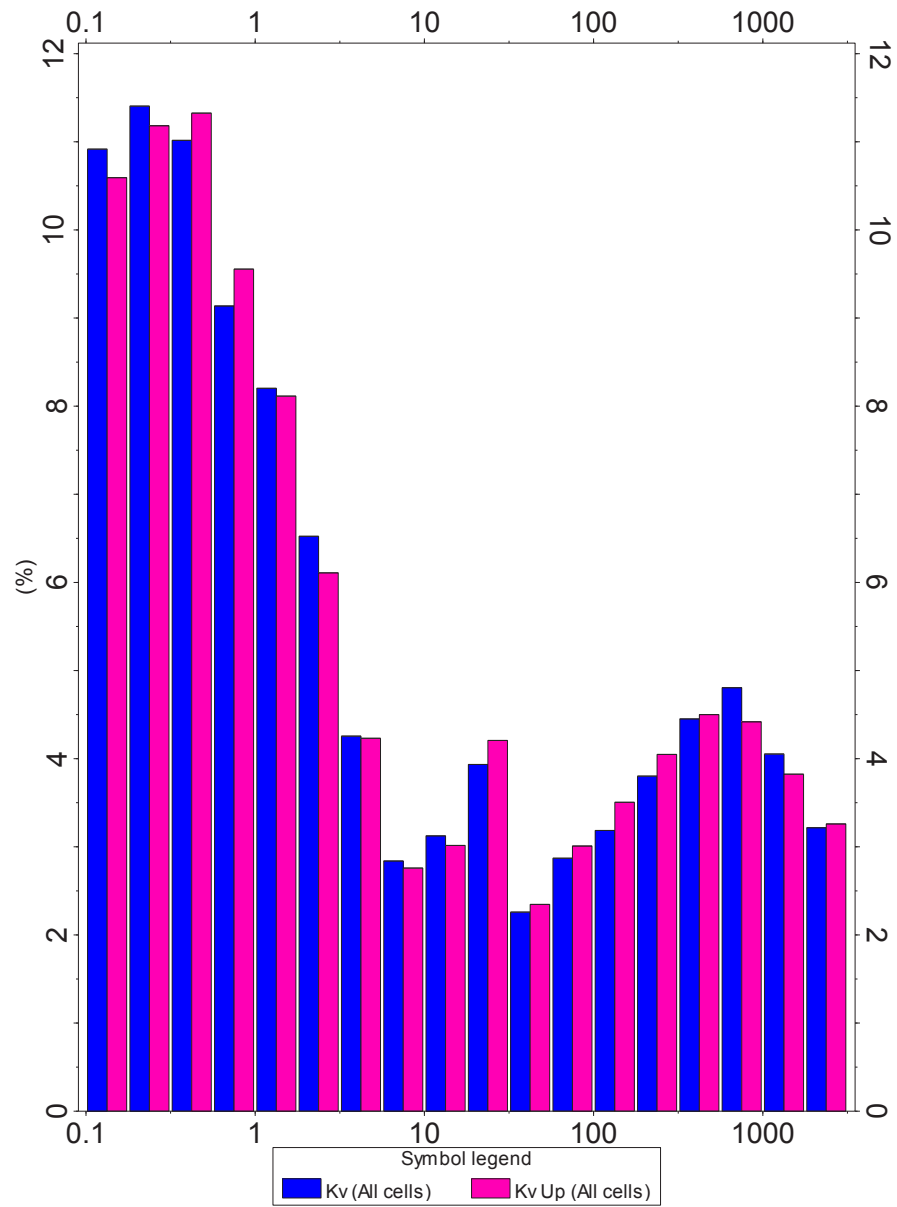


Figure 5.8b—Vertical permeability distribution histogram comparison for original and upscaled model properties. (Note: x-axis represents permeability in milliDarcy, mD.)

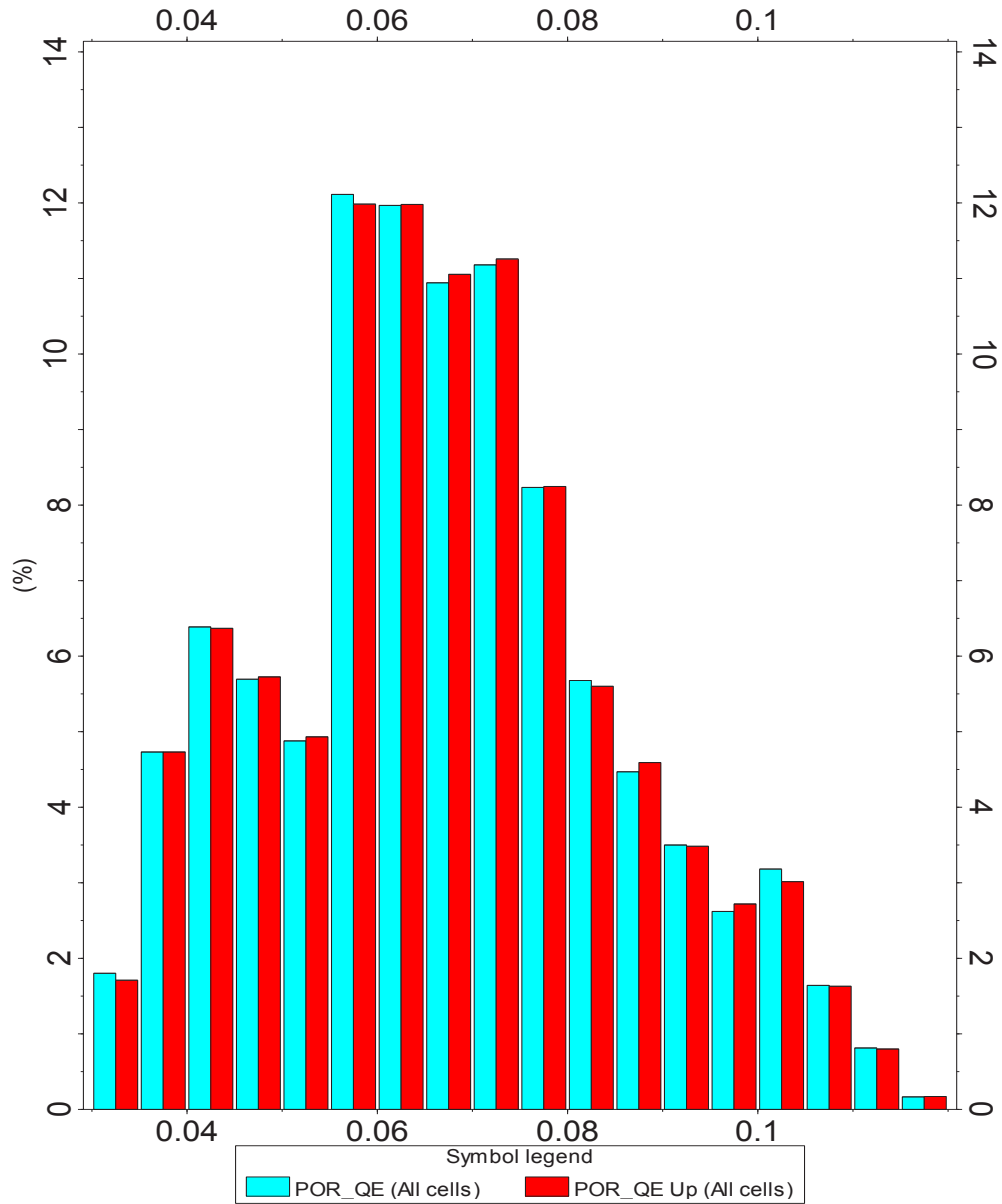


Figure 5.9—Porosity distribution histogram comparison for original and upscaled model properties. (Note: x-axis represents porosity.)

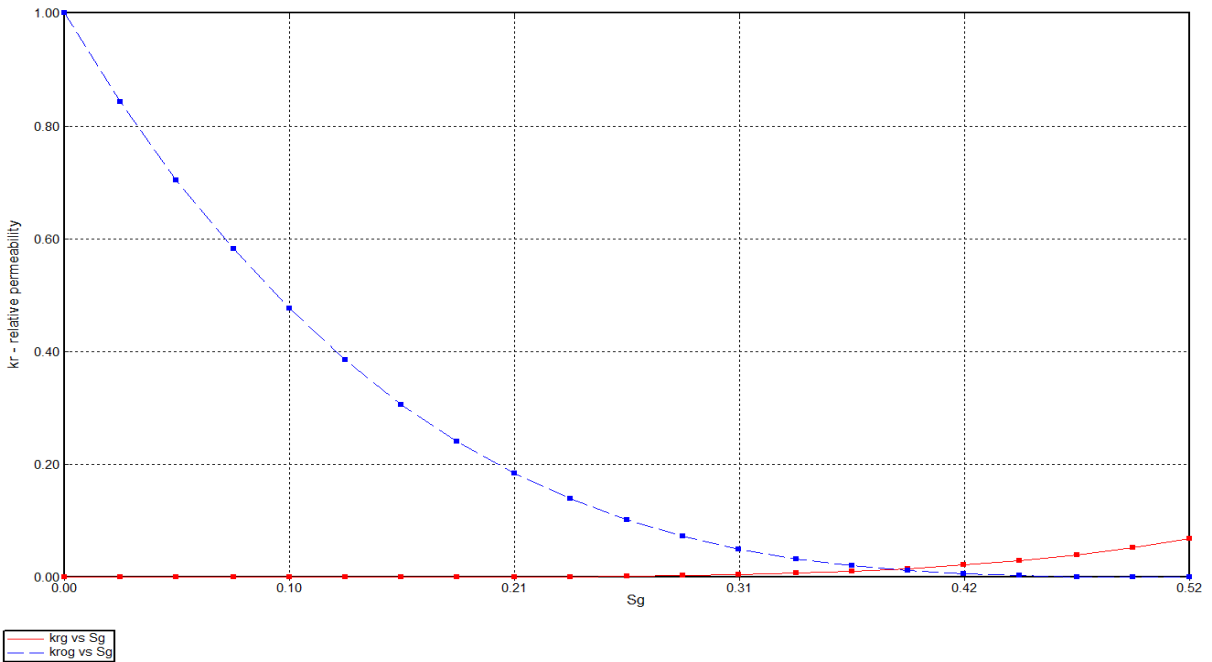
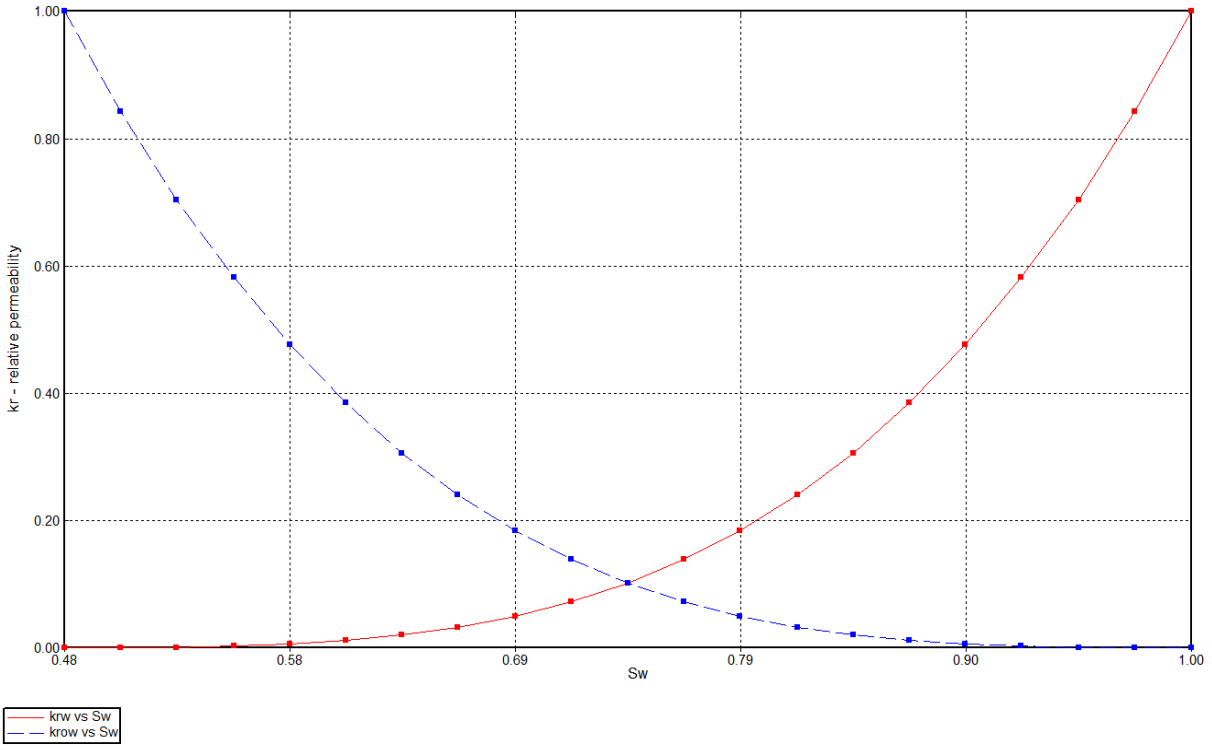


Figure 5.10—Relative permeability as a function of water and gas saturation (source: Bennion and Bachu [2007]).

Table 5.4—Model input specification and CO₂ injection rates.

Temperature	60 °C (140 °F)
Temperature Gradient	0.008 °C/ft
Pressure	2,093 psi (14.43 MPa) @ 4,960 ft RKB
Perforation Zone	4,910-5,050 ft
Perforation Length	140 ft (model layers 54 to 73)
Injection Period	9 months
Injection Rate	150 tons/day
Total CO ₂ injected	40,000 MT

5.4.5 Alternative Models

The base-case reservoir model has been carefully constructed using a sophisticated geo-model as discussed in Section 5.3, which honors site-specific hydrogeologic information obtained from laboratory tests and log-based analyses. However, to account for hydrogeologic uncertainties, a set of alternate parametric models were developed by varying the porosity and horizontal hydraulic permeability. Specifically, the porosity and permeability were increased and decreased by 25% following general industry practice (FutureGen Industrial Alliance, 2013). This resulted in nine alternative models, listed in Table 5.5. Simulation results based on all nine models were evaluated to derive the worst-case impacts on pressure and migration of the plume front for purposes of establishing the AoR and ensuring that operational constraints are not exceeded.

Table 5.5—Nine alternative permeability-porosity combination models. (Showing multiplier of base-case permeability and porosity distribution assigned to all model cells.)

Alternative Models	Base Porosity x 0.75	Base Porosity	Base Porosity x 1.25
Base Permeability x 0.75	K-0.75/Phi-0.75	K-0.75/Phi-1.0	K-0.75/Phi-1.25
Base Permeability	K-1.0/Phi-0.75	K-1.0/Phi-1.0	K-1.0/Phi-1.25
Base Permeability x 1.25	K-1.25/Phi-0.75	K-1.25/Phi-1.0	K-1.25/Phi-1.25

5.4.6 Reservoir Simulation Results

For the simulations, 40,000 metric tons (MT) of CO₂ were injected into the KGS 1-28 well at a constant rate of approximately 150 tons per day for a period of nine months. A total of nine

models representing three sets of alternate permeability-porosity combinations as specified in Table 5.5 were simulated with the objective of bracketing the range of expected pressures and extent of CO₂ plume migration.

The extent of lateral plume migration depends on the particular combination of permeability-porosity in each of the nine alternative models. These two parameters are independently specified in CMG as they are assumed to be decoupled. A high-permeability value results in farther travel of the plume due to gravity override, buoyancy, and updip migration. Similarly, a low effective porosity for the same value of permeability results in farther travel for the plume as compared to high porosity as the less-connected pore volume results in faster pore velocity. The high-permeability/low-porosity combination (k-1.25/phi-0.75) resulted in the largest horizontal plume dimension. In contrast, the highest induced pressures were obtained for the alternative model with the lowest permeability and the lowest porosity (k-0.75/phi-0.75). The results for these alternative models are discussed below along with the base-case model (k-1.0/phi-1.0).

5.4.6.1 CO₂ Plume Migration

Figure 5.11a–f shows the maximum lateral migration of the CO₂ plume in the injection interval (elevation 5,010 ft) for the largest areal migration case (k-1.25/phi-0.75). The plume grows rapidly during the injection phase (Figure 5.11a–c) and is largely stabilized by the end of the first year (Figure 5.11d). The plume at the end of 100 years (Figure 5.11f) has spread only minimally since cessation of injection and has a maximum lateral spread of approximately 1,750 ft from the injection well. It does not intercept any well other than the proposed Arbuckle monitoring well KGS 2-28, which as documented in Section 10, will be constructed in compliance with Class VI injection well guidelines.

The evolution of the maximum lateral extent of the plume is shown in Figure 5.12 for the maximum plume spread case (k-1.25/phi-0.75) along with the base case (k-1.0/phi-1.0) and the maximum pressure case (k-0.75/phi-0.75). As can be inferred from the plot, the extent of maximum lateral migration is fairly similar for all three cases, and the plume has largely stabilized

within three months of cessation of injection for all three cases.

The CO₂ plumes discussed above represent CO₂ in both the dissolved and free phases. The lighter free-phase CO₂, which could potentially rise to the USDW if any hypothetical vertical pathways were present inside the plume boundary, has a slightly smaller footprint, as shown in Figures 5.13a–f, which depicts the evolution of the free-phase plume from commencement of injection to 100 years after injection stops. The free-phase plume grows rapidly during the injection period and then continues growing gradually thereafter. The free-phase plume, however, is always contained within the total CO₂ plume (i.e., CO₂ in the dissolved and free phases). The stabilized free-phase plume at 100 years is shown in Figure 5.13g along with the total CO₂ plume at 100 years. The free-phase plume has a maximum lateral extent of approximately 1,700 ft and is contained within the total CO₂ plume. The plume only intercepts the proposed Arbuckle monitoring well KGS 2-28, which will be built to be in compliance with Class VI design and construction requirements. There are no additional natural or artificial penetrations that will allow CO₂ to escape upward into the USDW.

The extent of vertical plume migration for the fast vertical migration case ($k=1.25/\phi=0.75$) is also shown in Figures 5.11a–g and 5.13 a–g. Both the dissolved and the free-phase plumes remain confined in the injection interval (lower Arbuckle) because of the presence of the low-permeability baffle zones above the injection interval. This same information is shown in Figure 5.14, which shows the maximum extent of vertical migration for the base case and two alternative cases discussed above. For all three cases, the plume remains confined in the injection interval in the lower Arbuckle.

The simulation results discussed above are expected to represent conservative estimates of plume migration. This is because the present CMG simulations neglects mineral sequestration trapping and capillary forces. The effects of capillary forces, however, were studied in preliminary modeling exercises and were found to have a negligible effect on reservoir pore pressure response and extent of CO₂ lateral movement. Additionally, the modeling results presented in this document do not simulate convection cells, which as demonstrated recently by Pau et al. (2010) can greatly

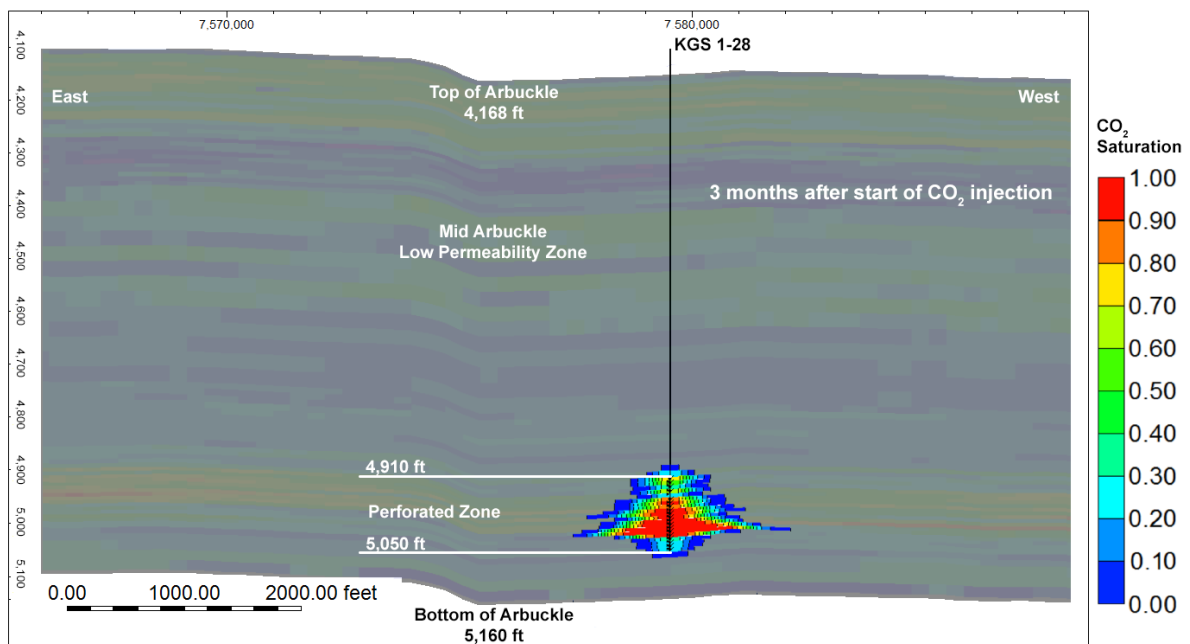
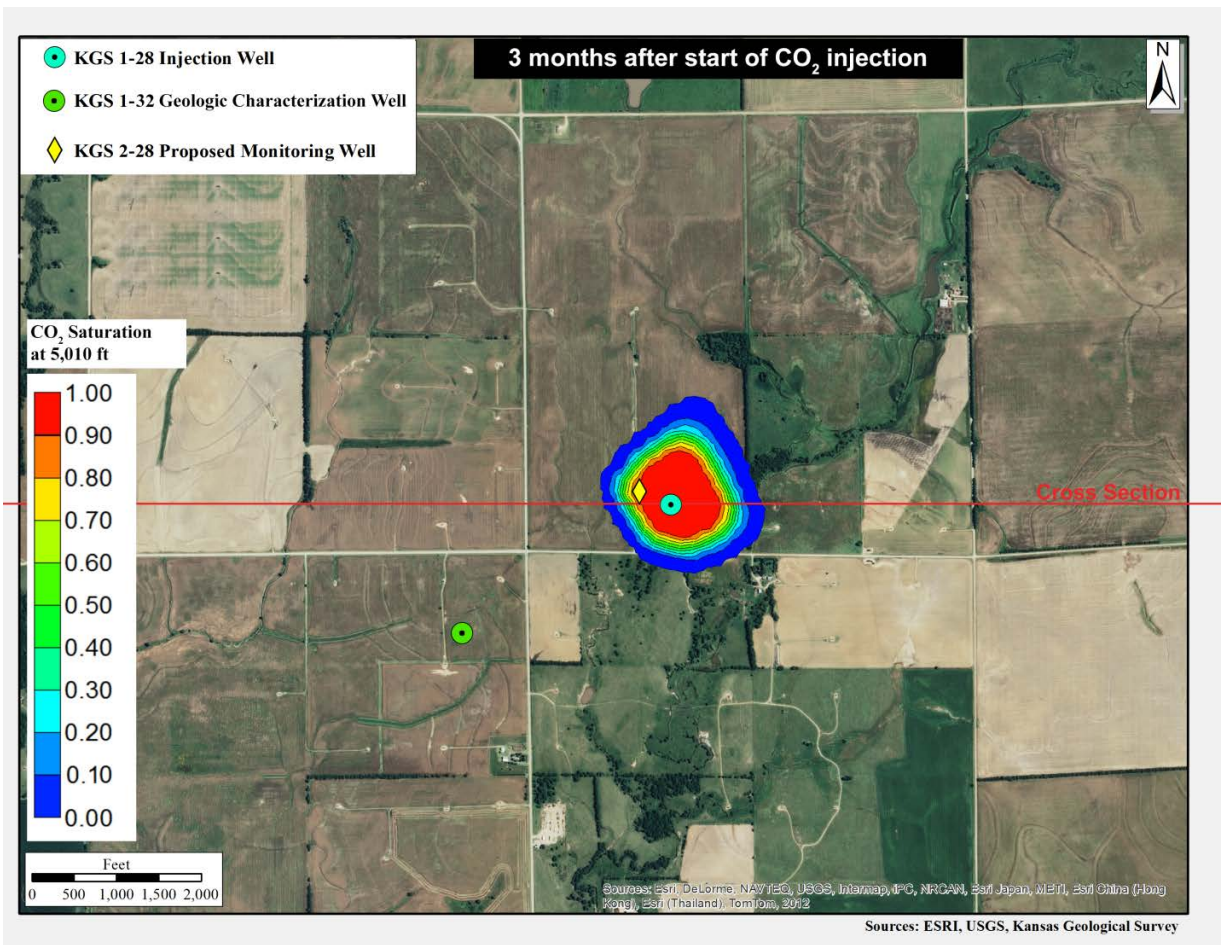


Figure 5.11a—CO₂ plume in aerial and cross-sectional view in the injection interval for the largest plume migration alternative model ($k=1.25/\phi=0.75$) at three months from start of injection. Background represents horizontal permeability distribution.

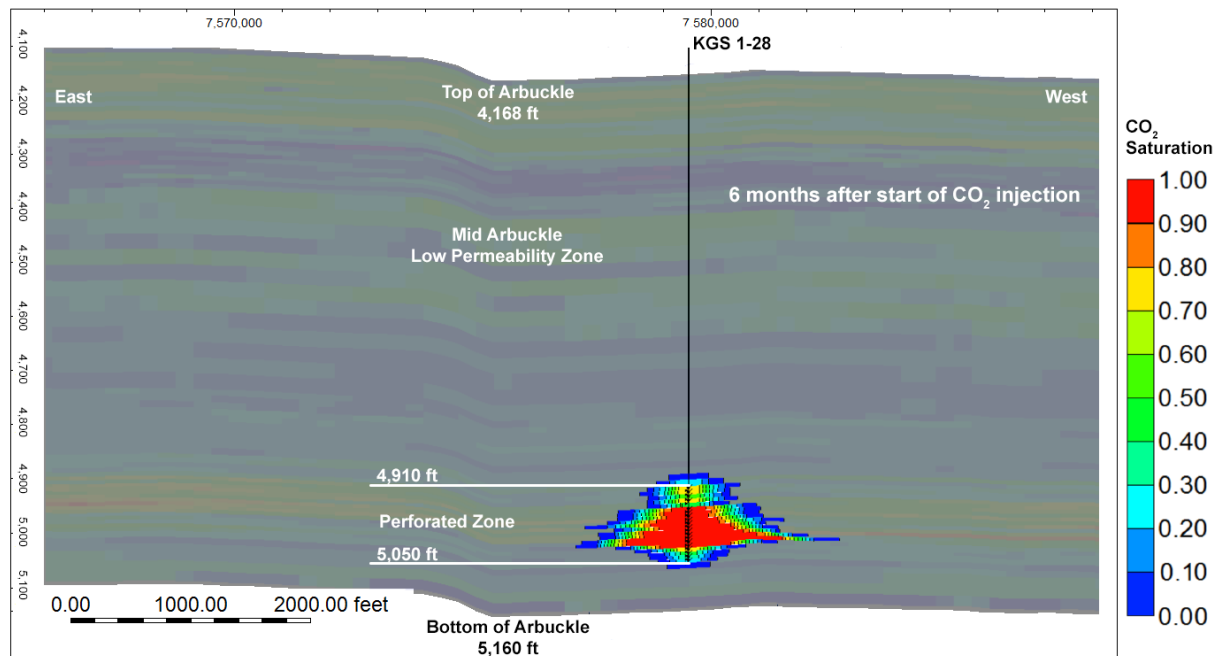
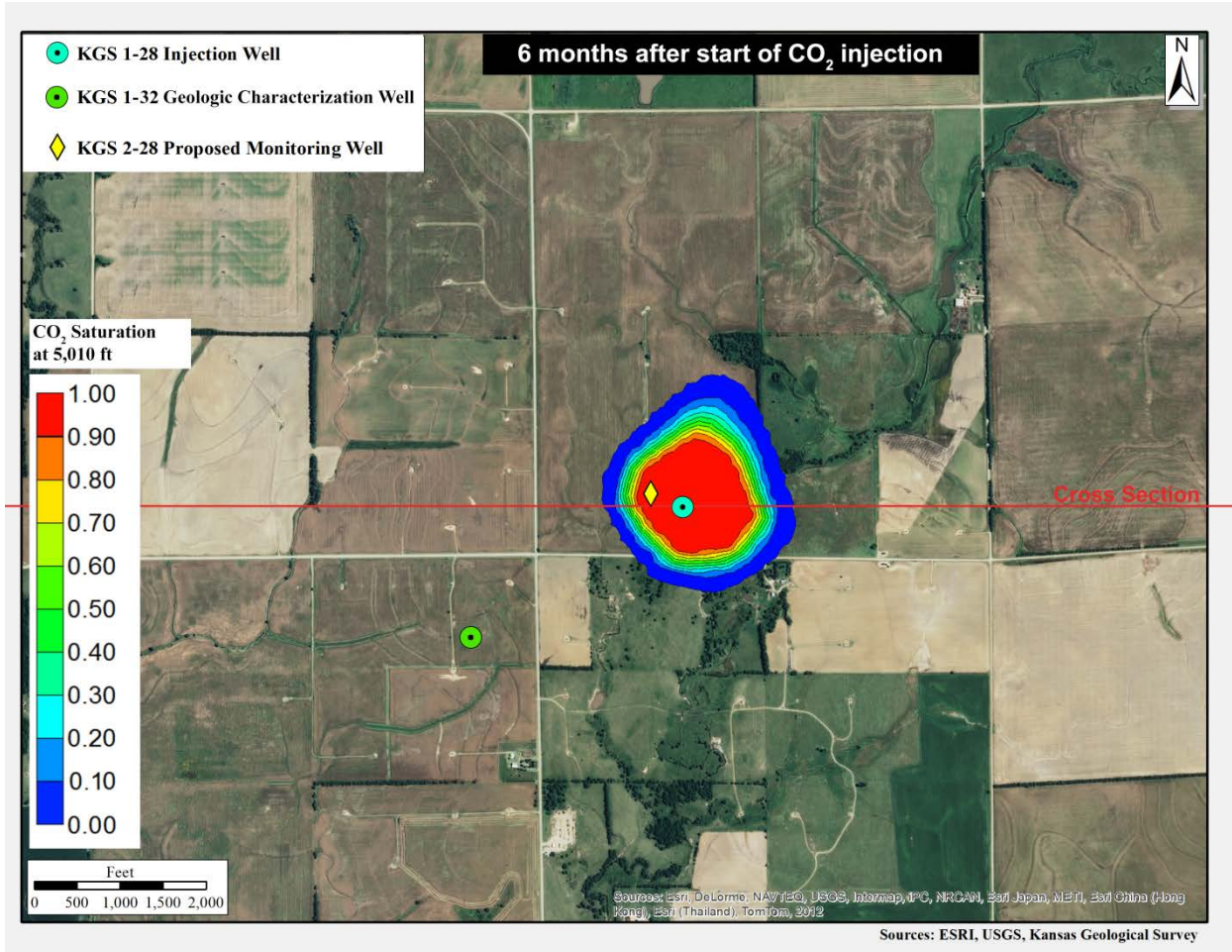


Figure 5.11b—CO₂ plume in aerial and cross-sectional view in the injection interval for the largest plume migration alternative model ($k=1.25/\phi=0.75$) at six months from start of injection.

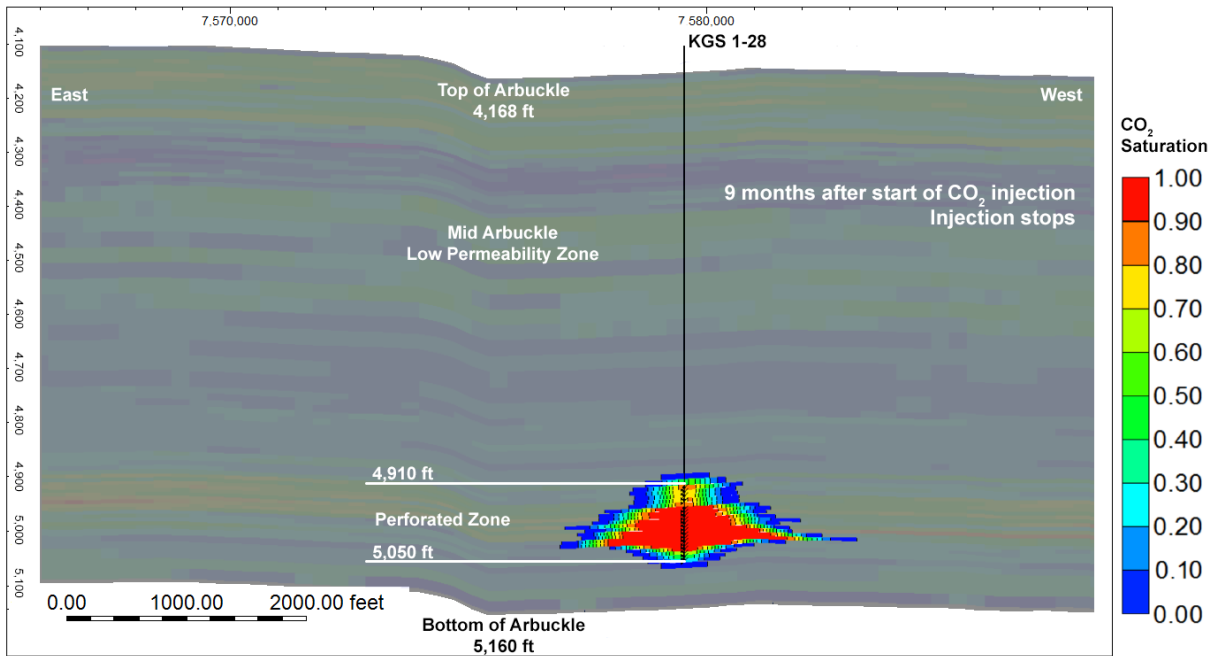
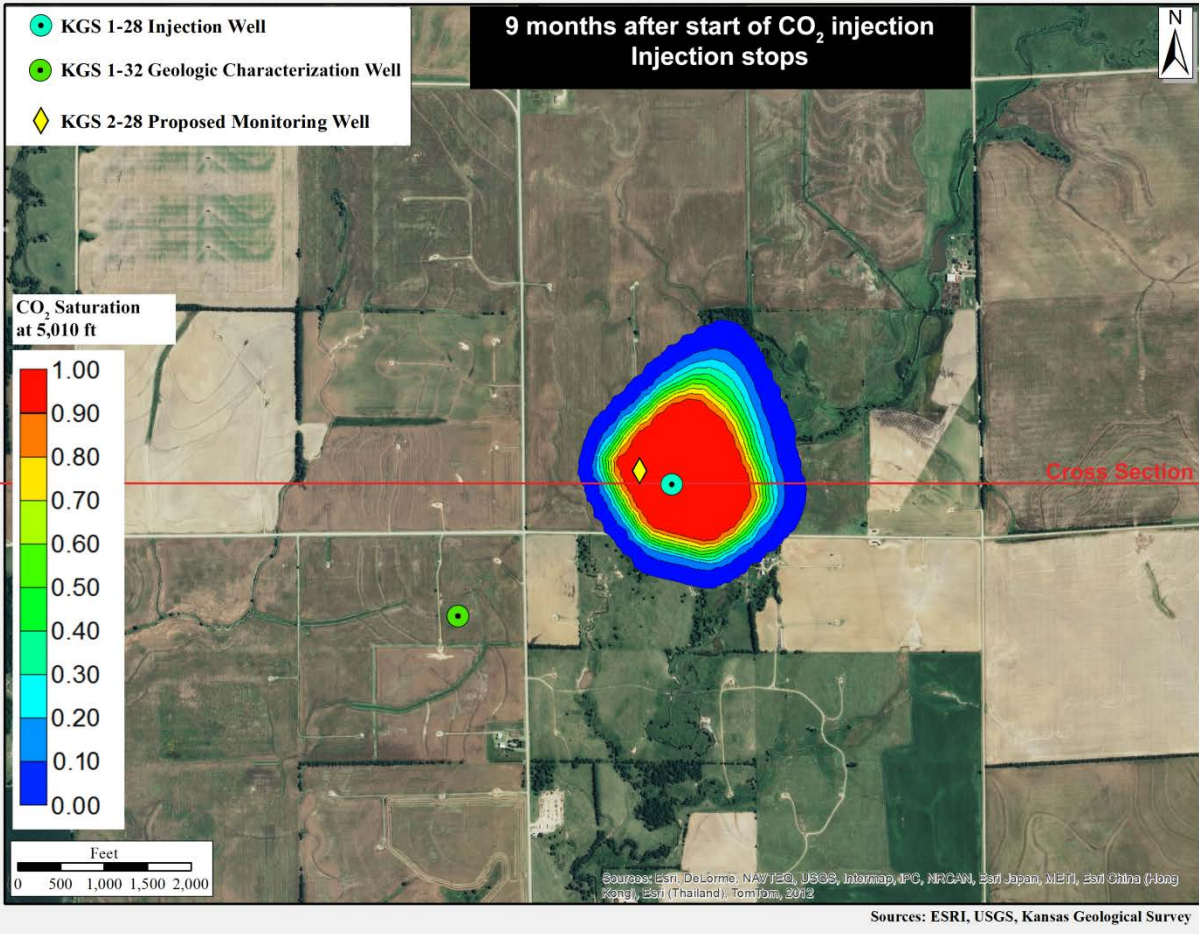


Figure 5.11c—CO₂ plume in aerial and cross-sectional view in the injection interval for the largest plume migration alternative model ($k=1.25/\phi=0.75$) at nine months from start of injection.

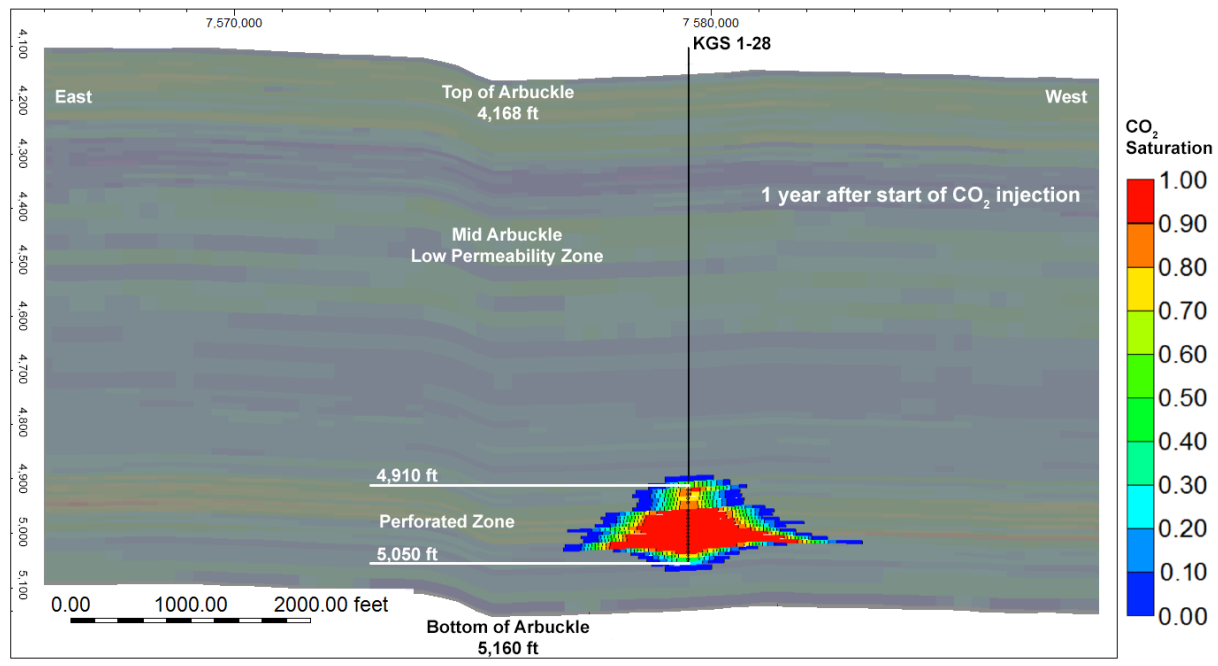
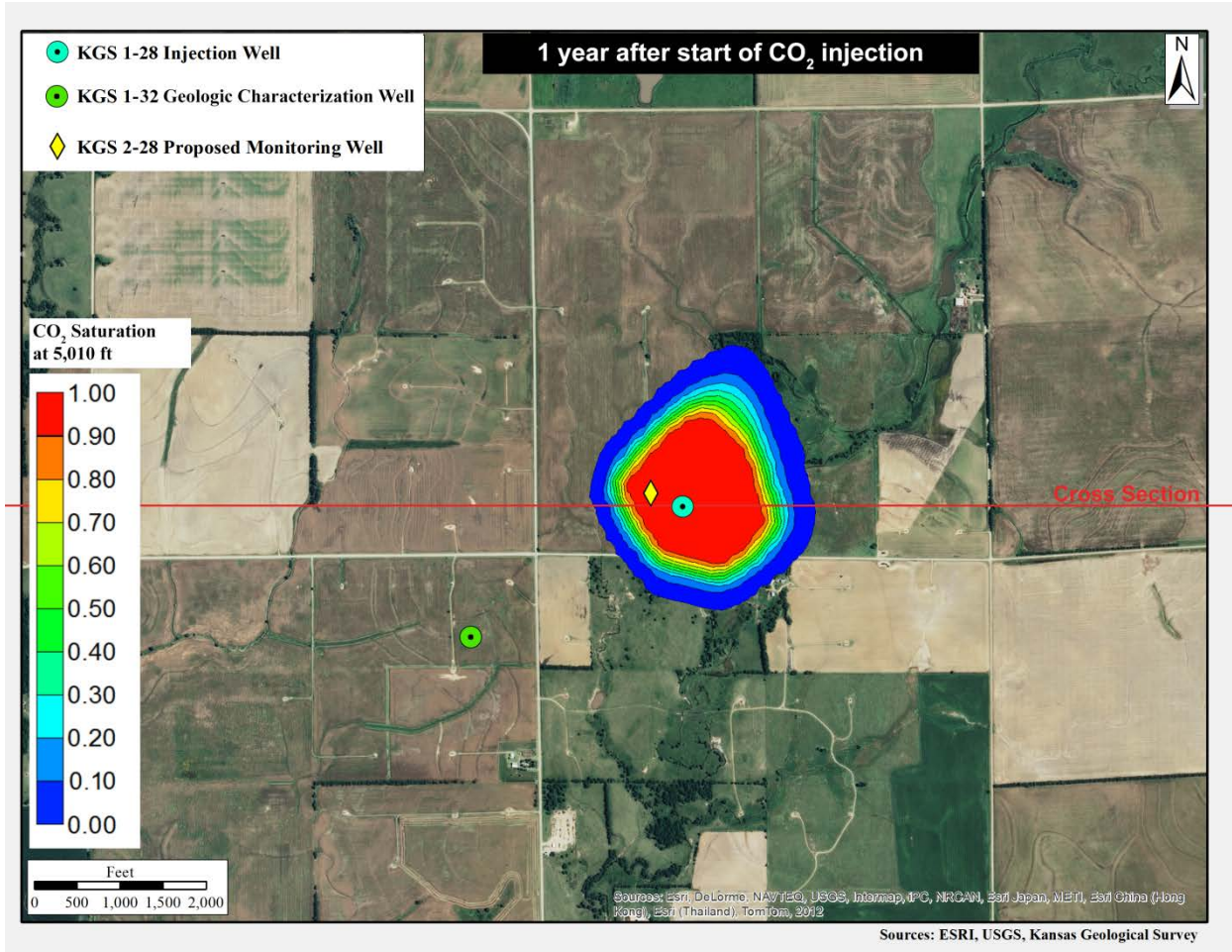


Figure 5.11d—CO₂ plume in aerial and cross-sectional view in the injection interval for the largest plume migration alternative model ($k=1.25/\phi=0.75$) at one year from start of injection.

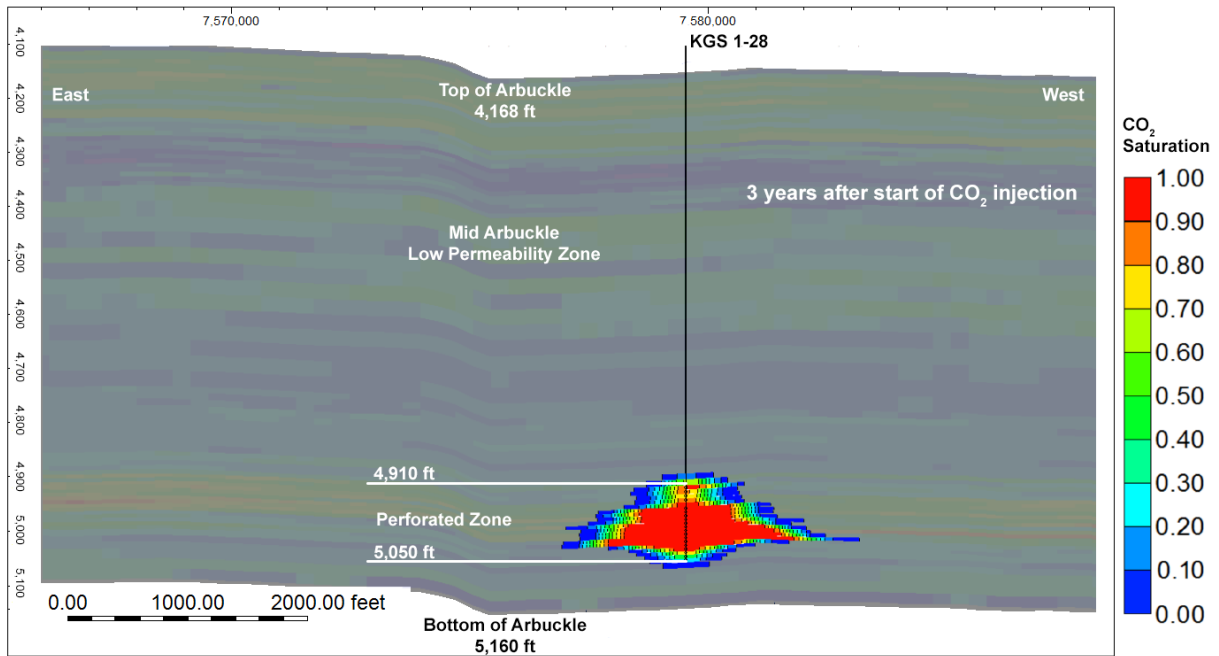
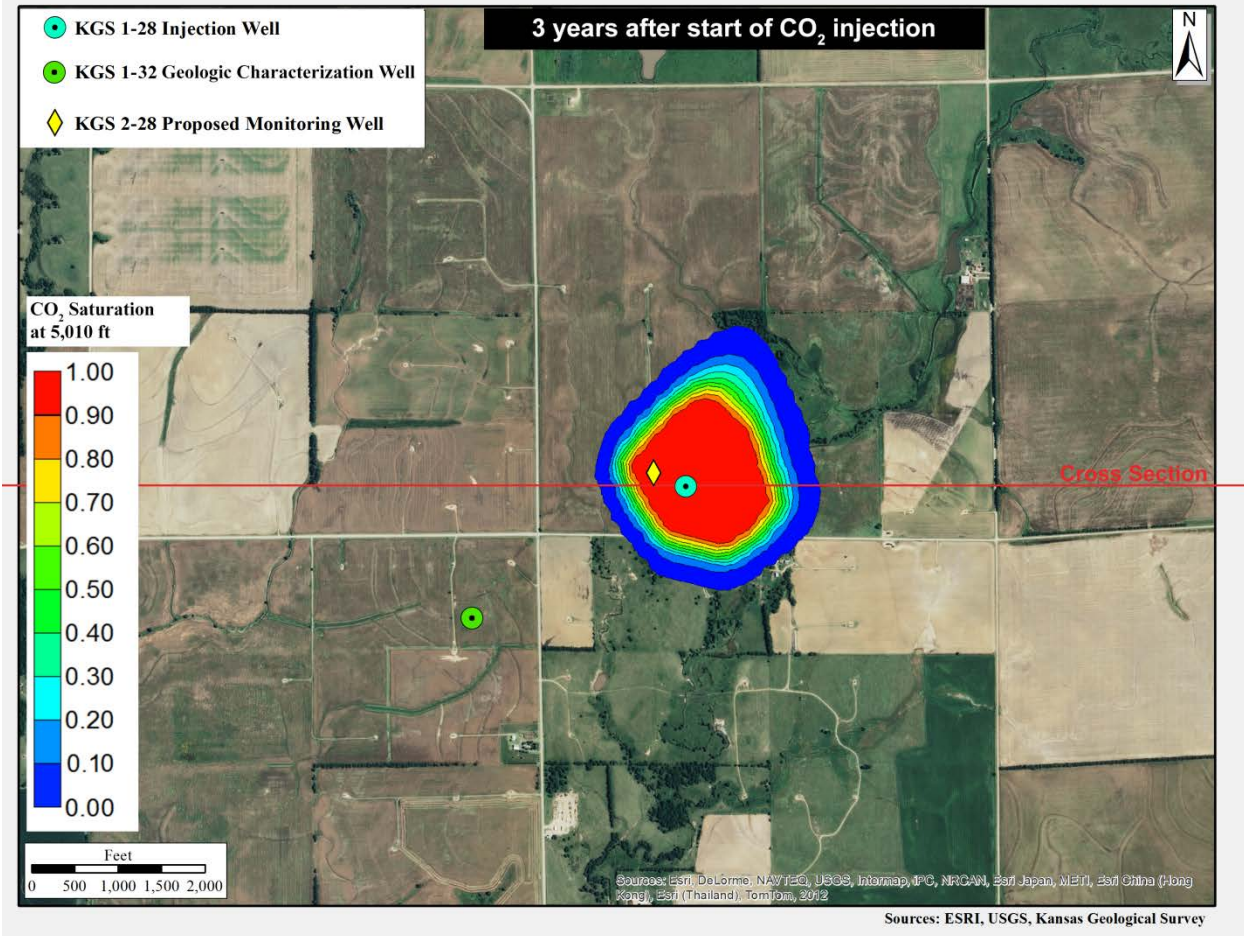


Figure 5.11e—CO₂ plume in aerial and cross-sectional view in the injection interval for the largest plume migration alternative model ($k=1.25/\phi=0.75$) at three years from start of injection.

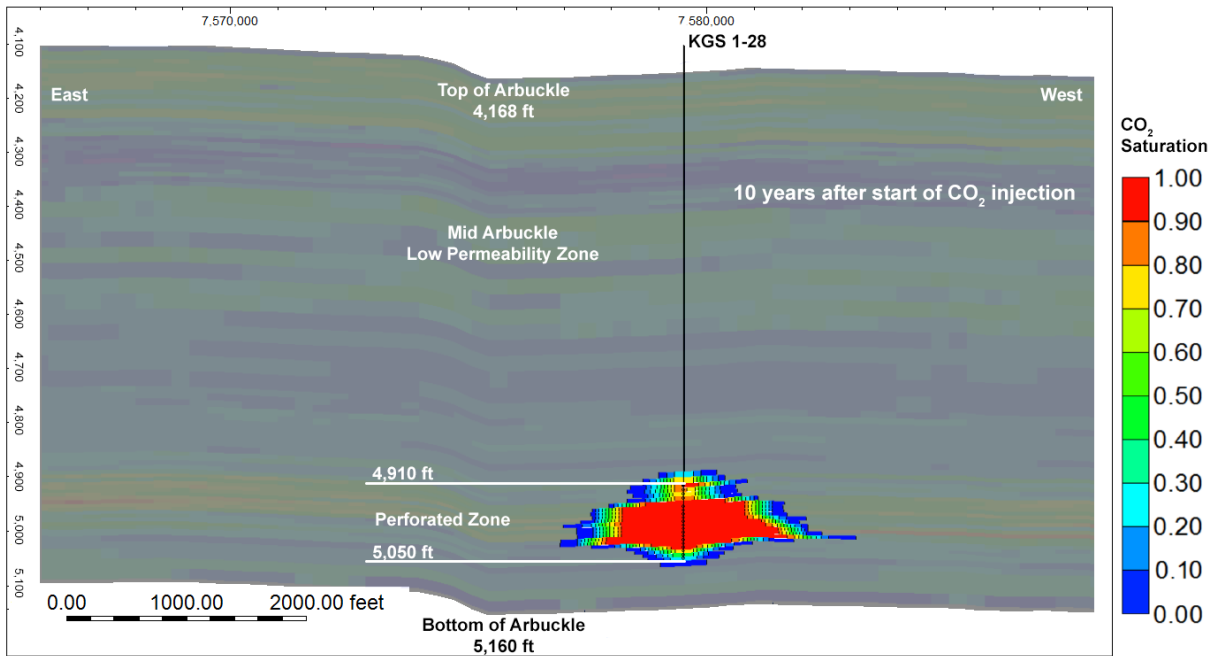
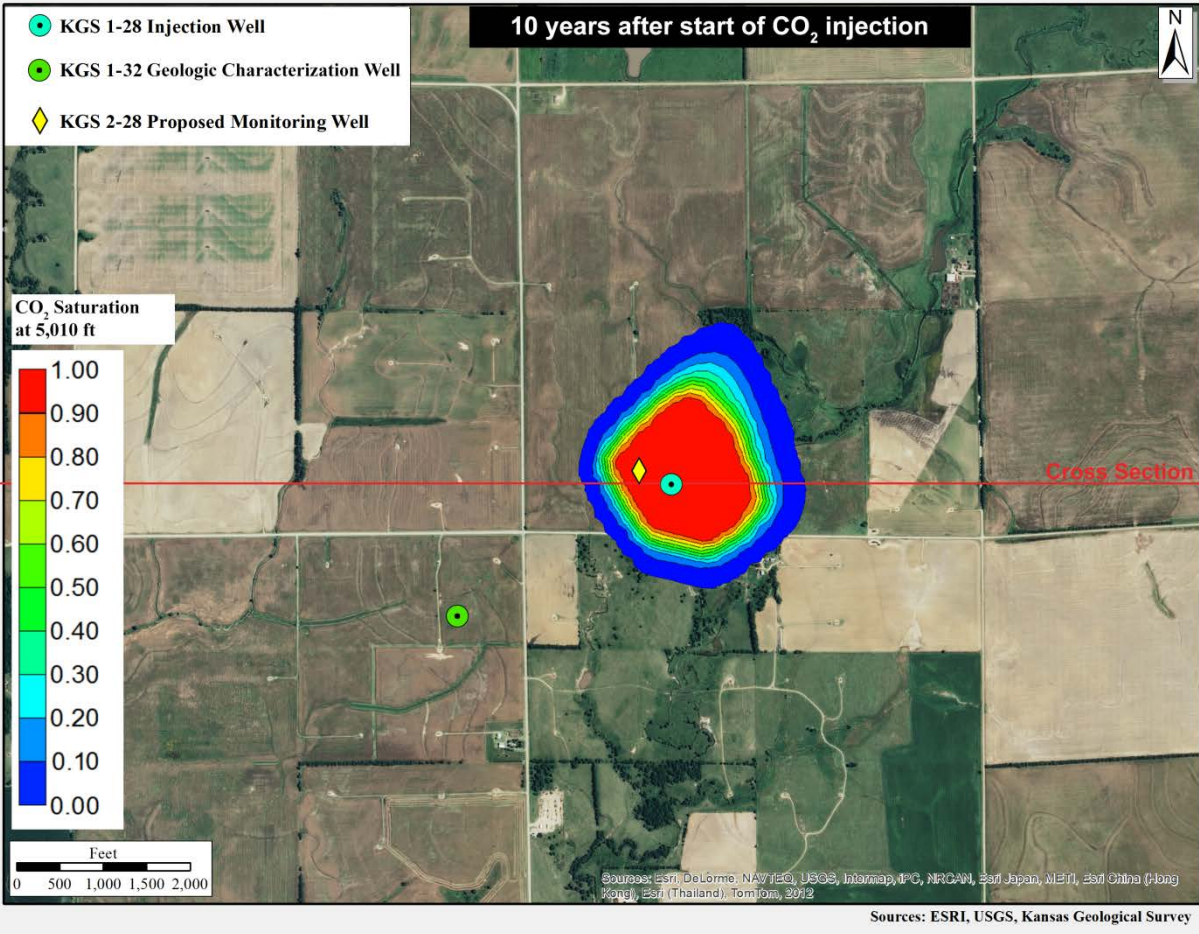
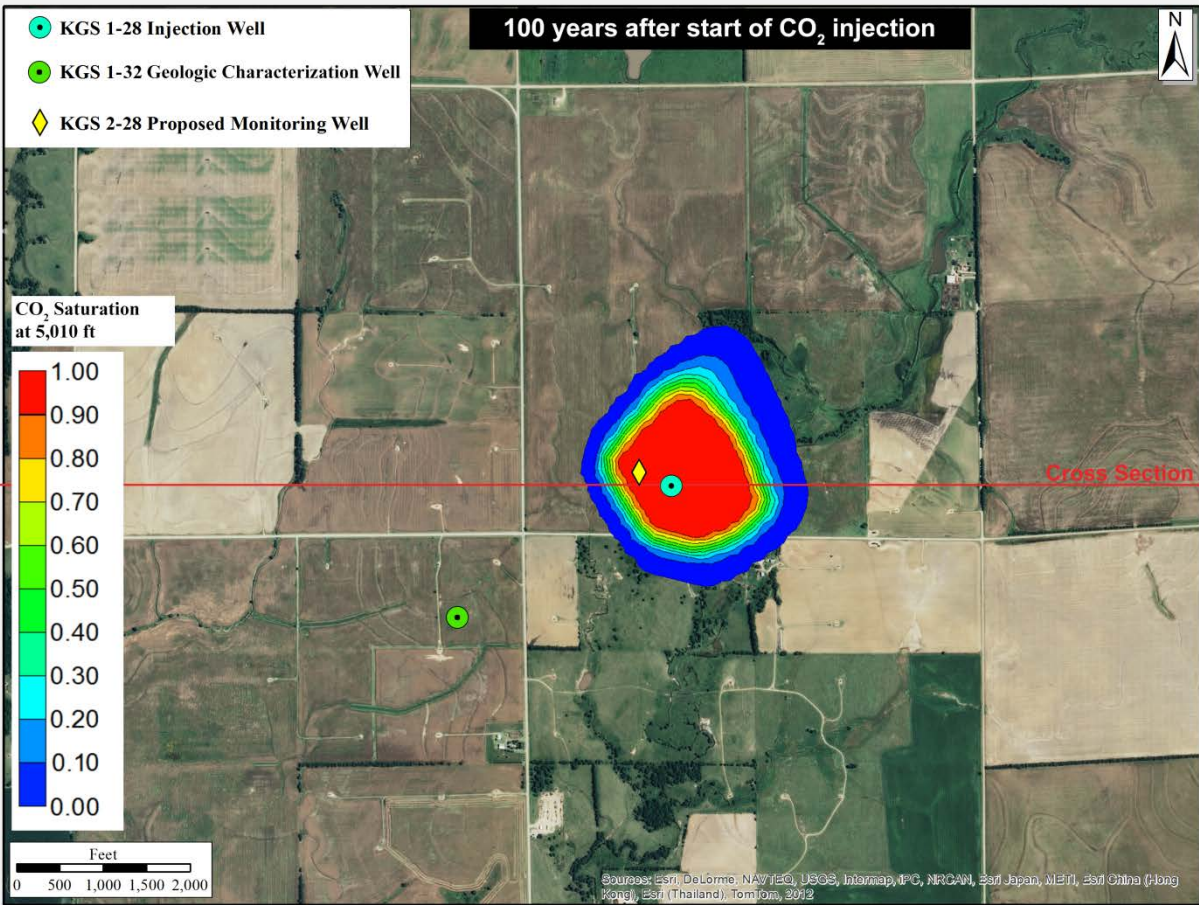


Figure 5.11f—CO₂ plume in aerial and cross-sectional view in the injection interval for the largest plume migration alternative model ($k=1.25/\phi=0.75$) at 10 years from start of injection.



Sources: ESRI, USGS, Kansas Geological Survey

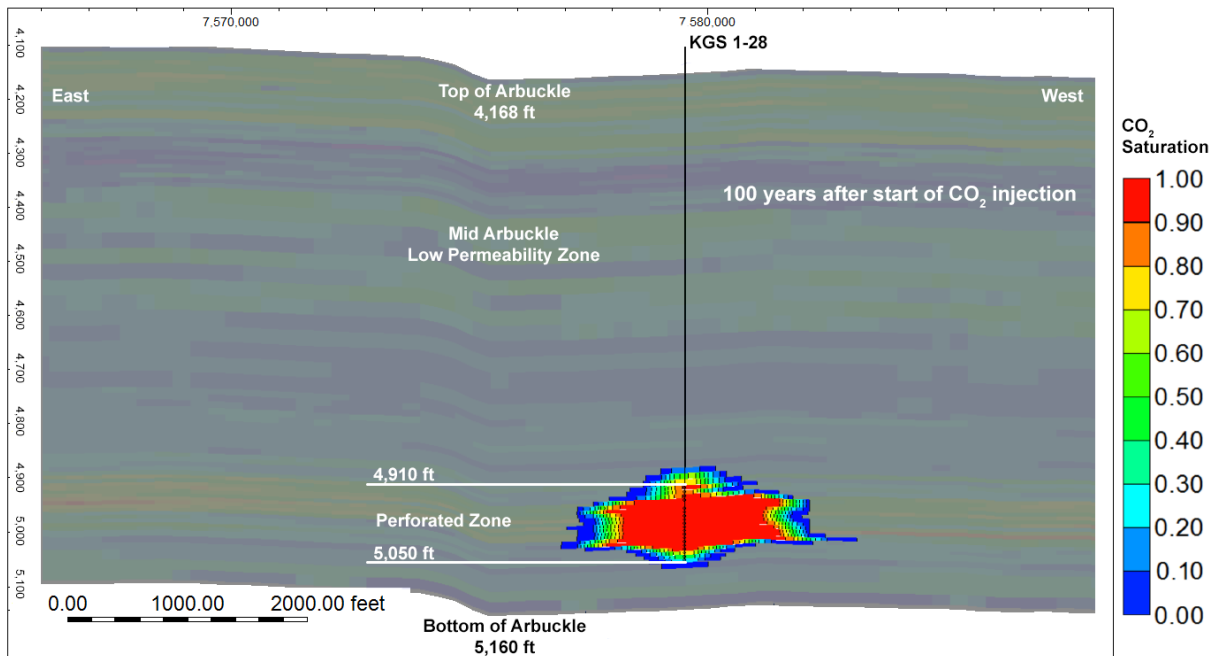


Figure 5.11g—CO₂ plume in aerial and cross-sectional view in the injection interval for the largest plume migration alternative model ($k=1.25/\phi=0.75$) at 100 years from start of injection.

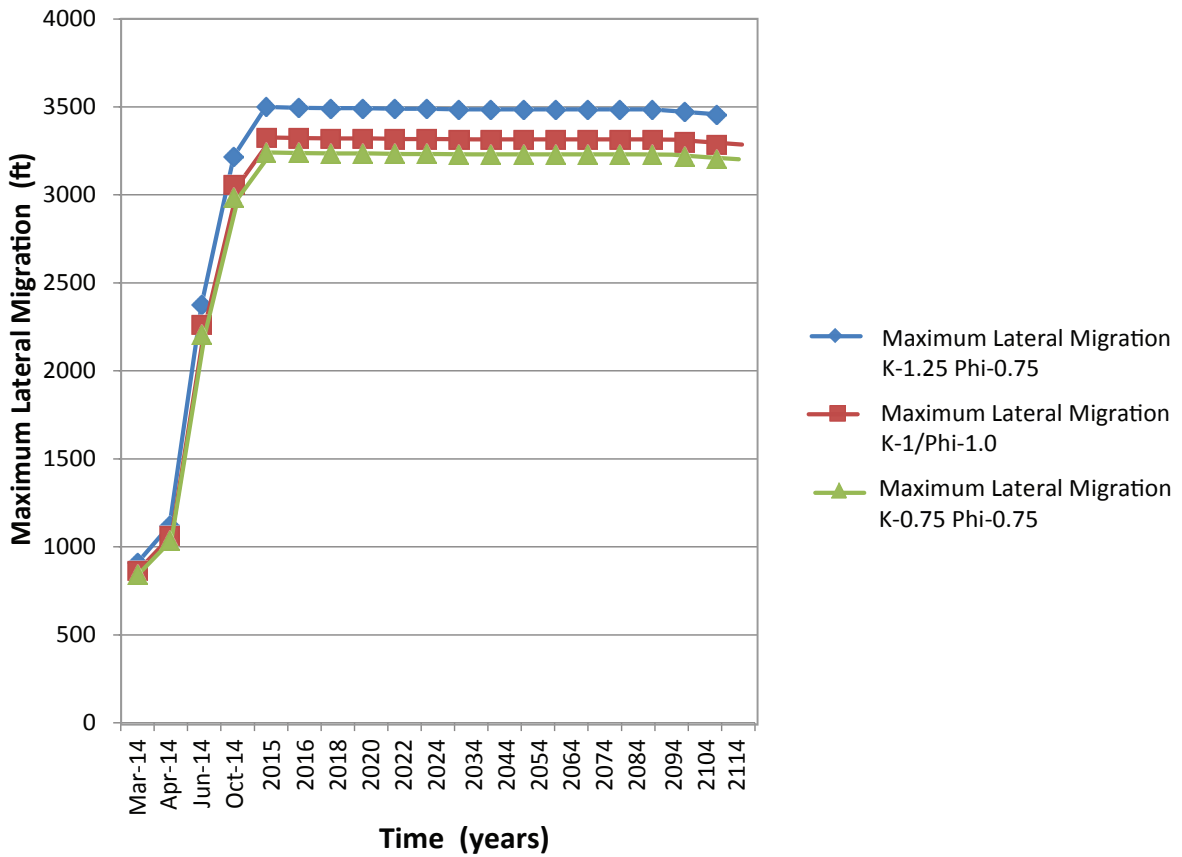


Figure 5.12—Maximum lateral extent of CO₂ plume migration (as defined by the 1% CO₂ saturation isoline) for the base case and for the two alternative models, which represent the maximum extent of plume and pressure-front migration.

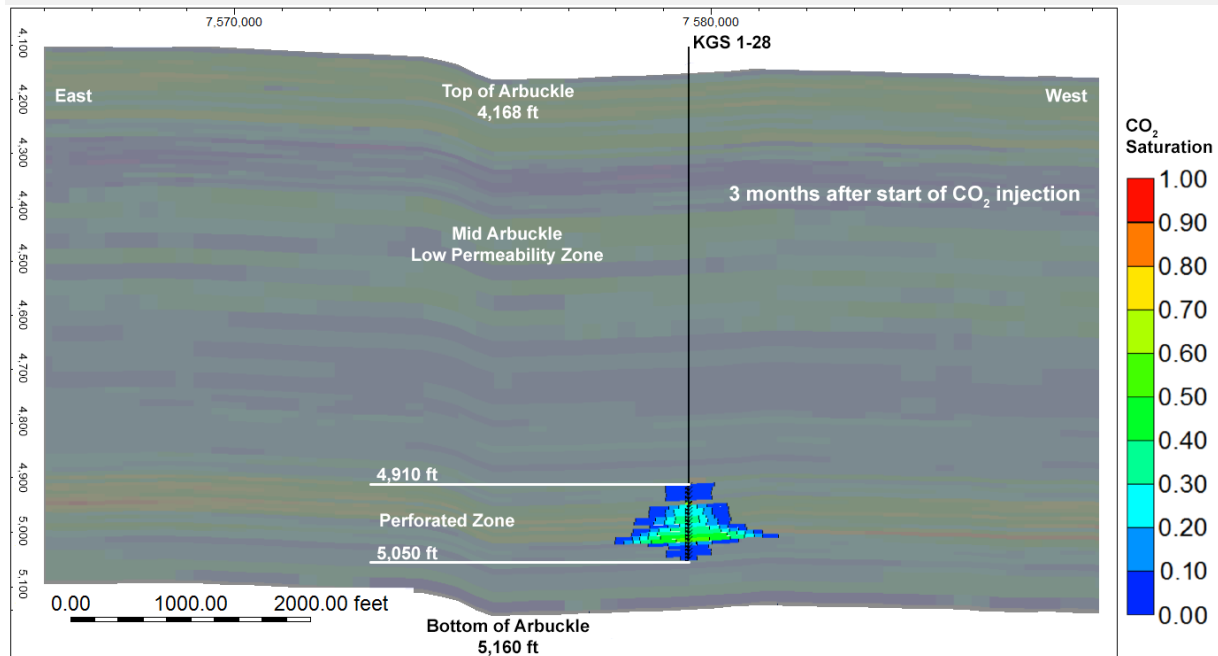
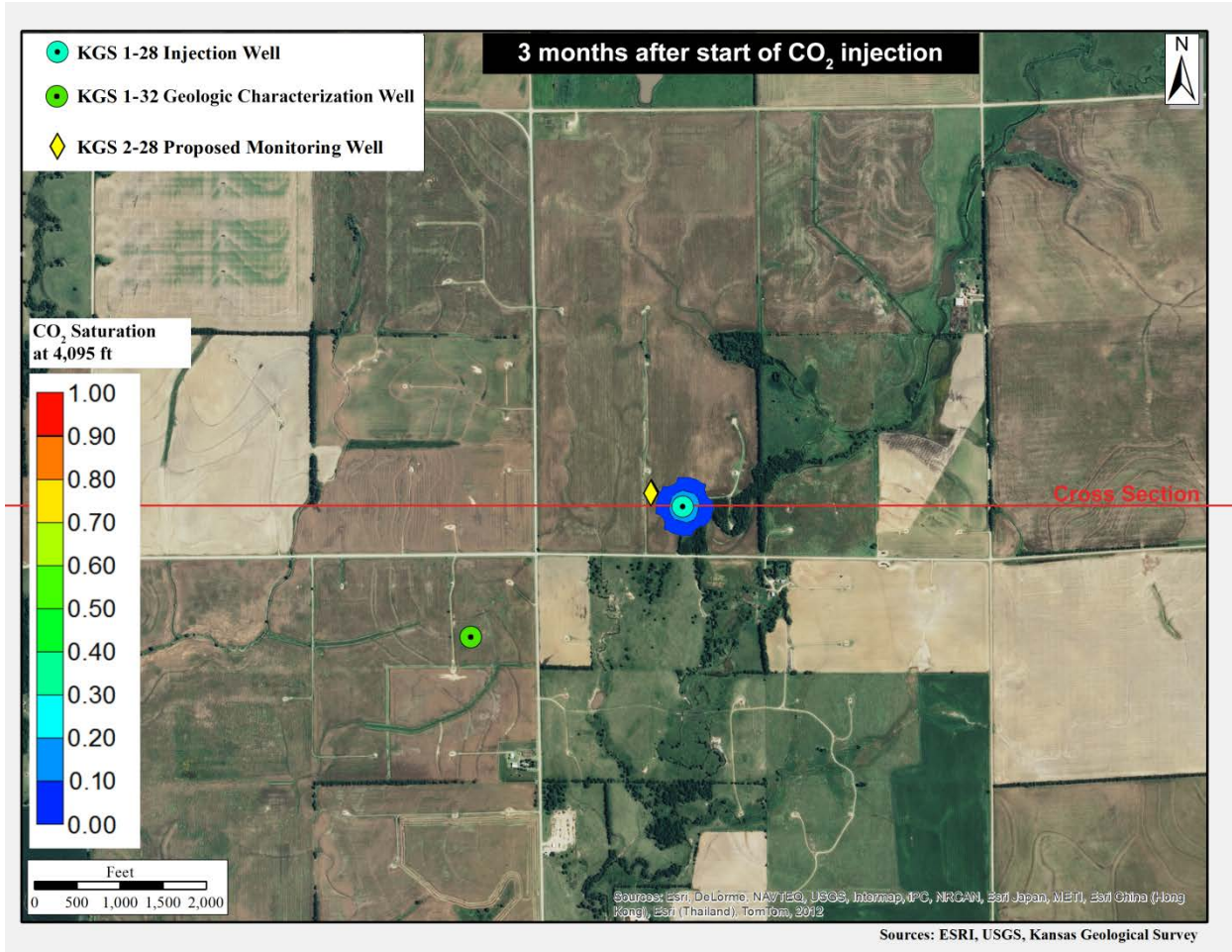


Figure 5.13a—Free-phase CO₂ plume in aerial and cross-sectional view for the largest migration alternative model ($k=1.25/\phi=0.75$) at three months from start of injection.

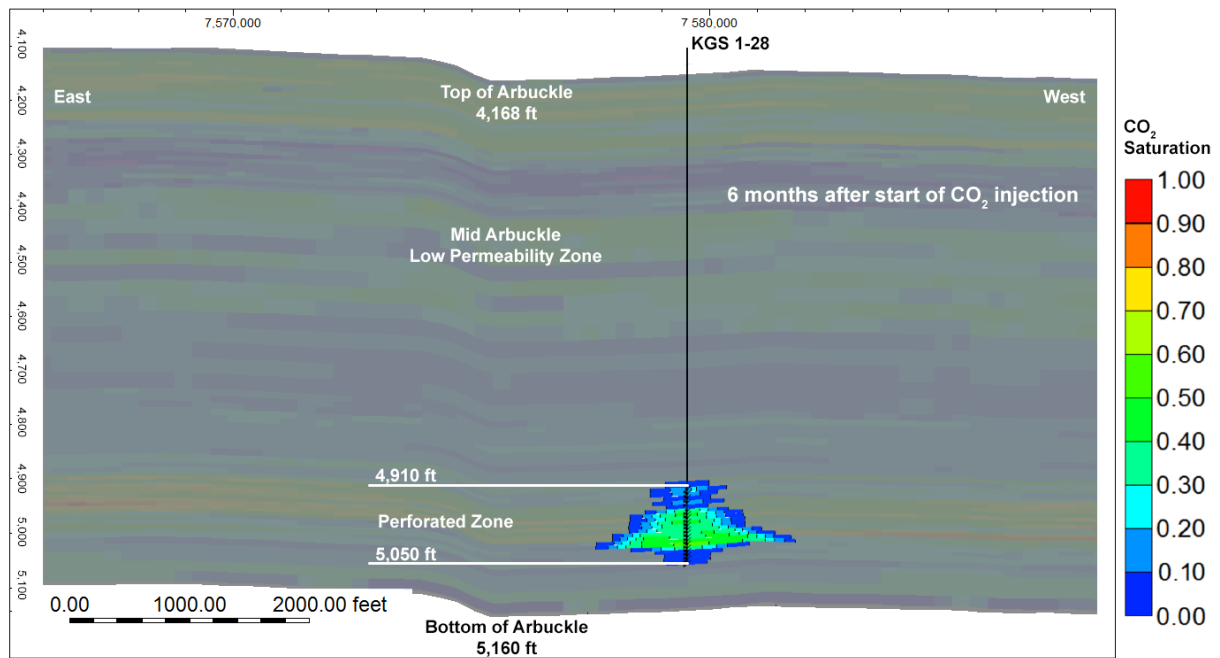
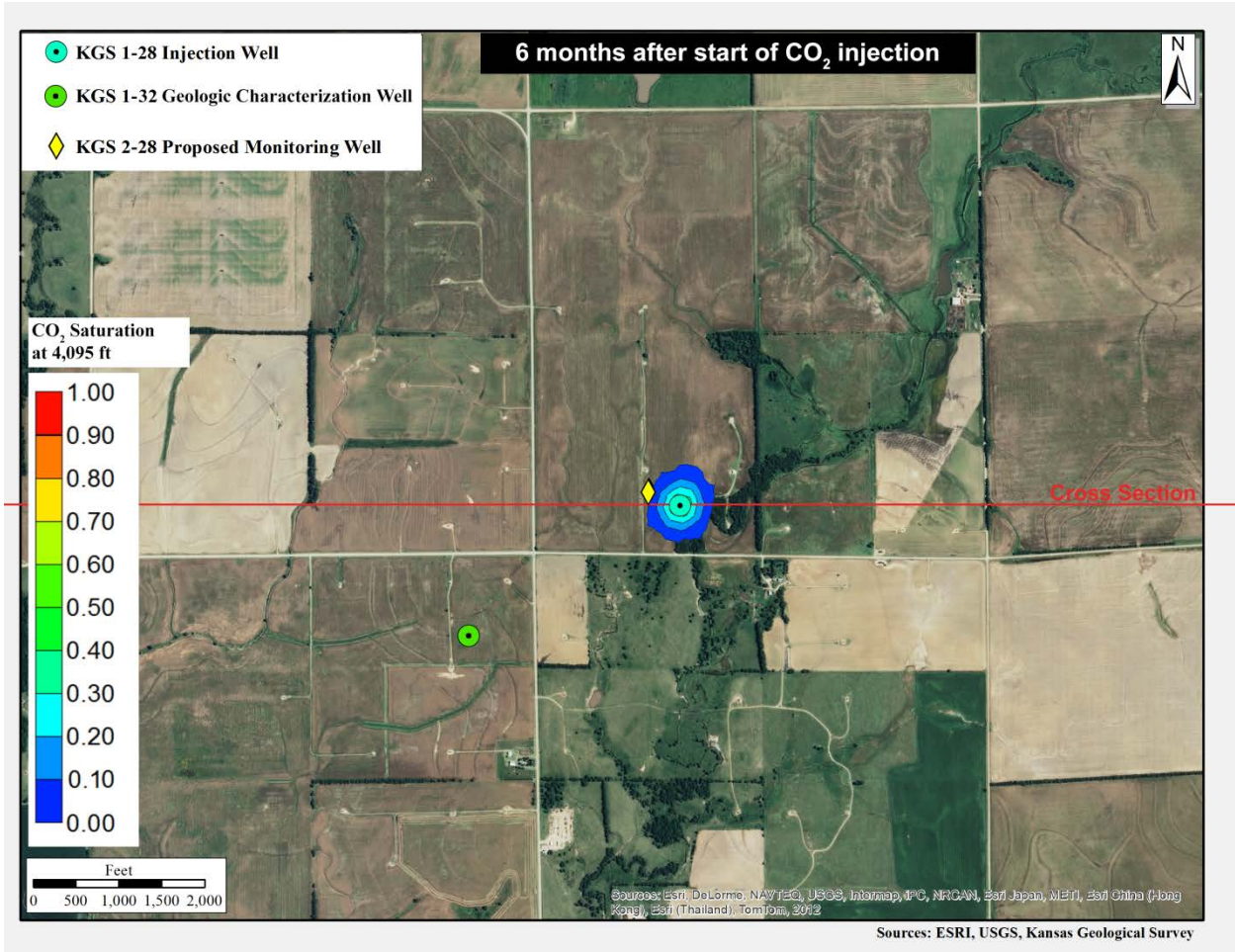


Figure 5.13b—Free-phase CO₂ plume in aerial and cross-sectional view for the largest migration alternative model ($k=1.25/\phi=0.75$) at six months from start of injection.

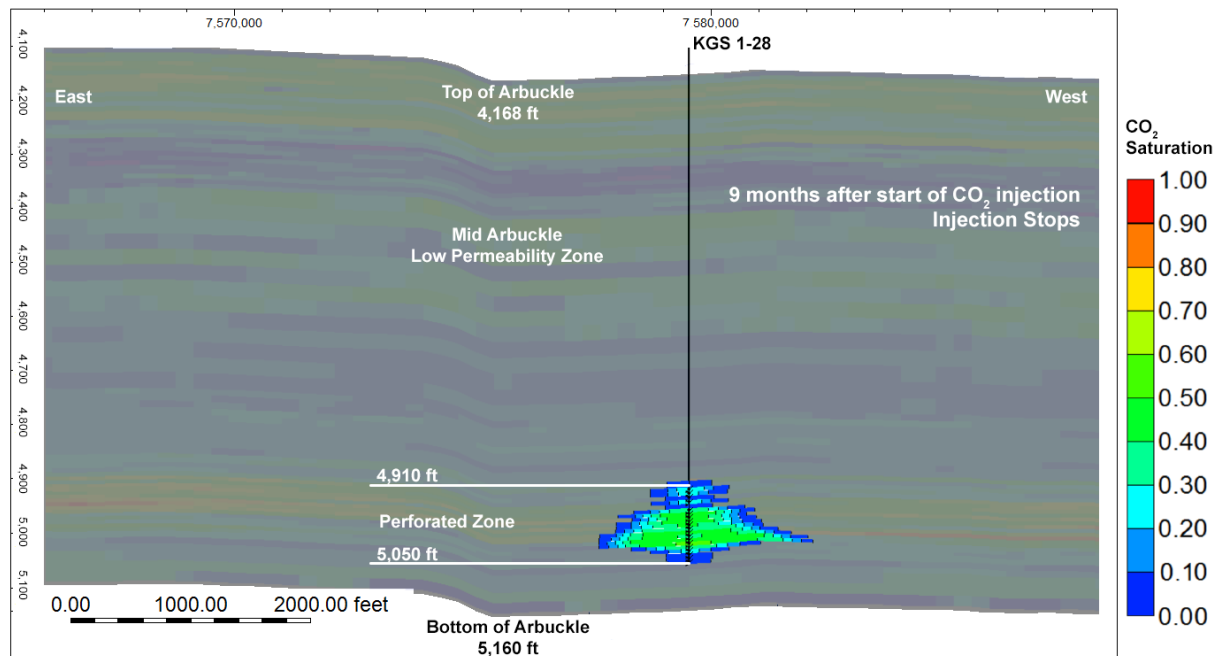
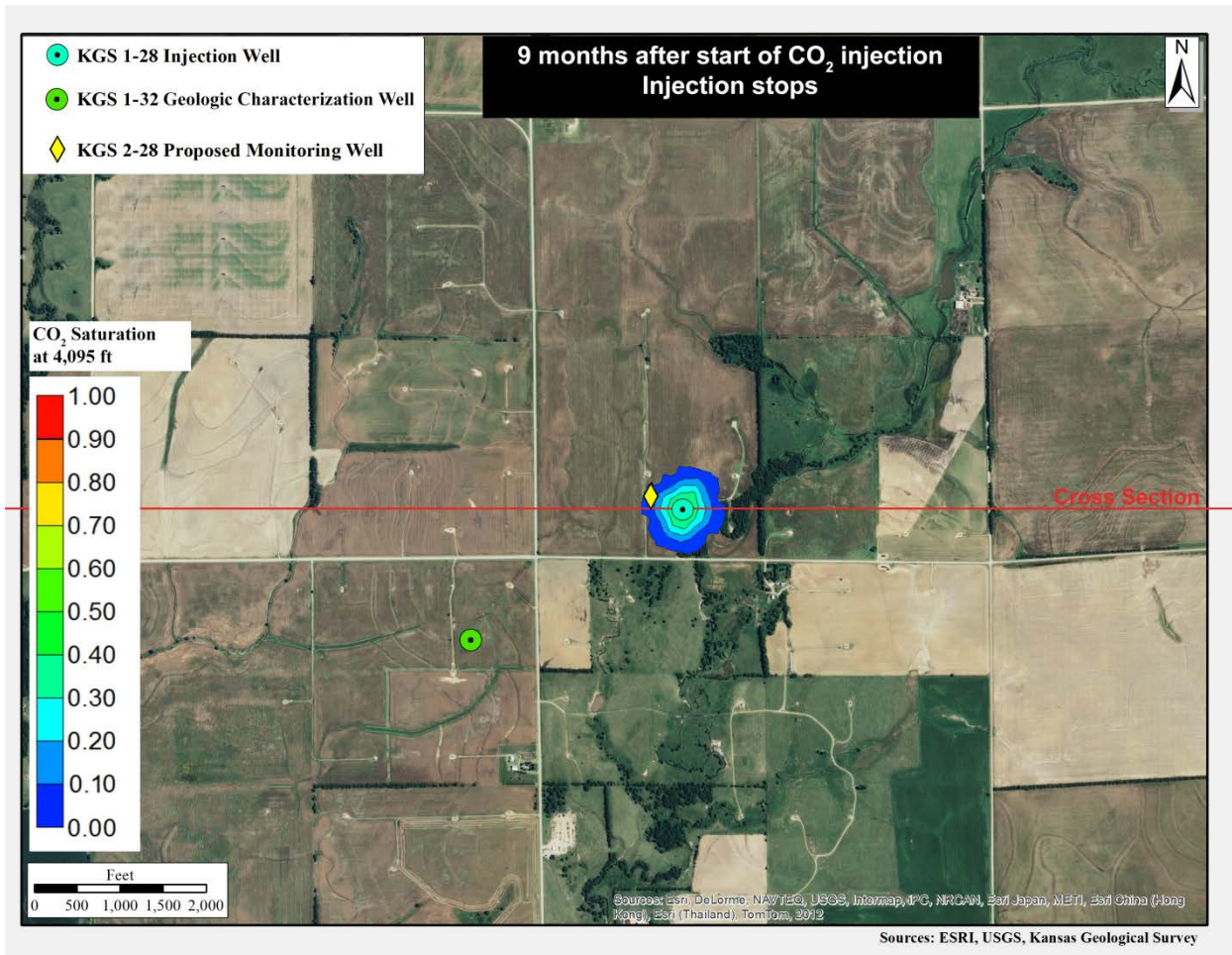


Figure 5.13c—Free-phase CO₂ plume in aerial and cross-sectional view for the largest migration alternative model ($k=1.25/\phi=0.75$) at nine months from start of injection.

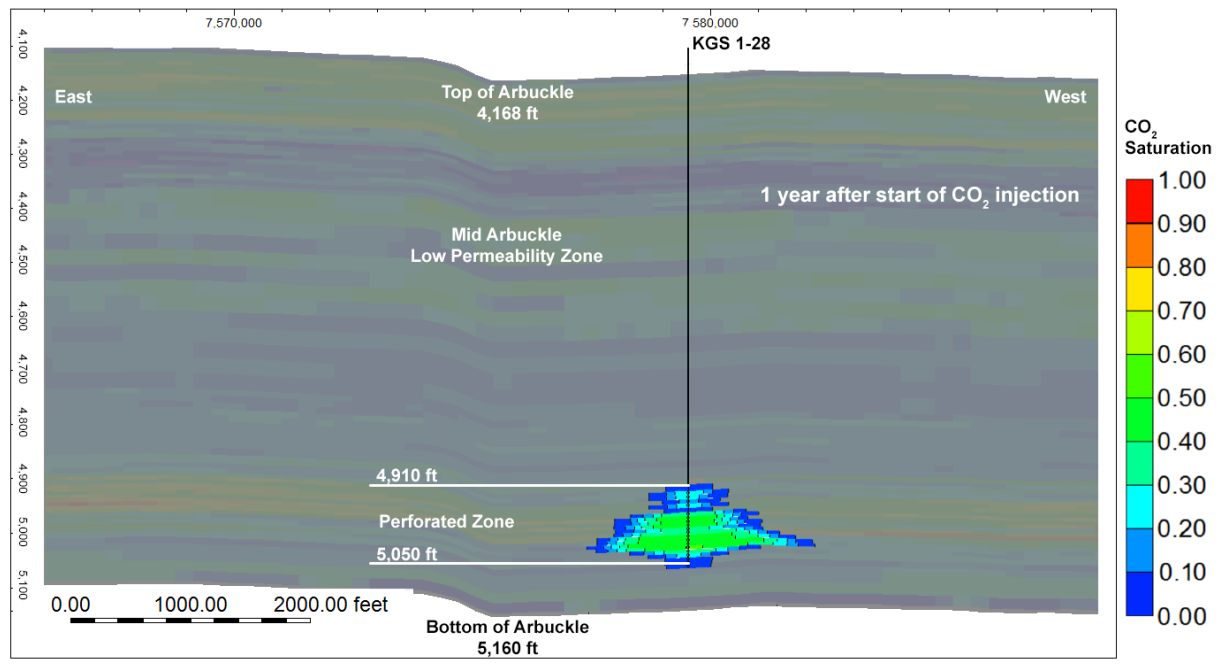
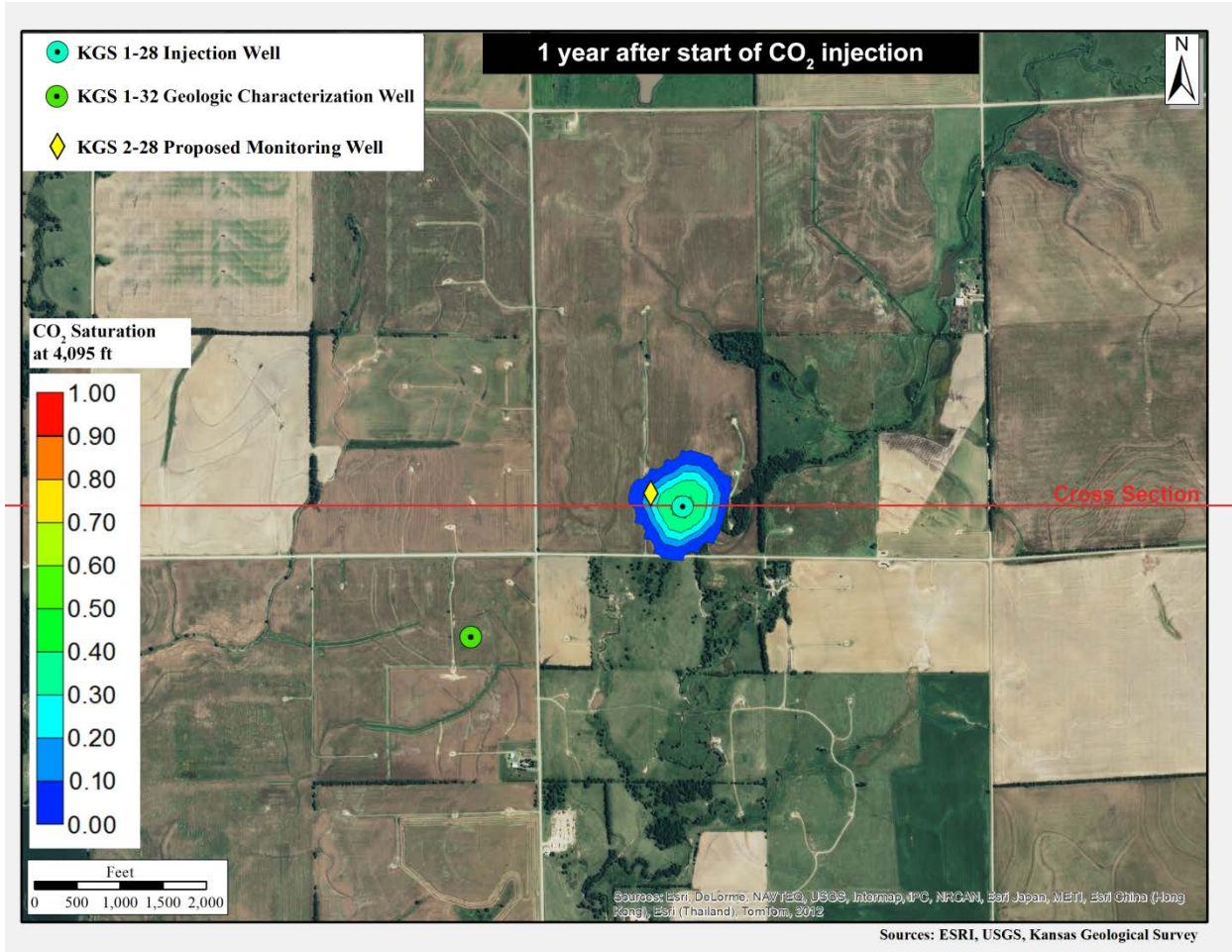


Figure 5.13d—Free-phase CO₂ plume in aerial and cross-sectional view for the largest migration alternative model ($k-1.25/\phi-0.75$) at one year from start of injection.

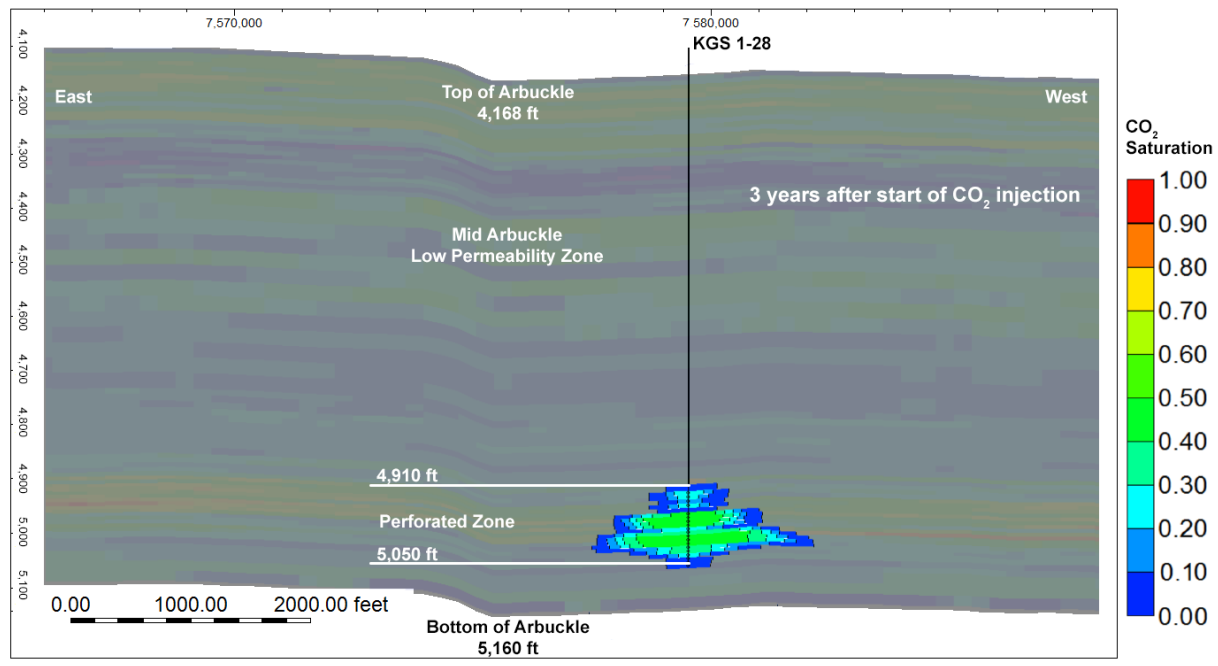
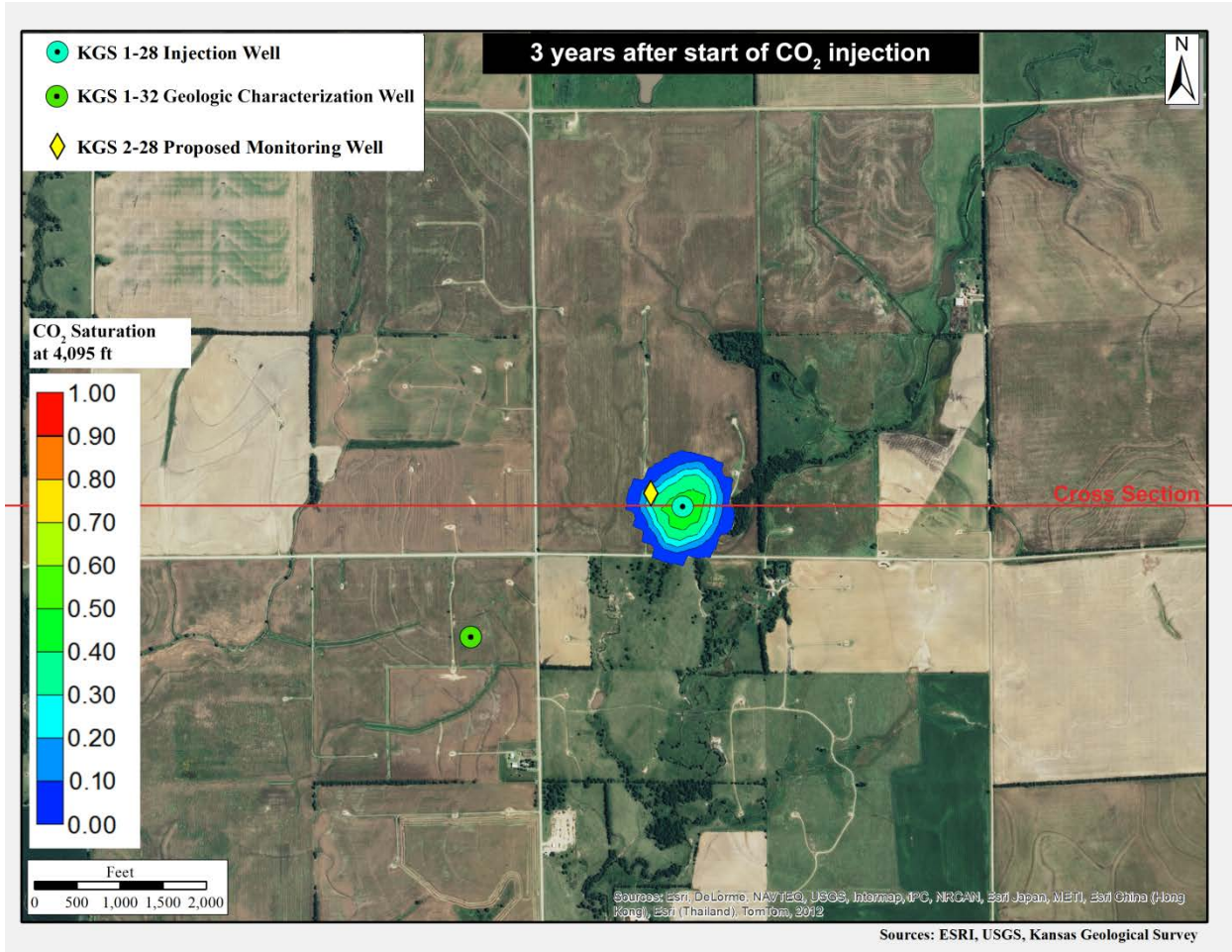


Figure 5.13e—Free-phase CO₂ plume in aerial and cross-sectional view for the largest migration alternative model ($k=1.25/\phi=0.75$) at three years from start of injection.

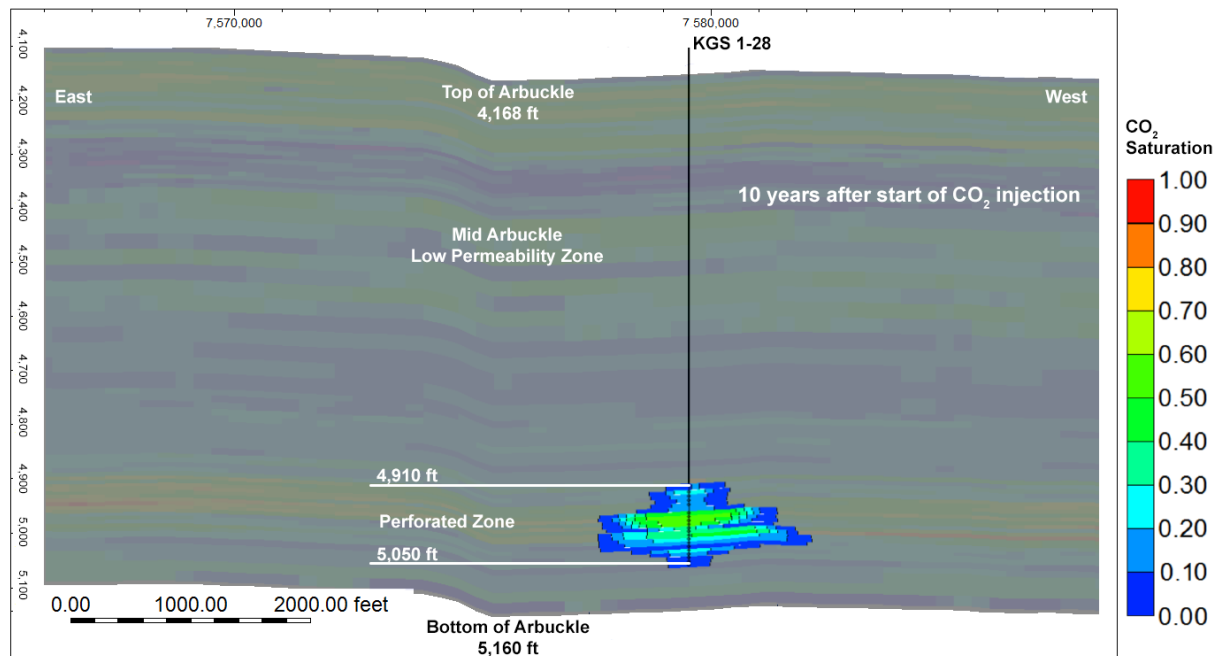
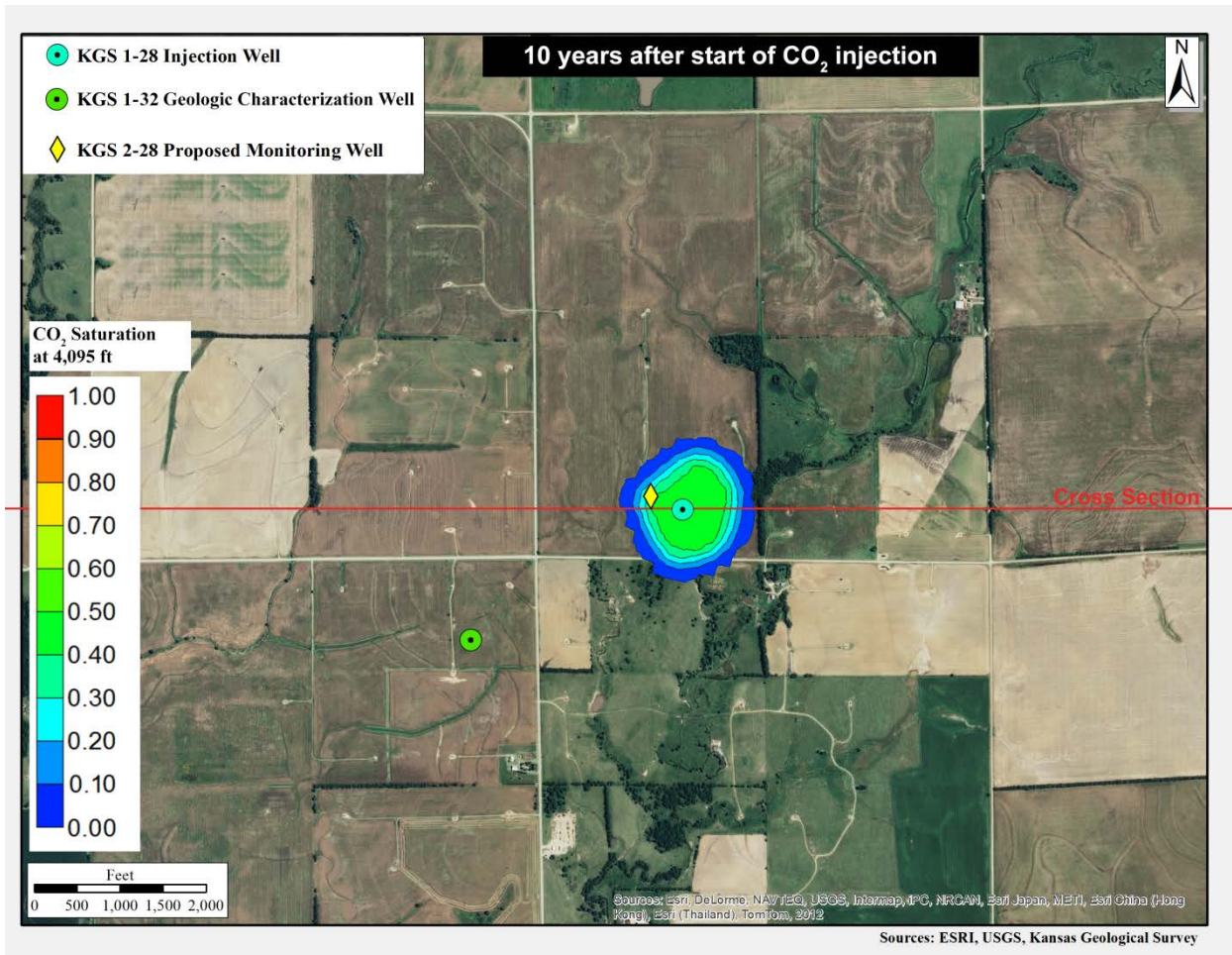


Figure 5.13f—Free-phase CO₂ plume in aerial and cross-sectional view for the largest migration alternative model ($k=1.25/\phi=0.75$) at 10 years from start of injection.

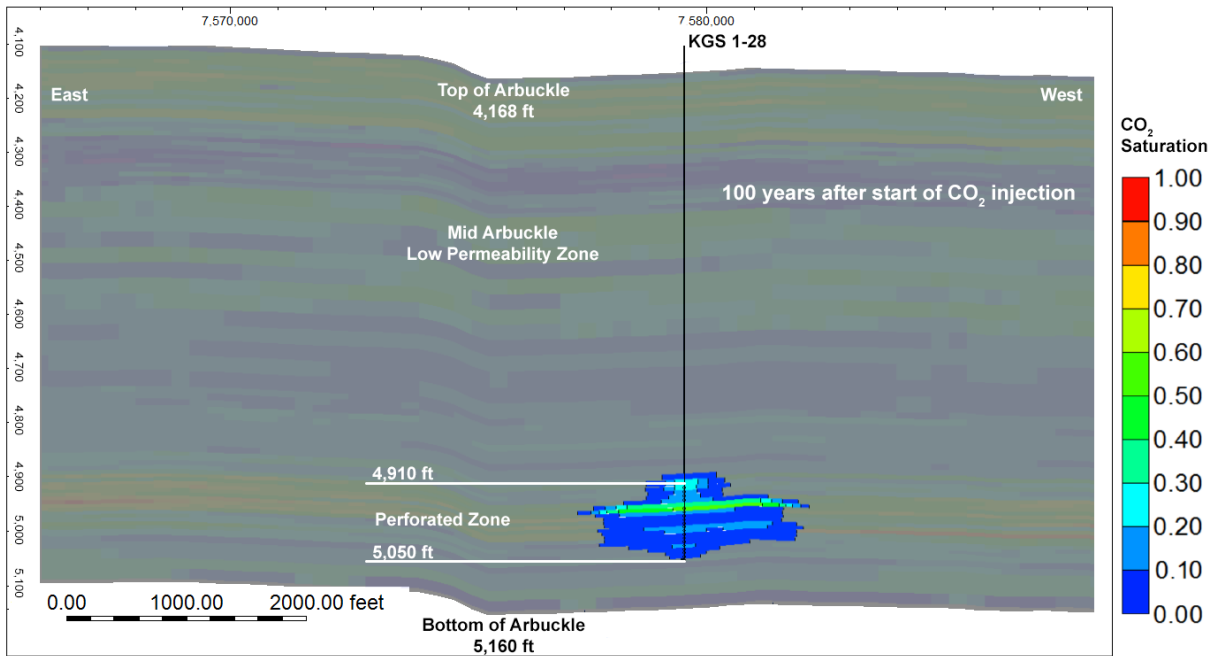
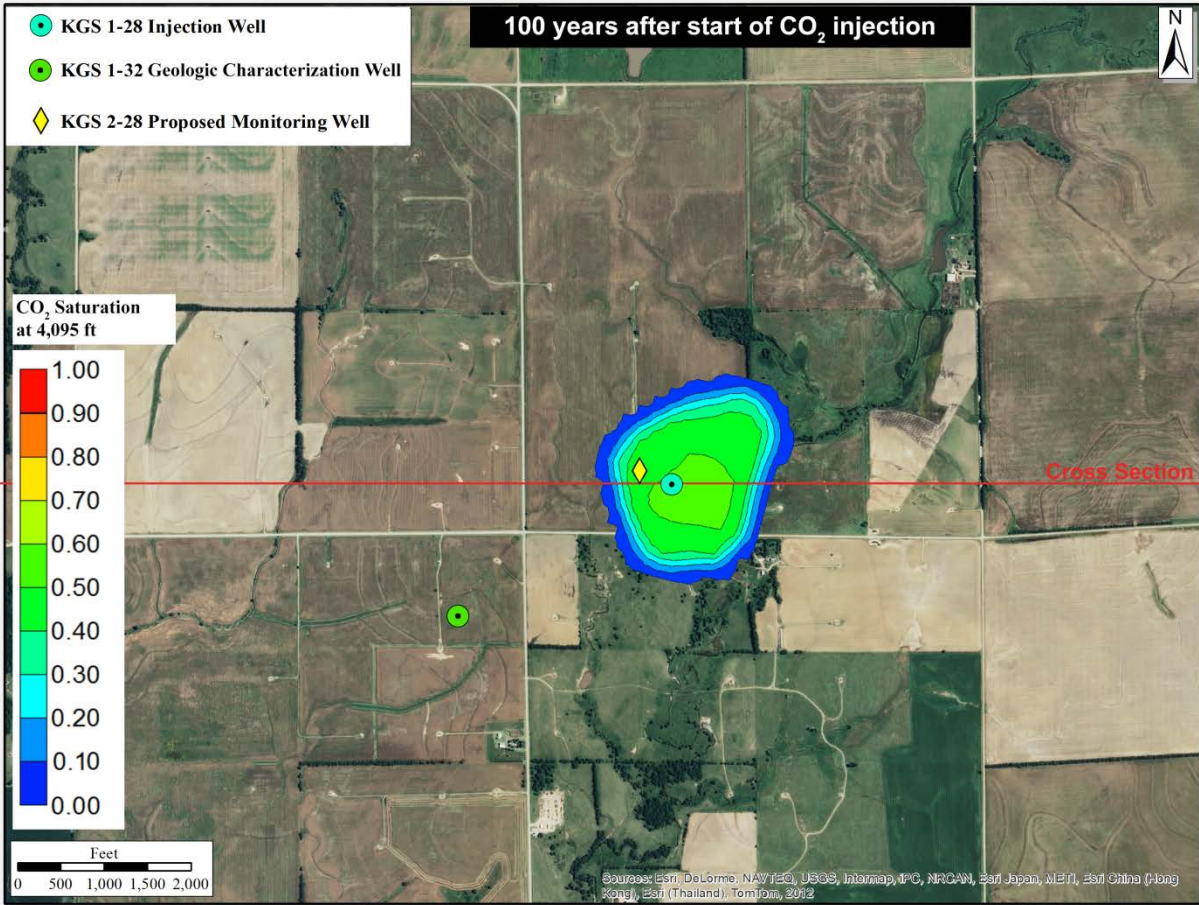


Figure 5.13g—Free-phase CO₂ plume in aerial and cross-sectional view for the largest migration alternative model ($k=1.25/\phi=0.75$) at 100 years from start of injection.

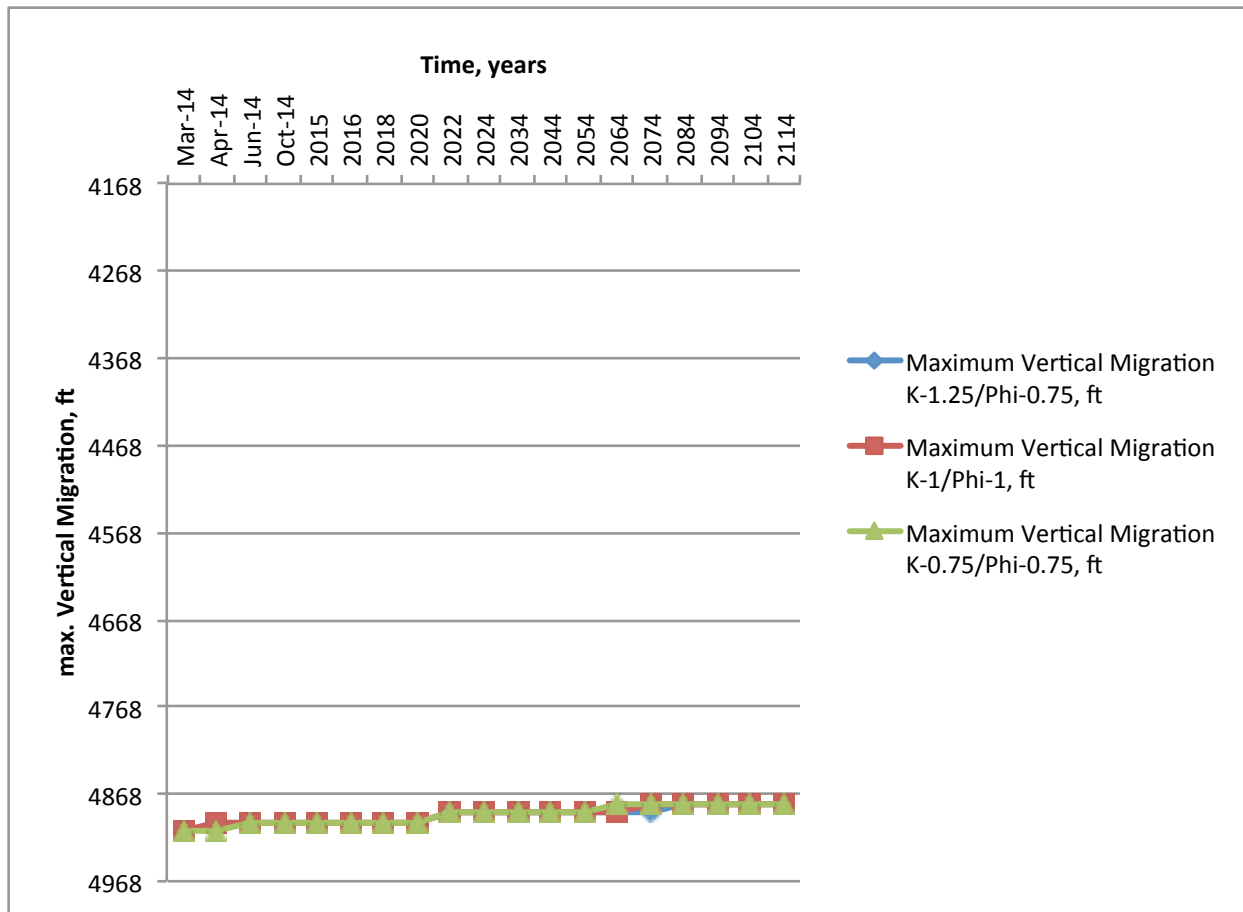


Figure 5.14—Maximum vertical extent of free-phase CO₂ migration for the two alternative cases that result in the maximum plume spread ($k-1.25/\phi-0.75$) and the maximum induced pressure ($k-0.75/\phi-0.75$) along with base case ($k-1.0/\phi-1.0$).

accelerate the dissolution rate. Because of time and computational constraints, these mechanisms were ignored, and therefore the storage rates and quantities are likely to be underestimated, thus ensuring that the projections presented in this application provide a “worst-case” scenario.

5.4.6.2 Simulated Pressure Distribution

Figure 5.15 presents the bottomhole pressure (at a reference depth of 5,050 ft) for the base case and the two cases that resulted in highest pressures and plume migration. The bottomhole pressures for all nine alternative cases are listed in Table 5.6. For all three cases presented in Figure 5.15, the pressure increases when CO₂ injection operations start and then drops to nearly pre-injection values when injection ceases. The pressure is influenced by permeability and porosi-

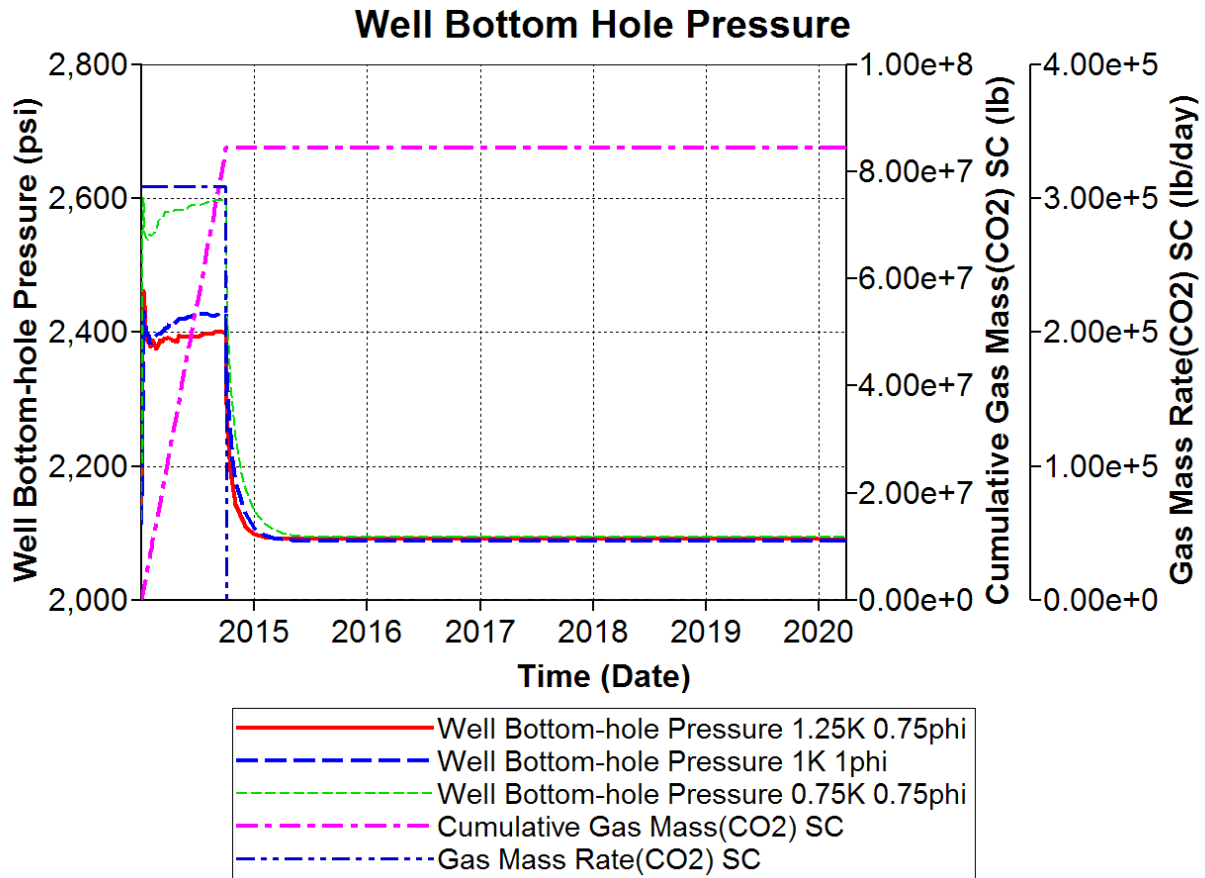


Figure 5.15—Well bottomhole pressure at the depth of 5,050 ft for the two alternative cases that result in the maximum plume spread ($k=1.25/\phi=0.75$) and the maximum induced pressure ($k=0.75/\phi=0.75$) along with base case ($k=1.0/\phi=1.0$).

ty, as these two parameters are independent (decoupled) variables in CMG. Therefore, as expected, the highest bottomhole pressure (BHP) of 2,535 psi at a depth of 5,050 ft is observed for the low permeability–low porosity case. This pressure represents an increase of 442 psi over pre-injection levels and results in a pressure gradient of 0.515 psi/ft, which is less than the maximum allowable pressure gradient of 0.675 psi/ft corresponding to 90% of the fracture gradient (0.75 psi/ft) as documented in Section 4.6.9.

Table 5.6—Maximal CO₂ migration extent and bottom-hole pressure for each of the nine alternative cases

Modeling Case	Case Identifier	CO ₂ Maximum Diameter of Areal Extent (ft)	Maximum Bottomhole Pressure, psi (@ 5,050 ft)	Maximum Bottomhole Pressure Increase (psi)
Low Permeability, Low Porosity	K-0.75/Phi-0.75	3,389	2,535	442
Medium Permeability, Low Porosity	K-1.0/Phi-0.75	2,629	2,462	369
High Permeability, Low Porosity	K-1.25/Phi-0.75	3,504	2,418	325
Low Permeability, Medium Porosity	K-0.75/Phi-1.0	2,218	2,512	419
Medium Permeability, Medium Porosity	K-1.0/Phi-1.0	2,433	2,428	335
High Permeability, Medium Porosity	K-1.25/Phi-1.0	3,203	2,415	322
Low Permeability, High Porosity	K-0.75/Phi-1.25	1,952	2,525	432
Medium Permeability, High Porosity	K-1.0/Phi-1.25	2,517	2,459	366
High Permeability, High Porosity	K-1.25/Phi-1.25	2,802	2,410	317

Figure 5.16 presents the change in pore pressure at the base of the confining zone (Simpson Group) for the base case and the two alternative cases that resulted in the highest pressures and plume spread. The maximum pressure increase at the end of the injection period is fairly small and varies between 8.9 psi and 13.1 psi. As observed for pressures at the bottom of the well, the highest pressure is noted for the low permeability/low porosity case (k-0.75/phi-0.75).

Figure 5.17a–d presents the lateral distribution of pressure in the Arbuckle injection interval (at an elevation of 4,960 ft) for the k-0.75/phi-0.75 case, which resulted in the maximum induced pore pressures. The pressures increase from commencement of injection to nine months and then drop significantly by the end of the first year (three months after operations stop). The pressures also drop very rapidly at short distances from the injection well at the end of the nine-month injection period, as shown in Figure 5.18. The pressures at the end of the nine-month in-

jection period drop from about 283 psi a short distance from the injection well to less than 11 psi at the geologic characterization well, KGS 1-32, which is approximately 3,500 ft southwest of the injection well. The maximum induced pressure at the model boundary is only 2–3 psi.

Figure 5.17a–d also shows the vertical pressure distribution for the maximum induced pressure case ($k=0.75/\phi=0.75$). The confining effect of the mid-Arbuckle baffle zones is evident in the plots as the large pressure increases are mostly restricted to the injection interval. The pressures decline rapidly at a short distance from the injection well. The pressures throughout the model subside to nearly pre-injection levels soon after injection stops, as shown in the one-year pressure plot in Figure 5.17d.

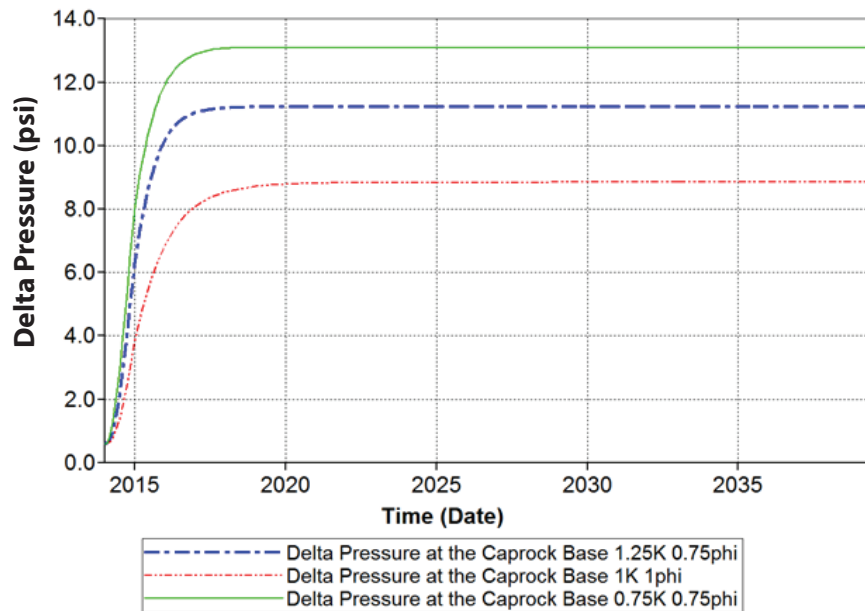


Figure 5.16—Change in pore pressure at the base of the confining zone (i.e., base of Simpson Group) at the injection well site for the two alternative cases that result in the maximum plume spread ($k=1.25/\phi=0.75$) and the maximum induced pressure ($k=0.75/\phi=0.75$) along with base case ($k=1.0/\phi=1.0$).

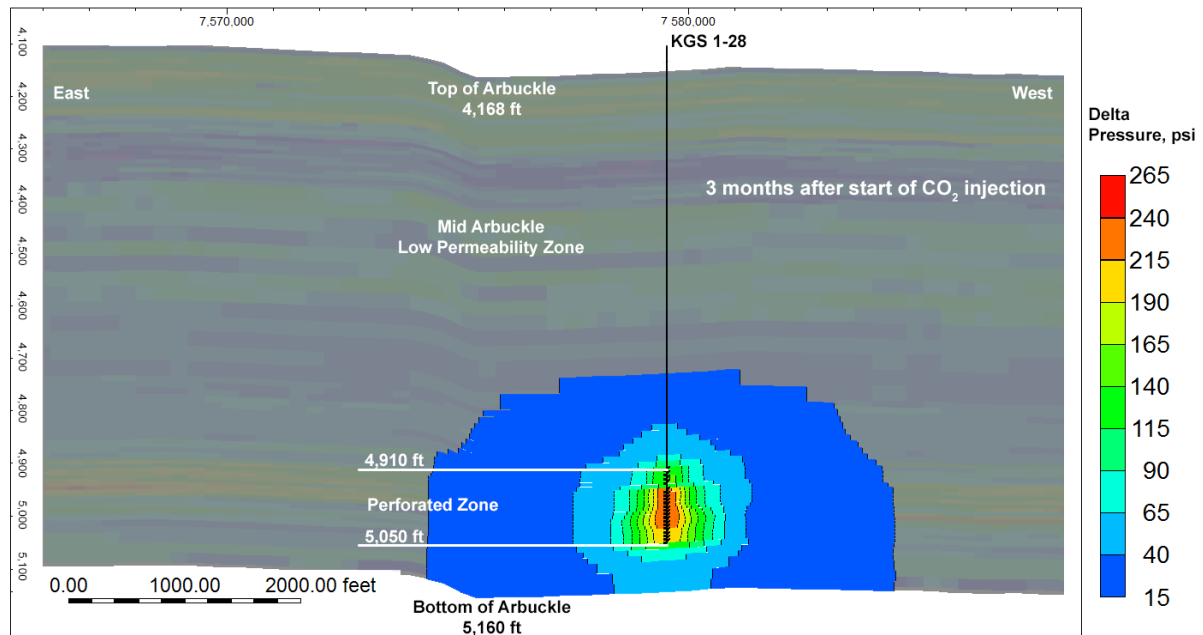
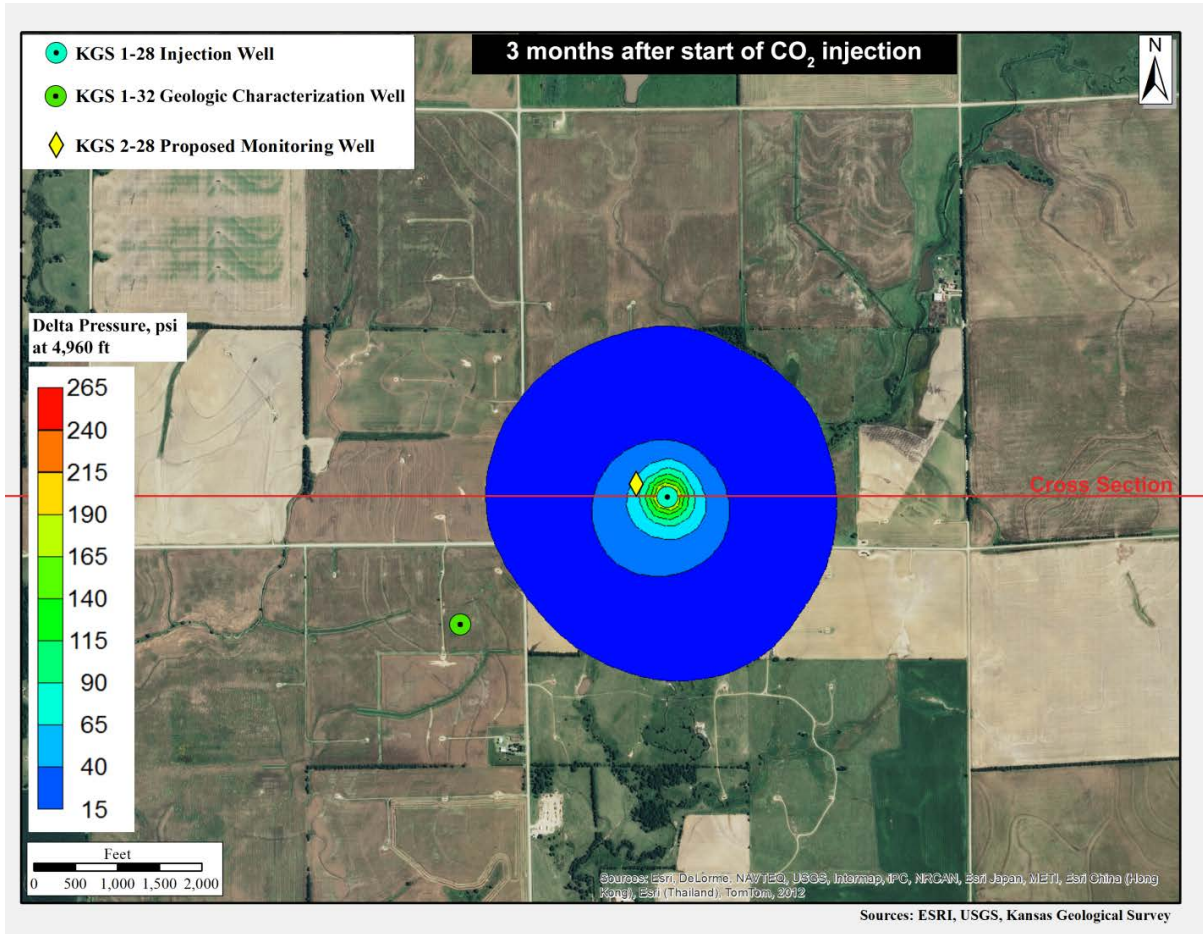


Figure 5.17a—Simulated increase in pressure in plan and cross-sectional view at three months from start of injection for the low permeability–low porosity ($k=0.75/\phi=0.75$) alternative case, which resulted in the largest simulated pressures.

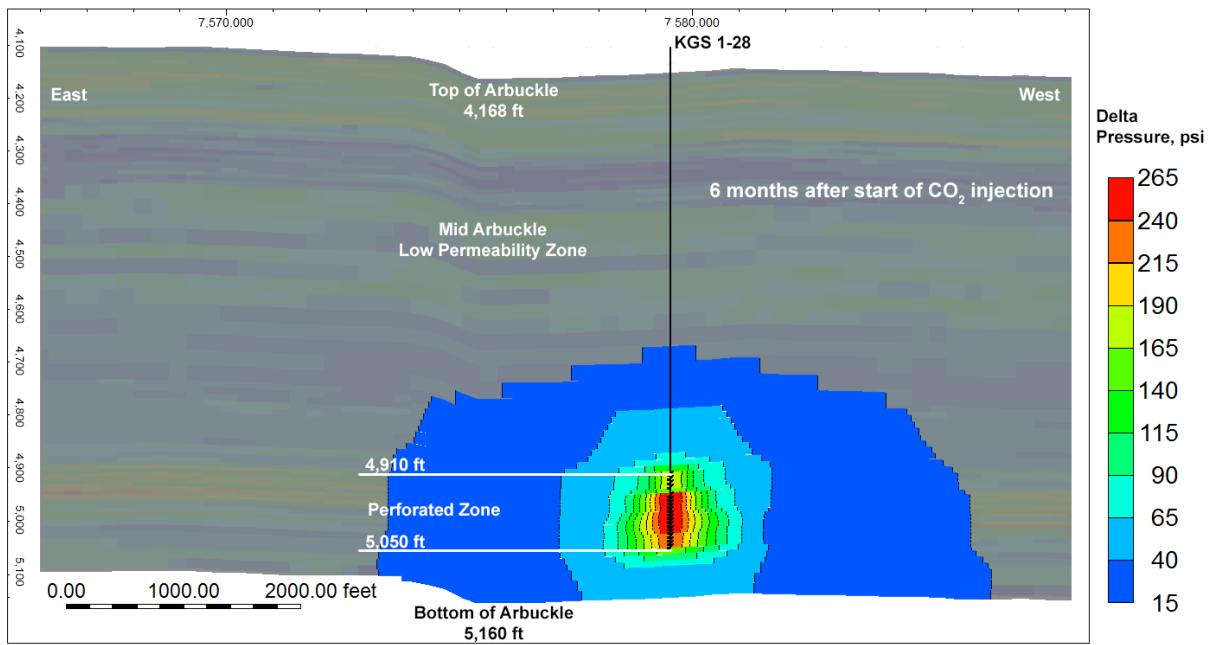
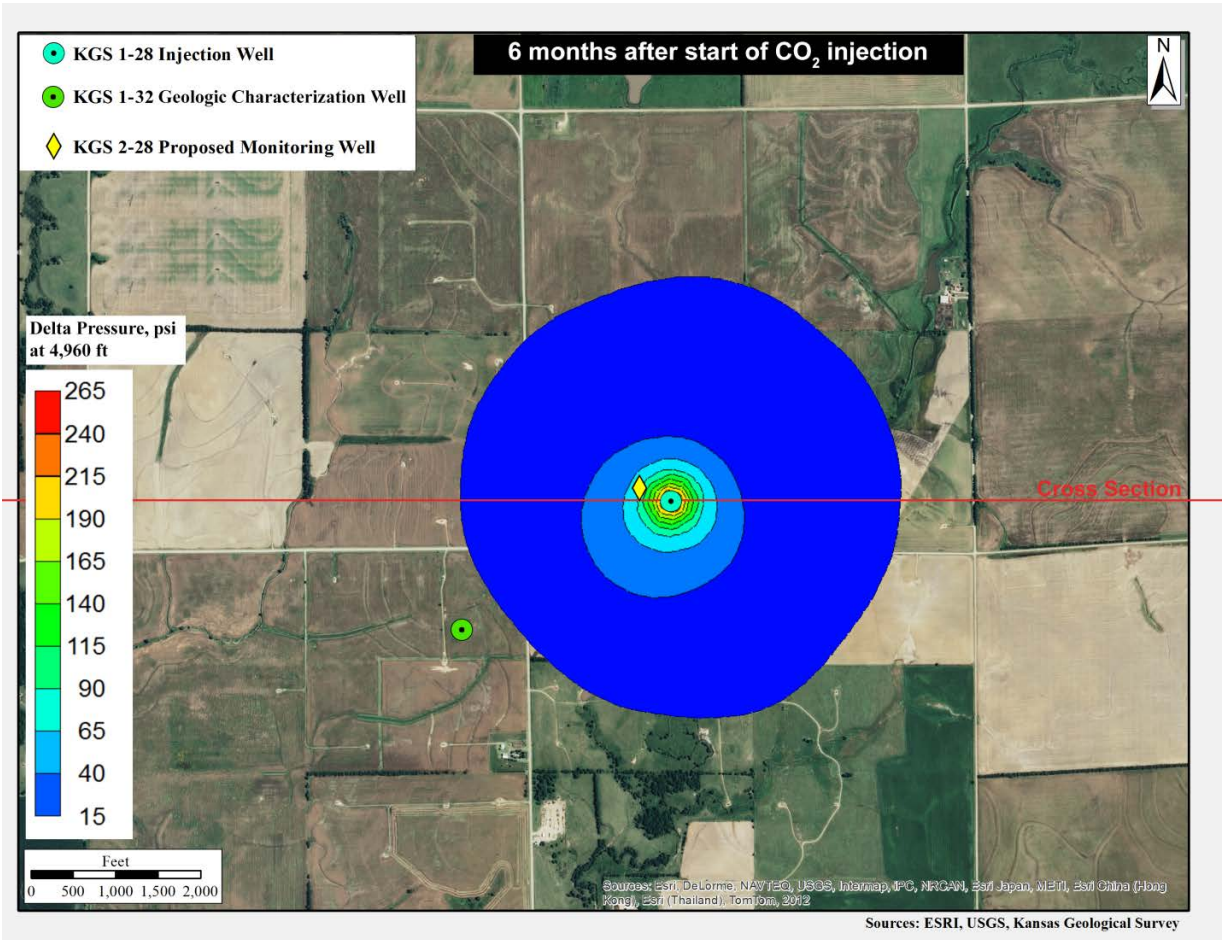


Figure 5.17b—Simulated increase in pressure in plan and cross-sectional view at six months from start of injection for the low permeability–low porosity ($k=0.75/\phi=0.75$) alternative case, which resulted in the largest simulated pressures.

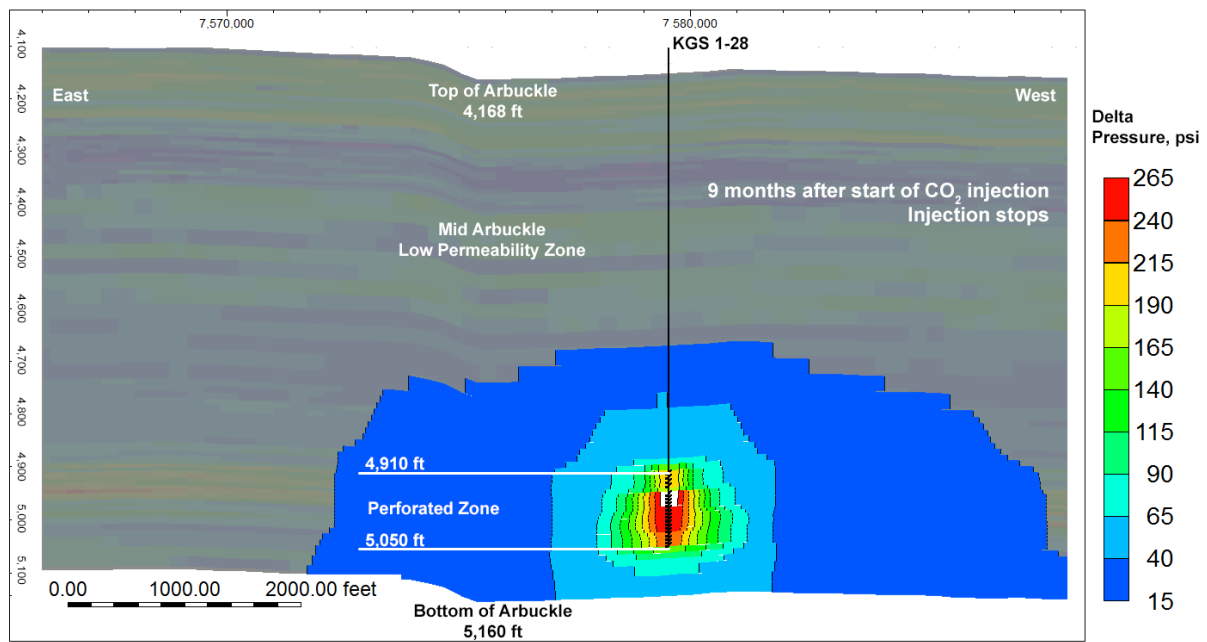
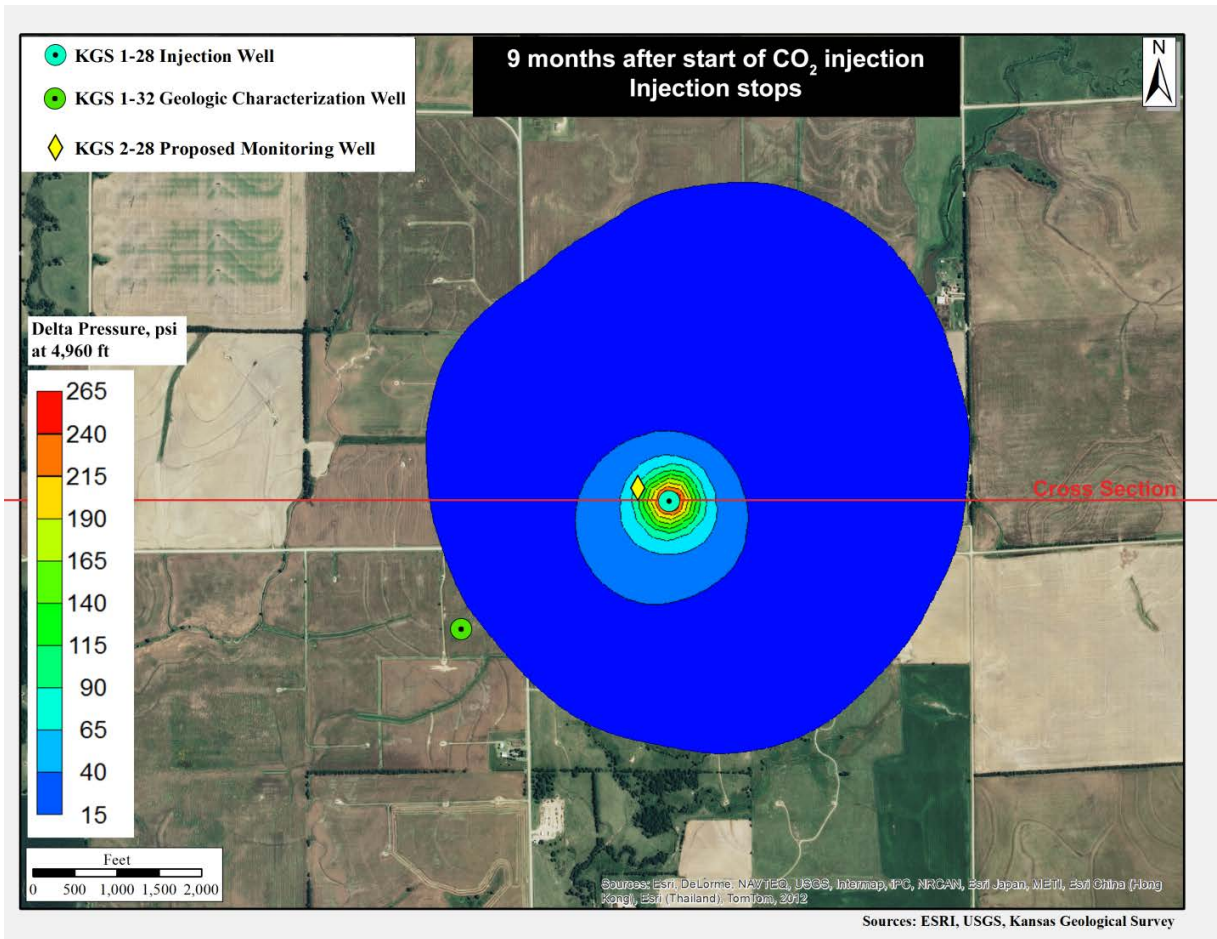


Figure 5.17c—Simulated increase in pressure in plan and cross-sectional view at nine months from start of injection for the low permeability–low porosity ($k=0.75/\phi=0.75$) alternative case, which resulted in the largest simulated pressures.

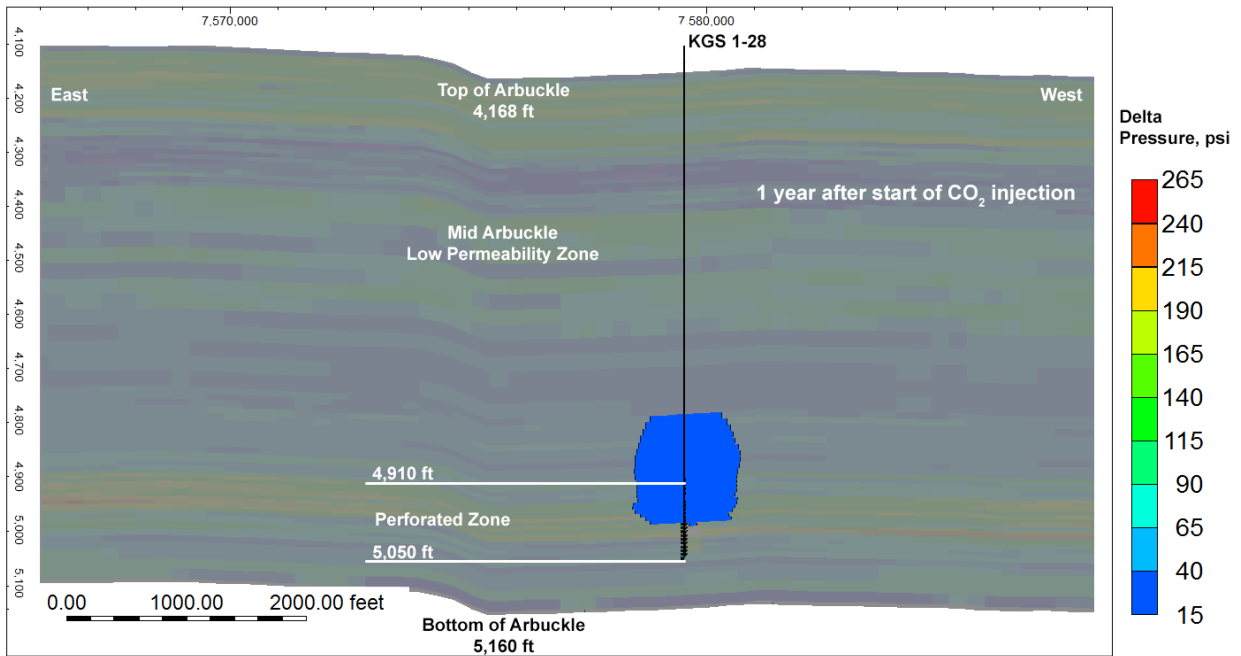
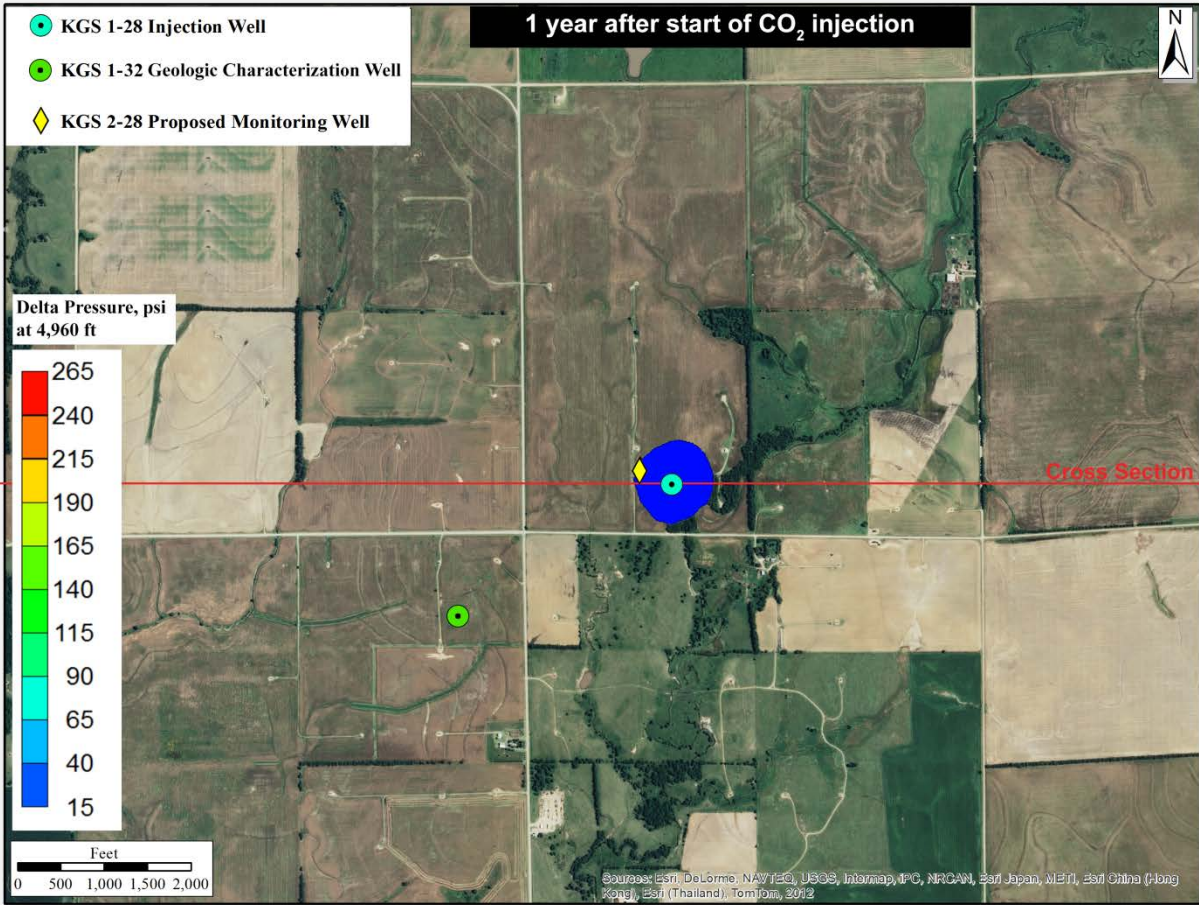


Figure 5.17d—Simulated increase in pressure in plan and cross-sectional view at one year from start of injection for the low permeability–low porosity ($k=0.75/\phi=0.75$) alternative case, which resulted in the largest simulated pressures.

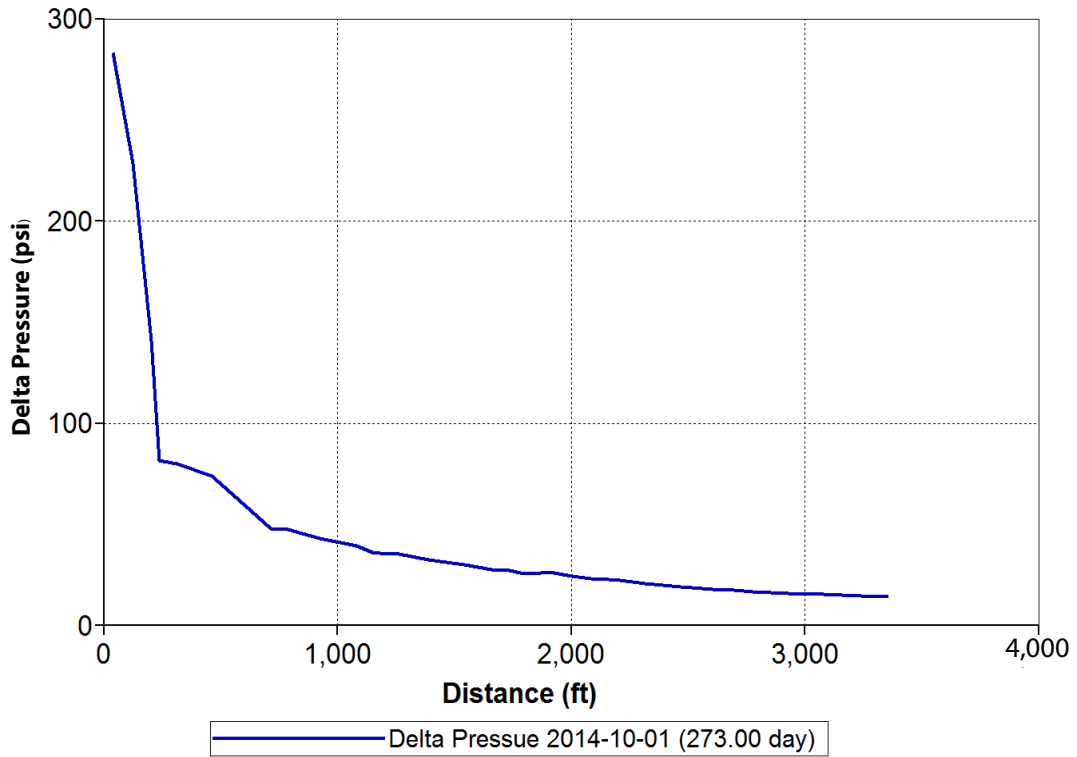


Figure 5.18—Pore pressure as a function of lateral distance from the injection well (KGS 1-28) at the end of the injection period (nine months) for the highest induced pressure case ($k=0.75/\phi=0.75$).

Section 9

Area of Review Delineation Re-Evaluation and Corrective Action Plan

Facility Name: Wellington Field Small Scale Carbon Capture and Storage Project

Injection well Location: Latitude 37.319485, Longitude -97.4334588
Township 31S, Range 1W, Section 28 NE SW SE SW

Facility Contact: Dana Wreath, Vice President

Contact Information: 2020 N. Bramblewood Street
Wichita, KS 67206
(316) 265-3311
Fax: (316) 265-8690

9.1 Introduction

Class VI Area of Review and Corrective Action requirements states in § 146.84 (b) that the owner or operator of a Class VI well must prepare, maintain, and comply with a plan to delineate the AoR for a proposed geologic storage project, periodically re-evaluate the delineation, and perform corrective action that meets the requirements of this section and is acceptable to the director. The Area of Review and Corrective Action Plan must include the following:

- (1) The method for delineating the AoR, including the model to be used, assumptions that will be made, and the site characterization data on which the model will be based;
- (2) A description of
 - (i) The minimum fixed frequency, not to exceed five years, at which the owner or operator proposes to re-evaluate the AoR;
 - (ii) The monitoring and operational conditions that would warrant a re-evaluation of the AoR before the next scheduled re-evaluation, as determined by the minimum fixed frequency.

- (iii) How monitoring and operational data (e.g., injection rate and pressure) will be used to inform an AoR re-evaluation; and
- (iv) How corrective action will be conducted to meet the requirements, including what corrective action will be performed before injection and what, if any, portions of the AoR will have corrective action addressed on a phased basis and how the phasing will be determined; how corrective action will be adjusted if there are changes in the AoR; and how site access will be guaranteed for future corrective action.

Additionally, §146.84 (e) also requires a re-evaluation of the AoR at the minimum fixed frequency, not to exceed five years, as specified in the Area of Review and Corrective Action Plan, or when monitoring and operational conditions warrant. The re-evaluation process must do the following:

- (1) Re-evaluate the AoR in the same manner as originally conducted;
- (2) Identify all wells in the re-evaluated AoR that require corrective action;
- (3) Perform corrective action on wells requiring corrective action in the re-evaluated AoR; and
- (4) Submit an amended Area of Review and Corrective Action Plan or demonstrate to the director through monitoring data and modeling results that no amendment to the plan is needed. Any amendments to the Area of Review and Corrective Action Plan must be approved by the director, must be incorporated into the permit, and are subject to the permit modification requirements at §144.39 or §144.41, as appropriate.

Section 5 presents the reservoir modeling conducted in support of the Wellington Arbuckle pilot project AoR. The conceptual model, model domain, modeled processes, geologic structure, hydrogeologic and CO₂ injectate properties, model mesh, initial and boundary conditions, model operational constraints, simulations software description, and simulation results are all documented in Section 5. Therefore, Section 5 is an integral part of the Area of Review and Corrective Action Plan and contents in Section 5 should be reviewed in conjunction with information presented in this section. This section summarizes how modeling information from Section 5 was used to

delineate the AoR, how the AoR will be re-evaluated over time, and the overall plan for demonstrating compliance with 40 CFR 146.84 requirements listed above.

9.2 EPA Area of Review (AoR)

The EPA AoR is based on the Maximum Extent of either the Separate-phase Plume or Pressure-front (MESPOP) methodology as explained in the EPA AoR guidance document (USEPA, 2011). The goal is to define the extent of the plume and pressure front within which any artificial or natural penetration (such as improperly plugged wells, transmissive faults or fractures) could have the potential to allow brines within the injection zone to migrate upward into the lowermost USDW. As documented in Sections 4.4 and 4.5, the lowermost USDW at the Wellington geologic storage site is the Upper Wellington Formation within the top 250 ft of the geologic column. Section 9.2.1 discussed the pressure-based AoR, and Section 9.2.2 discusses the plume-based AoR.

9.2.1 Pressure-Based AoR

The pressure-based AoR is defined by the following equation:

$$P_{i,f} = P_u \frac{\rho_i}{\rho_u} + \rho_i g (z_u - z_i) \quad \text{(Equation 9.1)}$$

Where,

$P_{i,f}$ = Minimum pressure (MPa) within the injection zone necessary to cause vertical flow from the injection interval into the USDW

P_u = Pressure (MPa) within the lowermost USDW (97 psi = 0.67 MPa),

ρ_u = Fluid density (kg/m³) within the USDW (1,000 kg/m³),

ρ_i = Fluid density (kg/m³) in the injection zone (1,130 kg/m³),

z_i = Injection depth (m) (5,050 ft = 1,539 m; bottom of injection interval),

z_u = depth of lowermost USDW (m) (250 ft = 76.2m)

g = acceleration due to gravity (9.81 m/sec²)

The pressure-based AoR is defined by the 327 psi (increase in pore pressure) isoline. It was derived as follows.

Based on water level hydrographs presented in Figure 4.15, the water table in the area is generally 8–12 ft below ground. In one well in western Sumner County, the water table is approximately 25 ft below ground level. To be conservative, it is assumed that the water table is also 25 ft below ground level at the Wellington site within the entire AoR. This equates to a hydraulic freshwater pressure at the base of the USDW (Upper Wellington formation; 250 ft below ground, elevation of approximately 1,000 ft / 305 m, msl) of approximately 0.67 MPa. It is assumed that the density of freshwater in the USDW is 1,000 kg/m³. Based on the DST at KGS 1-28, the chloride concentration in the injection zone is approximately 112,000 ppm, which results in a specific gravity of 1.13 (density of 1130 kg/m³) as per the brine density relationship for the Arbuckle Group presented in Figure 4.3.

Substituting the above values in Equation 9.1 above results in a pressure of 16.97 MPa (2,461 psi) at the bottom of the injection interval at 5,050 ft.

$$P_{i,f} = 0.67 \text{ MPa} (1,130 \text{ kg/m}^3 / 1,000 \text{ kg/m}^3) + 1,130 \text{ kg/m}^3 * 9.81 \times 10^{-6} \text{ m/s}^2 (1,539.2 \text{ m} - 76.2 \text{ m}) = 16.97 \text{ MPa} = 2,461 \text{ psi}$$

Working similarly, the pressure-based AoR at the top of the injection interval (4,910 ft) is derived as 16.502 MPa (2,393 psi) as shown in Table 9.1

Table 9.1—Pressure boundary for Area of Review delineation.

Depth (ft)	Pressure-Based AoR Boundary (psi)	Estimated Ambient Pressure (Section 5.2.4) psi	Delta Pressure (psi)
4,910 (top of injection zone)	2,393	2,066	327
5,050 (bottom of injection zone)	2,461	2,134	327

The ambient (pre-injection) pressure is approximately 2,134 psi at the bottom of the injection interval (5,050 ft) based on the pressure equation derived in Section 5.2.4, which implies that a pressure increase of 327 psi (due to CO₂ injection) is required for the brine from the Arbuckle to

migrate vertically to the base of the USDW outside of the CO₂ plume. As shown in Figure 5.18, the pore pressure in the formation drops to less than 300 psi within a few tens of feet from the injection well at the end of the injection period. Therefore, the only well within the pressure-based AoR is KGS 1-28, which has been constructed per Class VI guidelines.

9.2.2 Plume-Based AoR

The plume-based AoR is defined by the boundary that encompasses the injected free-phase CO₂ with a concentration greater than 1%. As discussed in Section 5.4.6.1, the maximum plume spread results for the alternative model with the largest permeability and the lowest porosity (K-1.25/phi-0.75). Figure 9.1 shows the free-phase CO₂ plume in the injection zone at 100 years, by which time the plume has largely stabilized. As shown in Figure 9.1, no existing or abandoned wells, other than the proposed injection well (KGS 1-28) and the proposed monitoring well (KGS 2-28), penetrate the top of the confining zone (Pierson formation)

9.3 Corrective Action Plan

Since both the existing well (KGS 1-28) and the future well (KGS 2-28) located in the AoR will be constructed in accordance with 40 CFR 146.86 (Injection Well Construction Requirements), no corrective action is anticipated for the wells within the AoR. The construction details for well KGS 1-28 and KGS 2-28 are documented in Sections 8 and 10 respectively and are summarized in Table 9.2.

Table 9.2—Existing or abandonment wells/boreholes that penetrate the confining zone within the AoR.

API Well Number	Lease Name	Well Class	Operator Name	Total Depth (ft)	Status	Spud Date	Completion Date	API Number	Elevation (ft, msl)	NAD83 Latitude	NAD83 Longitude
22590	Wellington KGS #1-28	Inactive Well	Berexco LLC	5,250	CO ₂ Injection	2/20/11	8/24/11	15-191-22590	1257	37.31951	-97.43378
Future Well	Wellington KGS #2-28	Proposed Well	Berexco LLC	5,250	CO ₂ Monitoring	N/A	N/A	N/A	1255 (Est)	37.319965	-97.434739

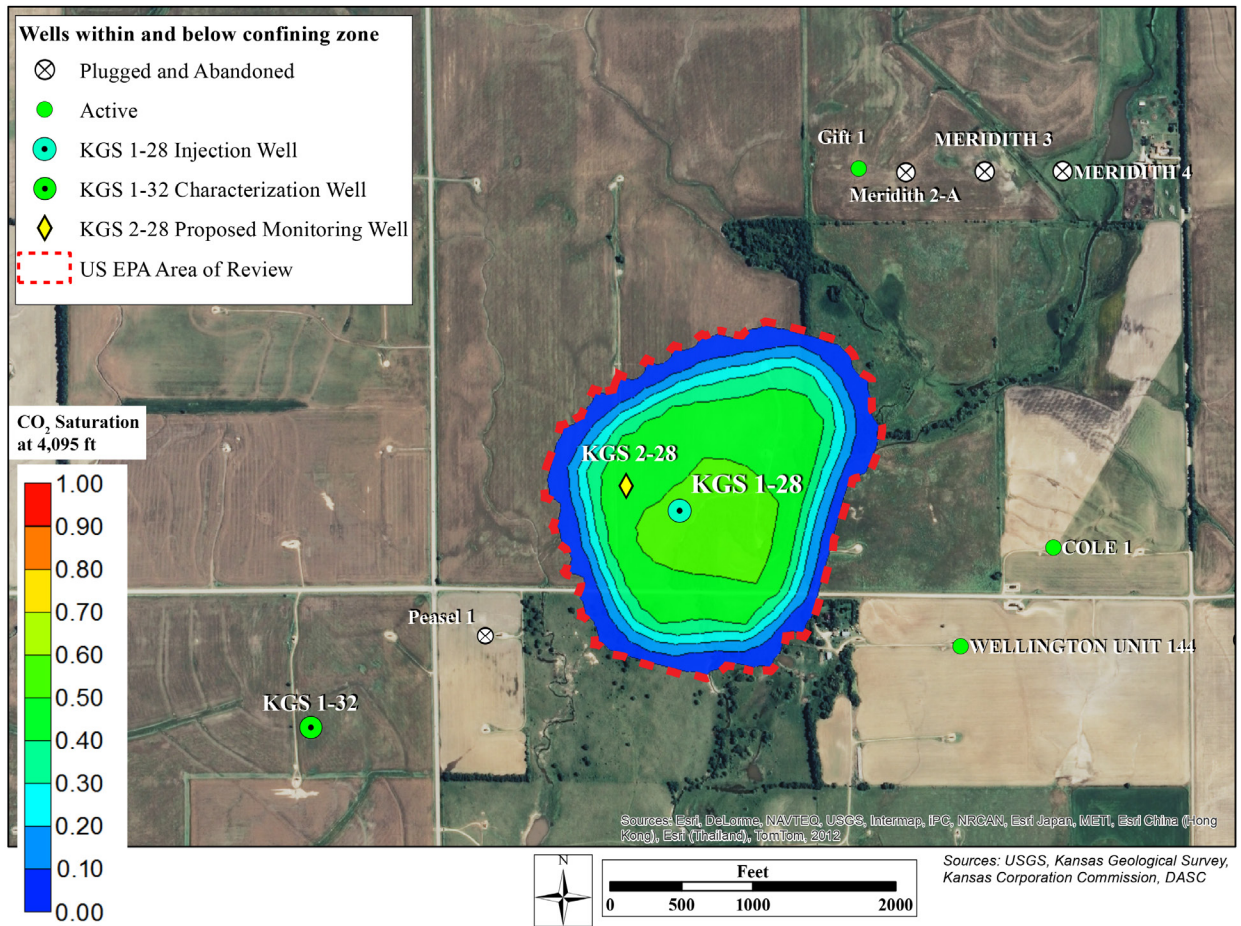


Figure 9.1—The plume-based AoR as defined by the 1% free-phase saturation isoline, which encompasses 99% of the injected CO₂ in free phase for the largest plume migration alternative model ($k=1.25/\phi=0.75$). Also shown are all existing, abandoned, and proposed wells that penetrate the top of the confining zone (Pierson formation) in the AoR and vicinity.

9.3.1 Area of Review Plan and Schedule

The AoR will be re-evaluated for this pilot-scale project according to the criteria presented below, or a demonstration will be made to the Director that an AoR re-evaluation is not required.

a) When the following operational parameters are exceeded:

- Average injection rate exceeds 300 tons/day for more than 1 week.
- The pressure at the top and bottom of the Arbuckle injection interval exceeds 90% of the fracture gradient as specified in the following table:

Depth (ft)	Expected Ambient Pressure* (psi)	90% of Fracture Gradient Based Pressure** (psi)
4,910	2,066	3,314
5,050	2,134	3,408

* based on pressure-depth relationship specified in Section 5.2.4.

** assuming fracture gradient of 0.75 psi/ft as specified in Section 4.6.9.

- b) If newly collected characterization data at KGS 2-28 are deemed to significantly alter the hydrogeologic properties specified in the reservoir model,
- c) When pressure and plume data recorded at the monitoring well (KGS 2-28) differ significantly from model projections,
- d) At the termination of injection,
- e) Just before site closure to demonstrate stability of the plume and pressure front, since an early site closure is requested for this short-term small pilot scale project,
- f) If the following events occur and re-evaluation is determined to be warranted based on evaluation of the event impact:
- Change in modeled direction of plume movement as detected by means other than the monitoring well (KGS 2-28) (evaluation within one month of detection),
 - Initiation of competing Arbuckle injection projects within the same injection formation within a 1-mi radius of the injection well (evaluation within one month of detection),

- A significant deviation of monitored wellhead operational data, or formation pressure and plume migration data
- Significant land use changes that would impact the USDW or site access (evaluation within one month of detection),
- New site characterization data that identify faults within the AoR (within one month of identification),
- Seismic events or other emergency events that trigger an AoR re-evaluation as specified in Section 13,
- Any other activity prompting a model recalibration.

The AoR re-evaluation will ensure that site monitoring data are used to update modeling results and that the AoR delineation reflects any changes in operational conditions. Figure 9.2 illustrates the general relationship between site characterization, modeling, and monitoring activities that is to be followed. At the end of injection and at closure, and if evaluation of the events listed above indicates that the event was significant, then §146.84 (e), which requires a re-evaluation when monitoring and operational conditions change, will be implemented:

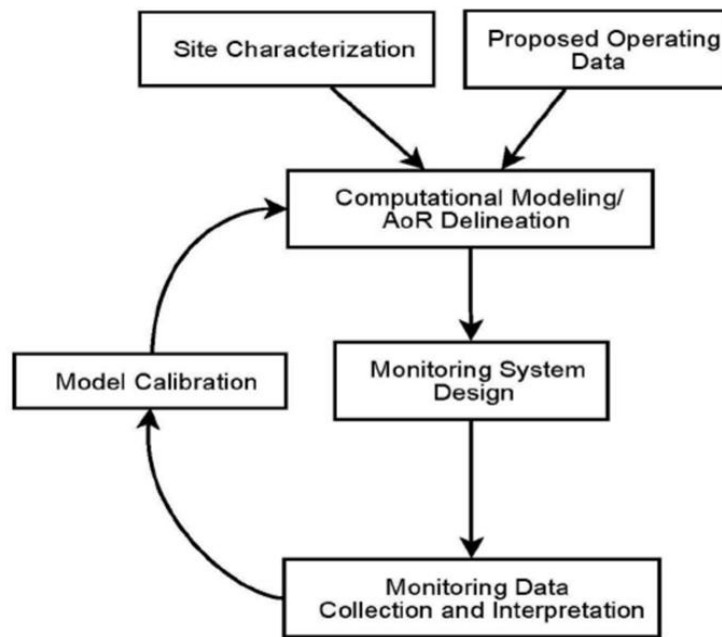


Figure 9.2—Flow chart of monitoring and modeling (source: EPA, 2011).

- (1) Re-evaluate the AoR in the same manner specified in paragraph (c) (1) of section 146.84;
- (2) Identify all wells in the re-evaluated AoR that require corrective action in the same manner specified in paragraph (c) of §146.84;
- (3) Perform corrective action on wells requiring corrective action in the re-evaluated AoR in the same manner specified in paragraph (d) of §146.84; and
- (4) Submit an amended Area of Review and Corrective Action Plan or demonstrate to the director through monitoring data and modeling results that no amendment to the plan is needed. Any amendments to the Area of Review and Corrective Action Plan must be approved by the director, must be incorporated into the permit, and are subject to the permit modification requirements at §144.39 or §144.41 as appropriate.

9.3.2 Corrective Action Plan and Schedule Following AoR Re-evaluation (§146.8 [b][2] [iv])

As discussed earlier, since both wells within the AoR are either constructed (KGS 1-28) or will be constructed (KGS 2-28) in accordance with 40 CFR 146.86, no corrective action is presently required. Should future modeling indicate that the AoR extends beyond the present AoR boundary and includes wells that penetrate the confining zone other than KGS 1-28 or KGS 2-28, the Corrective Action Plan will be revised to include the well name, well location, planned date of corrective action, planned corrective action method, and any other pertinent information required by the director. If the result of the re-evaluation requires corrective action(s), these will be implemented as expeditiously as possible in consultation with the EPA director.

9.3.3 Site Access (§146.8 [b][2][iv]):

The Wellington site is in close proximity to paved roads in the area, thereby providing easy access. Berexco is the operator of the Wellington oil field and has permission to access all well sites should that be necessary to perform any corrective action.

9.4 Compatibility of CO₂ with Arbuckle Brine and Minerals

No compatibility problems are anticipated in the injection zone. Conclusions from preliminary modeling results indicate that the CO₂ brine formation interactions and reactions from chemical processes will have a negligible effect on reservoir porosity. Additionally, the effects of mineralization and mineral precipitation are not expected to meaningfully reduce the formation permeability. The injection interval is mainly a dolomitic peloidal packstone-wackestone becoming a cherty packstone. Zones of autoclastic breccia have also been identified. Thin-section studies reveal extensive silica micro-porosity that contributes to high porosity values in the lower injection interval and that should facilitate injection. Microporous regions have high surface areas that increase reaction rates, which may lead to rapid dissolution.

9.5 Period of Data Retention

All modeling inputs and data used to support AoR delineation and re-evaluation will be retained for 10 years by Berexco/KGS.